

Molecular studies of the synaptic protein otoferlin

Dissertation

for the award of the degree

“Doctor rerum naturalium” (Dr. rer. nat.)

submitted by

Alexandra Müller

from

Siegen, Germany

Göttingen, 2016

Examination committee

Dr. Ellen Reisinger

(1st Reviewer, advisor, member of the thesis committee)
Molecular Biology of Cochlear Neurotransmission
Department of Otolaryngology

Prof. Dr. Thomas Dresbach

(2nd Reviewer, member of the thesis committee)
Department of Anatomy and Embryology
Center of Anatomy

Prof. Dr. Nils Brose

(Member of the thesis committee)
Molecular Neurobiology
Max-Planck-Institut für experimentelle Medizin, Göttingen

Prof. Dr. Silvio Rizzoli

Department of Neuro- and Sensory Physiology
University Medical Center Göttingen

Dr. Manuela Schmidt

Somatosensory Signaling Group
Max-Planck-Institut für experimentelle Medizin, Göttingen

Prof. Dr. Martin Göpfert

Cellular Neurobiology
Schwann-Schleiden-Forschungszentrum
University of Göttingen

Date of oral examination: 08.04.2016

Herewith I declare, that I prepared the PhD Thesis “Molecular studies of the synaptic protein otoferlin” on my own and with no other sources and aids than quoted.

Göttingen, 14.02.2016

Alexandra Müller

Science, my lad, is made up of mistakes, but they are mistakes which it is useful to make, because they lead little by little to the truth.

Jules Verne

Table of contents

1	Introduction	4
1.1	The mammalian ear	4
1.1.1	Anatomy of the ear	4
1.1.2	The Cochlea.....	6
1.1.3	The organ of Corti	6
1.1.4	Cochlear hair cells	7
1.1.5	Exocytosis at inner hair cells.....	8
1.1.6	Deafness.....	9
1.2	The ferlin protein family.....	9
1.3	Otoferlin	11
1.4	Interaction partners of otoferlin	13
1.5	Mutations in otoferlin	14
1.6	The “pachanga” mutation in the C ₂ F domain of otoferlin	15
1.7	The Gene Gun method for cell transfection	16
1.8	Aims of this study	18
2	Material.....	19
2.1	Chemicals	21
2.2	Organisms.....	21
2.3	Solutions for molecular biology	22
2.4	Vectors	23
2.5	Media and solutions for culturing.....	23
2.6	Solutions for immunohistochemistry.....	24
2.7	Solutions for SDS polyacrylamide gel electrophoresis and Western Blot	25
3	Methods.....	28
3.1	Molecular biology.....	28

3.1.1	Overview of cloning of mutated otoferlin constructs	28
3.1.2	Cloning of pEGFPN1mOtof delC ₂ A.....	35
3.1.3	Cloning of pEGFPN1mOtof delC ₂ B.....	37
3.1.4	Cloning of pEGFPN1mOtof delC ₂ C.....	39
3.1.5	Cloning of pEGFPN1mOtof delC ₂ F.....	42
3.1.6	Cloning of constructs containing a point mutation in otoferlin	45
3.1.7	Cloning of pEGFPN1mOtof RXR and pcDNA3mOtof RXR I515T	48
3.2	Kits.....	51
3.3	HEK cell culturing.....	52
3.4	Cycloheximide procedure for HEK cells	53
3.5	Gene Gun.....	54
3.6	Immunohistochemistry and Immunocytochemistry.....	55
3.7	Fluorescence Microscopy and image analysis	56
3.8	Proximity Ligation Assay.....	57
3.9	RNA-Isolation and generation of cDNA from organs of Corti	58
3.10	Real-Time PCR.....	60
3.11	Polyacrylamide gels and Western Blot of HEK cell lysates.....	61
4	Results.....	63
4.1	The mRNA level in <i>Otof</i> ^{#515T/I515T} mice is not reduced compared to wild type mice	63
4.2	HEK cells were transfected with otoferlin constructs.....	64
4.3	Western Blots with transfected HEK cell lysates	67
4.4	Immunostainings of organs of Corti from HA sumo mice.....	68
4.5	Proximity ligation assay to check for possible interaction partners of otoferlin.....	70
4.6	Measuring the reduction of wild type and mutated otoferlin protein over 2h via mass spectrometry showed little difference	77
4.7	Measuring the reduction of wildtype otoferlin and otoferlin I515T protein over 24h using mass spectrometry showed little difference	80
4.8	Differences between mouse and human otoferlin.....	82
4.9	Biolistic transfection of inner hair cells using different forms of otoferlin.....	84

5 Discussion..... 99

5.1 Determined mRNA levels in organs of Corti from *Otof*^{#515T/I515T} mice show no reduction in comparison to mRNA of wild type mice 100

5.2 Otoferlin protein as well as the temperature sensitive forms are not degraded by a proteasomal mechanism 100

5.3 Otoferlin is unlikely to be sumoylated 103

5.4 Gene Gun transfection could be successfully established for inner hair cells in our lab 104

5.5 It seems that a small amino acid stretch including a RXR motif is the reason for the I515T phenotype 106

5.6 Proximity ligation assay could not be established for use in inner hair cells 108

5.7 The otoferlin C₂F domain apparently plays a role for plasma membrane localization 110

5.8 Summary 112

References 113

Acknowledgements..... **Fehler! Textmarke nicht definiert.**

Appendix 121

1 Introduction

Mankind has been interested in our senses and how they function for a very long time. Already Aristotle in his work “De Anima” was thinking about our senses. Although he postulated that there are only five senses, namely sight, hearing, taste, smell and touch, which is not correct from today’s perspective, he nevertheless drew the conclusion that we have more than one sense so that we do not miss out on information. If we now confer his statements to today’s environment we could imagine the following situation. While having a nice dinner in the evening we see the person next to us, we hear music, we first smell and then taste the food. All the impressions sum up to a big picture in the end which can be impaired by just one sense missing. For instance, without the sense of hearing communication would be much harder, dangers for example those of traffic could not be detected that fast and we wouldn’t know the true pleasure of music.

1.1 The mammalian ear

1.1.1 Anatomy of the ear

The ear is subdivided into three parts called outer ear, middle ear and inner ear. Only the outer ear is visible whereas the other two parts are located inside the temporal bone. The outer ear consists of the pinna, the external ear canal and the tympanic membrane and is responsible for funneling the sound. Additionally the outer ear helps to localize sound coming from front, back, top or bottom but has no influence on the localization of sound from left or right (Heffner and Heffner, 2008). For this binaural hearing the detection of small differences in time and intensity coding is needed.

The middle ear is composed of the three smallest bones in the human body, malleus, incus and stapes, which can be summarized as ossicles. They are responsible for impedance matching between two media: air, having low impedance, and a non-compressible fluid with higher impedance, thus ensuring the transmission from sound from the outer ear to the inner ear. The middle ear increases the sound pressure using the leverage of the three ossicles for focusing the energy from the tympanic membrane onto the much smaller oval window of the cochlea (compare Fig. 1.1 A).

The inner ear is separated into the semicircular canals which are of great importance for balance and the cochlea. Inside the cochlea the organ of Corti as the organ of hearing is localized. Both parts of the inner ear rely on hair cells for detection of information.

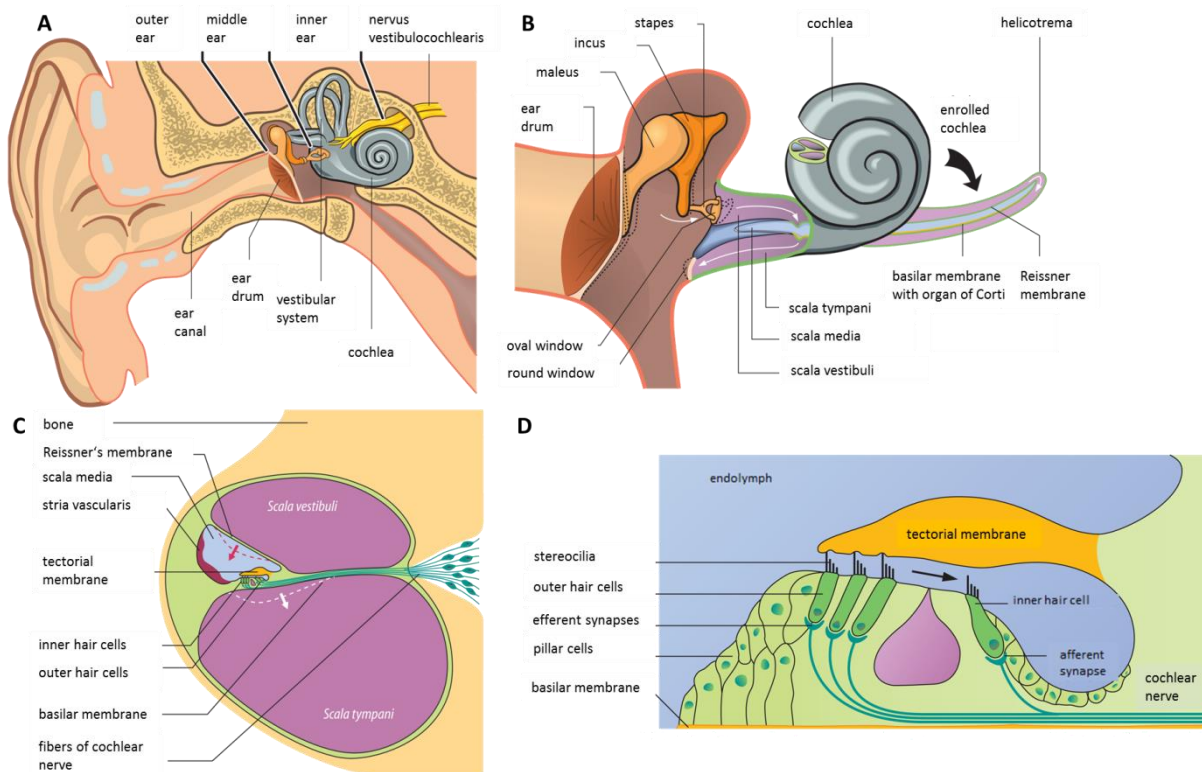


Figure 1.1: Drawings of the anatomy of the inner ear. **A)** The ear is separated into outer ear, middle ear and inner ear, the latter contains the vestibular system and the cochlea. **B)** The organ of Corti, on the one hand inside the cochlea and on the other hand enrolled is shown. **C)** The localization of the organ of Corti with outer hair cells and inner hair cells is depicted. **D)** The organ of Corti with tectorial and basilar membrane. Adapted from Schmidt/Thews, 1997

1.1.2 The Cochlea

The cochlea (compare Fig. 1.1 B) is composed of three fluid filled canals, namely scala tympani, scala media and scala vestibuli. In the scala media the organ of Corti is localized. Scala tympani as well as scala vestibuli are filled with perilymph whereas scala media is filled with endolymph. These two fluids differ regarding their ion concentrations. Endolymph is a high potassium solution whereas perilymph has a high sodium concentration. This difference plays an important role in the transduction of sound from the organ of Corti to the brain. Scala tympani and scala vestibuli are separated from scala media by the basilar and the Reissner's membrane, respectively. At the apex of the organ of Corti scala tympani and scala vestibuli are linked via the helicotrema. The human organ of Corti winds inside the cochlea about two and a half turns and is accompanied by the stria vascularis, a tissue rich in blood vessels which maintains the ion concentration of the endolymph (compare Fig. 1.1 C).

The third ossicle of the middle ear, the stapes, has contact to the oval window and transports the mechanical impulse from the ossicles to the fluid filled inner ear. The vibration of the ossicles is thus transmitted to the perilymph of the scala vestibuli and results in a pressure wave, called a travelling wave. The position of the travelling wave's maximum deflection within the cochlea depends on its frequency. Low frequency sounds lead to a maximum near the apex whereas high frequency sounds result in a maximum which is located near the base. This fact leads to tonotopic organization in the auditory pathway. The organ of Corti of mice has 1.75 turns and the detectable sounds range from 1 to 100kHz whereas the organ of Corti of humans is longer and can detect sound from 10Hz to 20kHz (Fettiplace and Hackney, 2006).

1.1.3 The organ of Corti

Our hearing organ, the organ of Corti, is situated on top of the basilar membrane. It consists of different cell types all having specific functions. Most important for hearing are the outer hair

cells, which can be found in three rows and the inner hair cells which only consist of one row. Both types are running the full length of the cochlea. Other cell types like pillar cells or Deiter's cells mechanically support the hair cells or maintain their ion homeostasis.

1.1.4 Cochlear hair cells

The hair cells in general are required for signal amplification and for converting the mechanical sound stimulus to an electrical signal. Outer hair cells mainly increase the amplitude of the deflection of the basilar membrane, while inner hair cells together with their synapses and spiral ganglion neurons are responsible for sound coding. In humans about 12,000 outer hair cells and 3,500 inner hair cells can be found (Dallos, 1992). Both types of hair cells possess so called stereocilia, long extensions on the apical part. Stereocilia of the outer hair cells are in direct contact with the tectorial membrane, unlike those of the inner hair cells (compare Fig. 1.1 D). Sound stimuli result in vertical vibration of the basilar membrane which lifts and lowers the organ of Corti. This in turn leads to a shearing force between the hair bundles of the outer hair cells and the tectorial membrane. Subsequently the fluid flow causes a deflection of the stereocilia of outer hair cells which in turn leads to opening of mechano-electrical transduction channels in the tips of the stereocilia. In consequence, potassium can enter the cell and depolarize it.

The lateral membrane of the outer hair cells is densely packed with prestin, a protein which has the ability to alter its conformation depending on the voltage (Oliver et al., 2001). Those conformational changes lead to contraction when the cell is depolarized and to elongation in hyperpolarized state (Kachar et al., 1986). This mechanism is required for the signal amplification in the cochlea (Liberman et al., 2002).

The movement of the oscillating outer hair cells is transferred back to the basilar and tectorial membrane and also to the fluid-filled interspace surrounding the organ of Corti. Movement in the endolymph leads to deflection of the inner hair cells' stereocilia. Same as in outer hair cells,

transduction channels open and because the endolymph is potassium rich, K^+ enters the cell through mechano-electrical transduction channels causing a depolarization. The depolarization leads to the opening of voltage-gated Ca^{2+} channels at the inner hair cell active zone, located at the basal part of an inner hair cell.

1.1.5 Exocytosis at inner hair cells

The active zone contains the ribbon synapse, the type of synapse present in sensory hair cells. The opening of voltage-gated Ca^{2+} channels leads to an influx of Ca^{2+} in the cell and to Ca^{2+} dependent exocytosis of glutamate filled vesicles at the ribbon synapse. Glutamate is detected by postsynaptic bouton-like terminals of SGN; the SGN depolarizes via activation of α -amino-3-hydroxy-5-methyl-4-isoxazole propionic acid (AMPA) receptors (Matsubara et al., 1996; Glowatzki and Fuchs, 2000). This leads to an action potential (AP) which is transmitted to the brain. Depending on the stimulus frequencies, action potentials in different hair cells are evoked and different auditory nerve fibers are stimulated.

A striking feature of the inner hair cells is a specialized synapse, the so called ribbon synapse. Additionally, these synapses function with a different compilation of proteins than other types of synapses. Conventional synapses depend on N-ethylmaleimide-sensitive factor attachment protein receptor (SNARE) complexes; the main proteins are SNAP-25, syntaxin-1 or -2 and synaptobrevin. The Ca^{2+} sensor for fast exocytosis at the central synapse is synaptotagmin-1 or -2 (Geppert et al., 1994). Already in 1999 it was shown that synaptotagmins 1–3, synaptophysin, and synapsin are absent from the inner hair cell synapse (Safieddine and Wenthold, 1999). Additionally, it was shown in 2011 that exocytosis at the hair cell ribbon synapse operates without SNARE proteins (Nouvian et al., 2011). It seems that this synapse has a different protein composition which includes otoferlin, a multi C_2 domain protein which is needed for exocytosis (Roux et al., 2006; Pangršič et al., 2012).

1.1.6 Deafness

Hearing impairment is a frequent sensory deficit. As much as one in thousand children is affected by severe to profound hearing impairment at birth. The same number becomes deaf before they reach adulthood (Morton, 1991). Half of the occurring hearing loss, can be attributed to genetic reasons; which can be subdivided into two main categories. 10% of the patients are affected by syndromic hearing loss whereas 90% suffer from a non-syndromic form of hearing loss which does not coincide with other symptoms. For the latter different types, such as DFNA (autosomal dominant form), DFNB (autosomal recessive form) and DFNX (X-chromosomal form) are known. 60 genes so far can be linked to DFNB (www.hereditaryhearingloss.org). One of those genes is otoferlin which causes DFNB9 (Yasunaga et al., 1999). Mutations of otoferlin lead to an incorrectly transmitted auditory signal to the brain which in turn results in severe to profound hearing loss (Marlin et al., 2010).

1.2 The ferlin protein family

Ferlins are a family of large proteins (~200 – 240kDa) playing a role in vesicle fusion as well as membrane trafficking and exocytosis. In mammals six ferlin genes (Fer1L1 – L6) are encoded. The first three have the synonyms dysferlin, otoferlin and myoferlin, respectively. The six ferlins can be subdivided into two groups according to the absence or presence of a DysF domain, the function of which is not yet clear (Patel et al., 2008; Sula et al., 2014). Type-I ferlins, having a DysF domain, are dysferlin, myoferlin and Fer1L5. Otoferlin, Fer1L4 and Fer1L6 are lacking the DysF domain and are accordingly classified as type-II ferlins. Ferlins have five to seven so called C₂-domains which are characteristic for this protein family. Additionally, all ferlins include a unique domain called the Fer domain (compare Fig. 1.2) the function as well as structure of which are not yet unraveled (Lek et al., 2010). While mutations in otoferlin and myoferlin can lead to different diseases, inherited form of profound, non-syndromic deafness (DFNB9) and

limp-girdle muscular dystrophy type 2B respectively (Liu et al., 1998; Yasunaga et al., 1999), no disease-causing mutations were identified for dysferlin, Fer1L4, Fer1L5 or Fer1L6 yet.

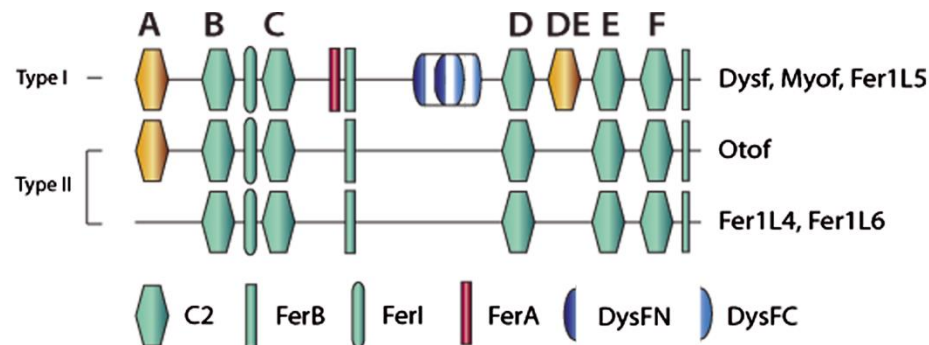


Figure 1.2: Domain topologies of mammalian ferlins: Ferlins of type I contain additionally FerA and FerB domains which are missing in ferlins of type II. Green: conserved features of all six ferlins, yellow: unique features. The DysF domain is separated into inner and outer part (adapted from Lek et al., 2010)

Scientists took an insight in the tissue-specific expression, sub-cellular localization and endocytic trafficking of human ferlins (Redpath et al., 2015). They overexpressed all ferlins except Fer1L4 in HEK293, Cos-7 cells and C2C12 myoblasts for localization studies. It turned out that dysferlin, myoferlin and Fer1L6 are plasma membrane ferlins, contrasting otoferlin, which predominantly localizes in intracellular compartments. The localization of otoferlin close to the membrane seems to be very important for hearing. It was shown in deaf *Otof^{ppga/pgga}* mice, which have a point mutation in the C₂F domain, that the otoferlin membrane staining is greatly reduced (Pangrsic et al., 2010) (see also section 1.6).

In HEK cells, dysferlin localizes to the plasma membrane and to endosomal vesicles (Evesson et al., 2010), whereas myoferlin only localizes to the plasma membrane (Bernatchez et al., 2009), otoferlin is predominantly intracellular (Redpath et al., 2015) and only at a very low level on the plasma membrane (compare Fig. 1.3). Getting even more into detail it was shown that myoferlin and dysferlin colocalize with markers for the secretory pathway and endosomes. Otoferlin in contrast shows colabelling with markers for the trans-golgi network.

Mutations or absence of certain ferlins have severe consequences. The ferlin in *Drosophila*, called misfire, plays a role in fertilization and embryonic development. Males with mutant misfire show defects in sperm plasma membrane breakdown post fertilization (Ohsako et al., 2003) whereas it was observed for females that some show abnormal egg markings. Those embryos behave abnormal in mitosis and development (Smith and Wakimoto, 2007). Fer-1 mutants in *C. elegans* are infertile (Achanzar and Ward, 1997).

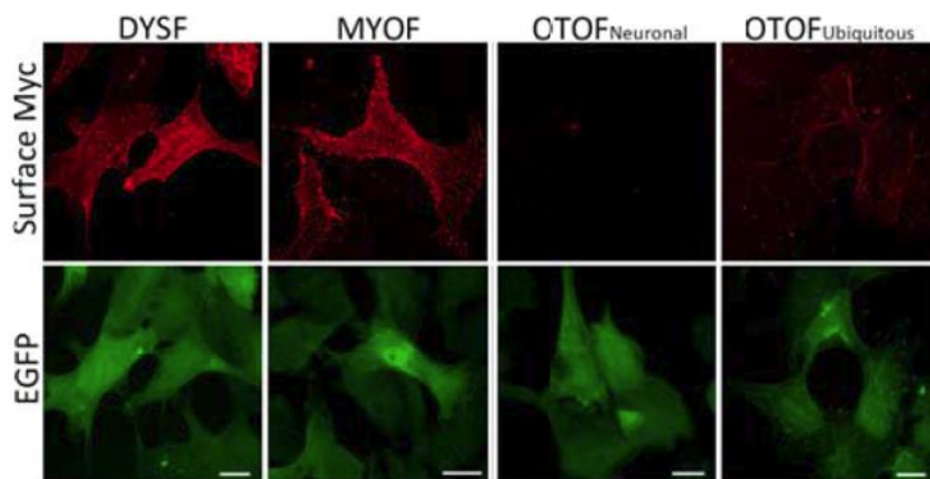


Figure 1.3: Surface labelling of different human ferlins. Using C-terminal α -Myc Tag, which is luminal for intracellular and extracellular for ferlins in the plasma membrane, HEK293 cells were labeled. Dysferlin and myoferlin are abundantly expressed at the surface, neuronal form of otoferlin is not expressed at the surface at all whereas otoferlin_{ub} is expressed in low amounts. Scale bars: 10 μ m (adapted from Redpath et al., 2015)

1.3 Otoferlin

Otoferlin, a ~220kDa protein and a member of the ferlin protein family consists of six C₂-domains (compare Fig. 1.4), C₂A to C₂F. A seventh C₂ domain between C₂D and C₂E, called C₂de is predicted but the similarity between this domain and other C₂-domains is very low compared to the similarity between C₂-domains among each other.

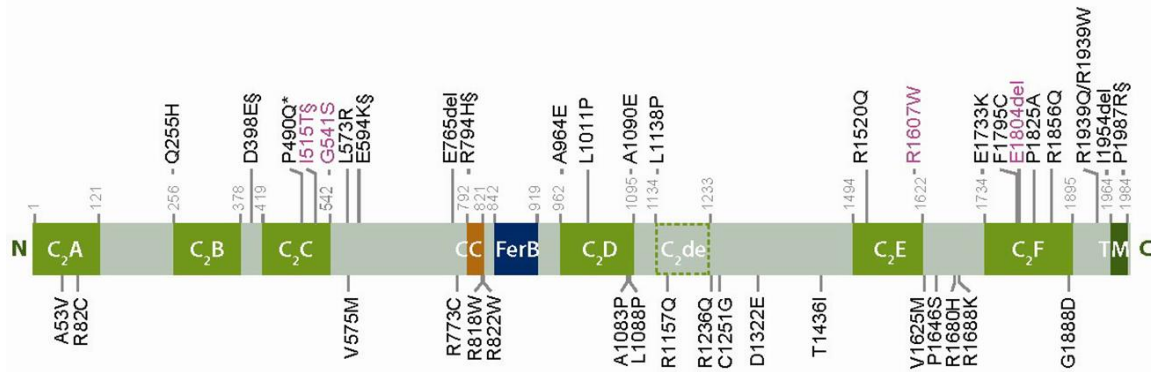


Figure 1.4: Protein domain structure of otoferlin showing all C₂ domains, the coiled coil domain (CC), a ferlin-specific motif (FerB) domain in the middle of the protein and the transmembrane domain (TM) at the C-terminus. Mentioned on top are pathogenic missense mutations and in frame deletions, on the bottom sequence variants. Mutations shown in purple have been associated with temperature sensitive hearing loss. (Taken from Pangršič et al., 2012)

The investigation of a generated otoferlin knockout mouse resulted in first ideas of the function of otoferlin (Roux et al., 2006). Although the number of ribbon-associated as well as docked vesicles is normal in these mutants, a great reduction in Ca²⁺ dependent exocytosis could be observed. From this it was concluded that otoferlin is fundamental for a late step of exocytosis (Roux et al., 2006), compare also Fig. 1.5). Inner hair cells of otoferlin knock out mice show spontaneous transmitter release as well as no detectable Ca²⁺ triggered exocytosis (Roux et al., 2006; Pangrsic et al., 2010). Apart from the inner hair cells, otoferlin can also be found in immature outer hair cells as well as in type I hair cells of the vestibular system, where it is important for synaptic exocytosis (Beurg et al., 2008; Dulon et al., 2009). Immunogold electron microscopy experiments from Roux et al. revealed, that otoferlin is localized to synaptic vesicles and the plasma membrane (Roux et al., 2006; Pangrsic et al., 2010) which would be similar to the localization of synaptotagmin. So far otoferlin is believed to function as a synaptotagmin-like Ca²⁺ sensor for fusion in inner hair cells (Roux et al., 2006) although this has not yet been demonstrated. Additionally, the investigation of an otoferlin mutant mouse line called “pachanga” raised the idea that otoferlin could play a role in vesicle replenishment and priming (Pangrsic et al., 2010). So far only of the C₂A domain the crystal structure was solved (Helfmann et al., 2011) and proved to not bind Ca²⁺ (Johnson and Chapman, 2010; Helfmann et al., 2011).

1.4 Interaction partners of otoferlin

Studies of otoferlin also include the identification of possible interaction partners of otoferlin. So far a few proteins are identified which seem to interact with otoferlin. It was shown that otoferlin directly interacts with syntaxin 1A, SNAP-25 and the L-type voltage gated Ca^{2+} channel $\text{Ca}_v1.3$ (Ramakrishnan et al., 2009). However, later studies revealed that SNARE proteins are absent in inner hair cells (Nouvian et al., 2011). Two other stated interaction partners are myosin6 (Roux et al., 2009) and Rab8b GTPase (Heidrych et al., 2009, 2008). Another proposed interaction partner of otoferlin is adapter protein complex 2 (AP-2) (Duncker et al., 2013; Jung et al., 2015). AP-2 is essential for coated-vesicle formation (Keyel et al., 2008; Rappoport, 2008) and it was stated that otoferlin and AP-2 interact in mature inner hair cells (Jung et al., 2015). Otoferlin is present in low amounts in the brain as well. It was shown that it interacts in the brain with Ergic2 (Endoplasmic reticulum-Golgi intermediate compartment protein 2), a protein with still unknown function (Zak et al., 2012).

However, none of these publications investigated an interaction in the inner hair cell itself but used different assays like surface plasmon resonance, pull-down and yeast two-hybrid assays. An examination whether these interactions take place in the inner hair cells as well would be meaningful.

Two promising candidates for an interaction with otoferlin were dynamin and OPA1 (optic atrophy protein, a dynamin like GTPase). Both were, amongst other proteins, identified in pull-down assays using mouse brain (performed by Sandra Meese (Molecular Structural Biology, Ralf Ficner) and Sunit Mandad (Bioanalytical Mass Spectrometry Group)). OPA1 is a dynamin-like protein, which can be related to auditory neuropathy as well (Santarelli et al., 2015). For dynamin the localization in inner hair cells was shown already using immunofluorescence stainings (Neef et al., 2014). Dynamin-1 together with clathrin seems to play a role in membrane retrieval (Neef et al., 2014).

1.5 Mutations in otoferlin

Research is directed at the different mutations that can occur in otoferlin and in identifying new ones. Silent mutations on the level of nucleotides happen quite often but either do not change the amino acid sequence or do change it to a similar amino acid, where the function of the protein is preserved. Some mutations lead to a premature stop codon which results in a shorter form of the protein, those mutations are then called “nonsense” mutation. If the stop codon is located close to the C-terminus the protein could still be at least partially functional. The earlier such a mutation occurs, the more likely it is that the protein is not functional. In another mutation form, parts of the nucleotide or amino acid sequence are deleted. The smaller the deleted protein sequence the more likely it is that the protein remains functional to some extent whereas a deletion of a single nucleotide causes a frameshift which changes the whole amino acid sequence. The most frequent is the so called “Spanish mutation” which, after the transition from cytosine to thymine, results in a premature stop codon at position 829 (Q829X) (Migliosi et al., 2002).

While most mutations in otoferlin lead to profound prelingual deafness, some mutations are known to cause different phenotypes. An interesting form of deafness is a transient form of hearing-loss, occurring when the patients’ core body temperature rises by as little as 1°C (Starr et al., 1998), for example because they become febrile or do sports. When the body temperature decreases again, the hearing status of affected patients returns to the previous level with a time lag of three to four days (Marlin et al., 2010). So far six of those temperature sensitive mutations have been described, all induced by an in frame mutation and a substitution of an amino acid or an amino acid deletion causing an in frame deletion. The described temperature-sensitive mutations are I515T (Varga et al., 2006b), G541S (Matsunaga et al., 2012), G614E (Romanos et al., 2009), R1080P (Romanos et al., 2009) R1607W (Wang et al., 2010) and E1804del (Marlin et al., 2010), and with compound heterozygosity for G614E and R1080P. In patients pure tone audiometry showed normal hearing to mild hearing impairment

at normal body temperature but severe to profound hearing impairment at a temperature of 38°C (Marlin et al., 2010). I515T and G541S mutation are located in the C₂C domain, R1607W in the C₂E domain and E1894del in the C₂F domain. Since those mutations affect different domains of the protein, it will be interesting to find out whether they share the same general mechanism like fast degradation or heat instability.

1.6 The “pachanga” mutation in the C₂F domain of otoferlin

The C₂F domain of otoferlin already was the subject of intensive studies. The interest was raised because a mutation called “pachanga” (pga) was found in this domain. Mice having this mutation, *Otof*^{pga/pgs}, were profoundly deaf (Schwander et al., 2007; Pangrsic et al., 2010). In comparison with normal hearing wild type mice and *Otof*^{-/-} mice, the latter also being profoundly deaf, differences could be observed (compare Fig. 1.5). In immunofluorescence stainings the otoferlin level in *Otof*^{pga/pgs} mice shows a strong reduction compared to the wild type, whereas staining is completely missing in *Otof*^{-/-} mice (compare Fig. 1.5, B). Apart from an overall reduction of otoferlin staining in the inner hair cells of *Otof*^{pga/pgs} mice it is visible, that the membrane staining is strongly reduced. In *Otof*^{-/-} mice exocytosis is nearly absent. In contrast in *Otof*^{pga/pgs} mice at least fusion of the readily-releasable pool seems to be intact, but sustained exocytosis is strongly reduced (compare Fig. 1.5 A). Comparing the results of Ca²⁺ uncaging of mutant to wild type mice, wild type mice show the release of a large pool of vesicles within milliseconds (indicated by black line, compare Fig. 1.5 C). Although the time constant of *Otof*^{pga/pgs} mice is comparable to the one seen in *Otof*^{+/+} mice, the fast component itself is greatly reduced (indicated by arrow, compare Fig. 1.5 C).

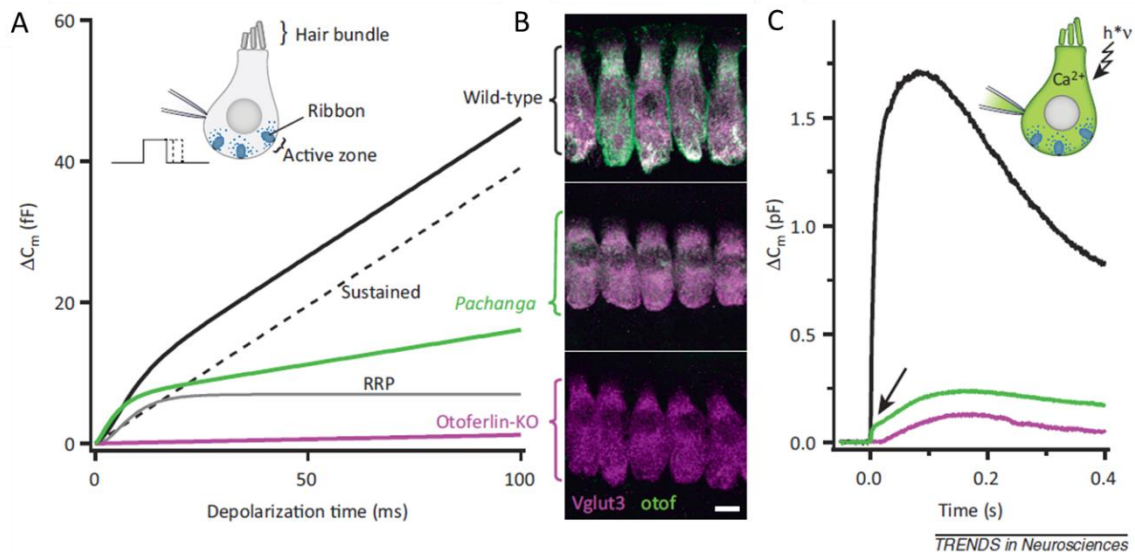


Figure 1.5: Exocytosis and expression of otoferlin in *Otof*^{+/+}, *Otof*^{pga/pga}, *Otof*^{-/-} mice. **A)** Behavior of sustained exocytosis (dashed line) and readily-releasable pool (RRP, grey line) of wild type mice (black) and both mutants (*pga* in green, knock out in purple) after depolarization. **B)** Immunofluorescence staining with α -otoferlin (green) and α -Vglut3 (vesicular glutamate receptor 3, purple) to show expression in inner hair cells, wild type IHCs on top, *pga* IHCs in the middle, otoferlin knockout IHCs on the bottom. **C)** Exocytosis upon Ca^{2+} uncaging (adapted from Pangršič et al., 2012)

1.7 The Gene Gun method for cell transfection

Different ways for transfecting cells like lipofection (for example using Lipofectamine®, Thermofisher) exist, but none of them proved successful so far for transfecting cochlear inner hair cells (Kirsten Reuter-Jessen and Ellen Reisinger, personal communication).

So far it has been shown that inner hair cells can be genetically manipulated by virus transfection and it was efficient for adeno-associated virus (AAV) serotype 1/2, adenovirus (Ad) serotype 5 and lentivirus (Luebke et al., 2001; Bedrosian et al., 2006). Otocyst as well as postnatal injection of mice ranging between p3 to around p14 has been established in our laboratory (Reisinger et al., 2011; Jung et al., 2015), both methods depend on the usage of AAV virus and lead to transfected inner hair cells in varying number. Unfortunately AAV virus has a

restricted capacity of roughly 2.5kb – 3kb which is smaller than the size of otoferlin (~6kb). Moreover, production of AAVs is laborious and usually takes several weeks of time.

A relatively new transfection method is the Gene Gun or biolistic (neologism combining bio and ballistic) transfection, invented by Nelson Allen, John Sanford and Ed Wolf (Klein et al., 1987; Sanford et al., 1987). Originally designed to infect plant cells, it uses helium pressure and cDNA coated gold or tungsten particles for transfection. Particles of varying size are coated with the desired cDNA and those gold particles are shot into the tissue of interest. Transfection of *Drosophila* embryos (Baldarelli and Lengyel, 1990), HEK293 and HeLa cells (O'Brien et al., 2001), larvae of *Bombyx mori* (Thomas et al., 2001) and bullfrog sacculle (Zhao et al., 2012) was proven successful. Thomas et al. self-built a shooting module since the results obtained with the BioRad module were not satisfying. They used coated gold particles and a helium pressure of either 1100psi or 1800psi. However, Baldarelli and Lengyel used tungsten instead of gold particles, the transfection pressure is not noted. Same as Thomas et al., O'Brien et al. modified the BioRad Gene Gun for their purposes. They troubled having either a too high pressure (175psi) thus destroying the cells or lower pressure (50 – 100psi) with low efficiency before modification. After modification the pressure could be decreased and transfections lead to transfected cells. Furthermore, Zhao and colleagues used a self-built setup using common laboratory equipment to reduce helium pressure. They were able to increase the pressure up to 200psi and still observe healthy looking cells. Additionally in all those differences in pressure and further modifications also the preparation of Gene Gun bullets differed regarding carrier (gold or tungsten), particle size (1 μ m – 1.6 μ m in diameter), amount of DNA (4 μ g – 50 μ g) and preparation protocol. It seems that, depending on the tissue that has to be transfected, all the different parameters have to be modified to get satisfying results.

Advantage of Gene Gun transfection over virus transduction are that even large constructs, larger than possible in virus transduction, as well as two constructs in parallel can be used. Furthermore, transfection is relatively cheap and fast.

1.8 Aims of this study

The aim of my PhD project could be separated into three major parts.

First, I was aiming to transfect inner hair cells with a variety of mutated otoferlin constructs. To reach this aim I combined cloning approaches to generate the otoferlin mutants and established biolistic transfection of inner hair cells using Gene Gun.

Secondly, I was interested in the underlying mechanism of temperature sensitive hearing loss. For that purpose I subcloned temperature sensitive otoferlin mutations and compared the protein expression at normal body temperature of 37°C as well as at elevated temperature of 38.5°C. Therefore different approaches such as overexpression of proteins in HEK cells, quantitative Real-Time PCR and immunofluorescence stainings had to be performed to elucidate the effect of temperature on otoferlin.

Third, I was working on the identification of interaction partners of otoferlin by applying proximity ligation assays, a method that serves to visualize protein interaction in inner hair cells. Although interaction partners of otoferlin are identified using different methods, none of those were reviewed if the proteins interact in inner hair cells as well. Since this method was so far not used in our lab, it had to be established.

2 Material

Lab Equipment	
Adjustable pipettes	Brand
Agarose gel electrophoresis chambers	BioRad
Cell incubator Midi 40	Thermo Scientific
Cell incubator HERAcell 150i	Thermo Scientific
Cell incubator HERA cell	Thermo Scientific
Centrifuge Heraeus Fresco 17	Thermo
Centrifuge Heraeus Pico 17	Thermo
Centrifuge 5424R	Eppendorf
Centrifuge Avanti® J-30I	Beckmann Coulter
Electrophoresis Power Supply MP 300V (for agarose gel electrophoresis)	major science
Electrophoresis Power Supply EPS 301 (for Western Blots)	GE healthcare
Gel documentation UV system	INTAS
Helios® Gene Gun	BioRad
Gene Gun Tubing Prep Station	BioRad
Gene Gun Tubing Cutter	BioRad
Microscope Axiovert 40 CFL with HBO 50 lamp	Zeiss
Microscope SP5	Leica
NanoVue plus	GE Healthcare
Real-Time PCR 7500 Sequence detection system	Applied Biosystems
Sonification water bath Transonic 820/H	Elma
Sonification Sonopuls	Brandelin
Sonification Sonifier 250	Branson
Sterile work bench HERA safe	Thermo Scientific
Sterile work bench Safe 2020	Thermo Scientific

Thermocycler My Cycler	BioRad
Thermocycler T100™ Thermal Cycler	BioRad
Thermomixer comfort	Eppendorf
Thermomixer Compact	Eppendorf
Western Blot chemiluminescence detection Chemo Cam	INTAS
Western Blot/SDS gel electrophoresis Mini PROTEAN® 3 cell	BioRad

Kits	
DNA Clean Up Zymoclean™ Gel DNA Recovery Kit	Zymo Research
Gel Extraction Zymoclean™ Gel DNA Recovery Kit	Zymo Research
NucleoBond® PC 100	Machery-Nagel
Plasmid extraction peqGOLD Plasmid Miniprep Kit I	peqlab
Size Standards	
Gene Ruler 100bp Plus	Thermo Scientific
Gene Ruler 1kb Plus	Thermo Scientific
Page Ruler™ Plus prestained	Thermo Scientific
Consumables	
Amersham™ Hybond ECL for Western Blot, nitrocellulose membrane	GE Healthcare
Cell Scaper	Corning
Cell Strainer	Corning
Falcon tubes Cellstar® Tubes	greiner bio-one
Lipofectamine®	Thermofisher
Minisart syringe filters	Sartorius
Petri dishes Cellstar®	greiner bio-one
Polypropylene Round-Bottom Tubes for plasmid isolation	Corning
Syringes	BD plastipak™
Cell culturing	
Cell Tak	Corning

DMEM	Gibco
DMEM/F-12	Gibco
DPBS (1x)	Gibco
HBSS (1x)	Gibco
HEPES buffer solution 1M	Gibco
HI NBCS	Gibco
Lipofectamine® 2000	Invitrogen
OptiMEM	Gibco
Penicillin/Streptomycin 5,000units each	Gibco
Trypsin 0.25% EDTA (1x)	Gibco
Western Blotting Substrate Pierce® ECL Plus	Thermo Scientific

2.1 Chemicals

Used chemicals were provided from Serva, Roth, Sigma or Invitrogen. Unless a district company was preferred the chemicals with the lowest prize were chosen.

2.2 Organisms

For mouse experiments different mouse strains were used; wild type mice C57/Nbl6, *Otof*^{-/-} *Otof*^{f515T/1515T} and *His6-HA-SUMO1* mice. Animal handling and experiments complied with national animal care guidelines, and were approved by the University of Göttingen Board for animal welfare and the animal welfare office of the state of Lower Saxony.

For HEK cell experiments HEK293T cells were used.

2.3 Solutions for molecular biology

11.1x PCR Buffer

45mM	Tris-HCL pH 8.8
11mM	ammonium sulphate
4.5mM	MgCl ₂
6.7mM	2-mercaptoethanol
4.4μM	EDTA pH 8.0
1mM	of each dNTP
113μg/ml	BSA

50x TAE Buffer

0.4M	Tris
0.4M	pure acetic acid
10mM	EDTA pH 8.0
ad 1l	H ₂ O

DNA Loading Dye

50%	Glycerol
1mM	EDTA pH 8.0
0.15%	Bromphenol Blue

2.4 Vectors

Following vectors were used for cloning. All vectors already contained mOtoferlin as an insert which was not inserted by myself. The vector pBlueScript was used without any insert as well.

pBlueScript KS(-)	Agilent Technologies
pcDNA3	Invitrogen
pEGFPN1	Clonotech

2.5 Media and solutions for culturing

Medium for culturing HEK cells

89%	DMEM media
1%	Penicillin/Streptomycin (final concentration 10µg/ml)
10%	NBCS

Culturing organs of Corti

Medium

95%	DMEM/F-12 media
5%	NBCS

Cell Tak

For allowing the attachment of biolistic transfected organs of Corti to the surface of a cover slip those were coated. Cell Tak was mixed in a ratio of 1:6 to 1:10, depending on the vial, with

0.1M NaHCO₃ (pH 8.0) buffer. The mixture was incubated until bubbles began to form. 14µl were pipetted on a coverslip and let dry.

2.6 Solutions for immunohistochemistry

PBS (Phosphate Buffered Saline)

140mM	NaCl
8mM	Na ₂ HPO ₄
2.7mM	KCl
1.5mM	KH ₂ PO ₄

PB (Phosphate Buffer)

240mM	Na ₂ HPO ₄ H ₂ O
-------	---

GSDB/DSDB (goat serum dilution buffer/donkey serum dilution buffer)

16%	normal goat serum/normal donkey serum
450mM	NaCl
0,3%	Triton X-100
20mM	phosphate buffer, pH 7,4

Wash Buffer

450mM	NaCl
20mM	phosphate buffer
0,3%	Triton X-100

Mowiol Mounting Medium

2.4g Mowiol 4-88 were dissolved into 6g glycerol and 12ml H₂O_{bidest} were added. The solution was stirred for several hours at room temperature. Subsequently 0.2M Tris pH8.5 was added and the solution was heated for 1-2h at 50°C. After Mowiol was dissolved the solution was centrifuged (500g, 15min) and 2.5% DABCO was added. Mounting medium was stored at -20°C for longer storage, for short time storage it was kept at 4°C.

2.7 Solutions for SDS polyacrylamide gel electrophoresis and Western Blot

Composition of SDS polyacrylamide gels

For 5ml running gel and 1ml stacking gel the following mixtures were used:

Running gel 6%

H ₂ O	2.6ml
30% Acrylamid (Rotiphorese® Gel 30 (37,5:1))	1ml
1.5M Tris (pH 8.8)	1.3ml
10% SDS	50µl
10% ammonium persulfate	50µl
TEMED	4µl

Stacking gel 5%

H ₂ O	680µl
30% Acrylamid (Rotiphorese® Gel 30 (37,5:1))	170µl
1.5M Tris (pH 6.8)	130µl
10% SDS	10µl
10% ammonium persulfate	10µl
TEMED	1µl

2x Laemmli sample buffer

50mM	Tris pH 6.8
2%	SDS
0.1%	Bromophenolblue
10%	87% glycerin
ad 90ml	H ₂ O _{dest}

Directly before use 800µl buffer were mixed with 200µl 1M DTT.

Running buffer

25mM	Tris-HCl
192mM	Glycine
0.1%	SDS

Transfer buffer

25mM	Tris-HCl
192mM	Glycine
20%	Methanol

Ponceau S staining solution

0.2%	Ponceau S
5%	acetic acid
190ml	H ₂ O _{dest}

Blocking solution

5%	skimmed milk powder
diluted in PBS	

PBS (Phosphate Buffered Saline)

140mM	NaCl
8mM	Na ₂ HPO ₄
2,7mM	KCl
1.5mM	KH ₂ PO ₄

Coomassie staining solution

2.5g	Brilliant Blue
475ml	EtOH
100ml	acetic acid
425ml	H ₂ O

The bottle was kept light protected at room temperature, the solution could be reused.

3 Methods

3.1 Molecular biology

3.1.1 Overview of cloning of mutated otoferlin constructs

Since the importance and the role of a single C₂ domain of otoferlin is not yet clear I generated otoferlin deletion constructs with a single missing C₂ domain using site directed mutagenesis by overlap PCR (Ho et al., 1989). With that constructs it should be possible to investigate correct folding by transfecting and staining transfected HEK cells with each construct. Additionally, the distribution inside an inner hair cell using biolistic transfection and subsequent immunofluorescence staining can be observed. With the help of site directed mutagenesis and overstretching primers it is possible to amplify a DNA section without a certain sequence and thus receive a shorter construct. An overview of the general workflow for generating the deletion constructs is shown in Fig. 3.1, deviations are mentioned in the sections explaining the cloning of a certain construct. To visualize the obtained product a vector map is depicted. The sequences of C₂ domains were chosen according to the sequences predicted by Jiménez and Bashir, 2007 with exception of the C₂A domain the sequence of which was determined using Helfmann et al., 2011.

Cloning strategy and primer design were performed with the help of *Gentle*. Sequence was checked for correctness using *Gentle* and NCBI tool *blast*. To delete a C₂ domain it was usually started with two so called adapter PCRs. For those, suitable primers were used. Each pair consisted of one overstretching primer together with a primer that bound upstream or downstream of a chosen enzyme cutting site, matching with the orientation of the overstretching primer of course. The sequences of the overstretching primers were complementary so that they did align together in the following so called overlap PCR (Ho et al.,

1989). The two cleaned products obtained in the previous adapter PCRs were mixed together and supplemented with common PCR ingredients. The used PCR programs are mentioned in the respective section. The product from the overlap PCR was cleaned and blunt subcloned into pBlueScript vector. The vector was transformed into XL1Blue cells. Colony PCRs were performed on the next day using the non-overstretching primers from the respective previous adapter PCRs. The whole PCR mix was loaded on an agarose gel to check for insert containing colonies. With those a plasmid preparation was performed. Three preparations were sent for sequencing. In case of correct sequence insert-containing pBlueScript vector was digested using the enzymes previously chosen. The final vector pEGFPN1mOtof was digested using the same enzymes. Using a common ligation mixture, insert (obtained in overlap PCR) and vector (pEGFPN1mOtof) were ligated together. The product was transformed in XL1Blue cells and plasmid preparation was performed subsequently. Three plasmids were again sent for sequencing.

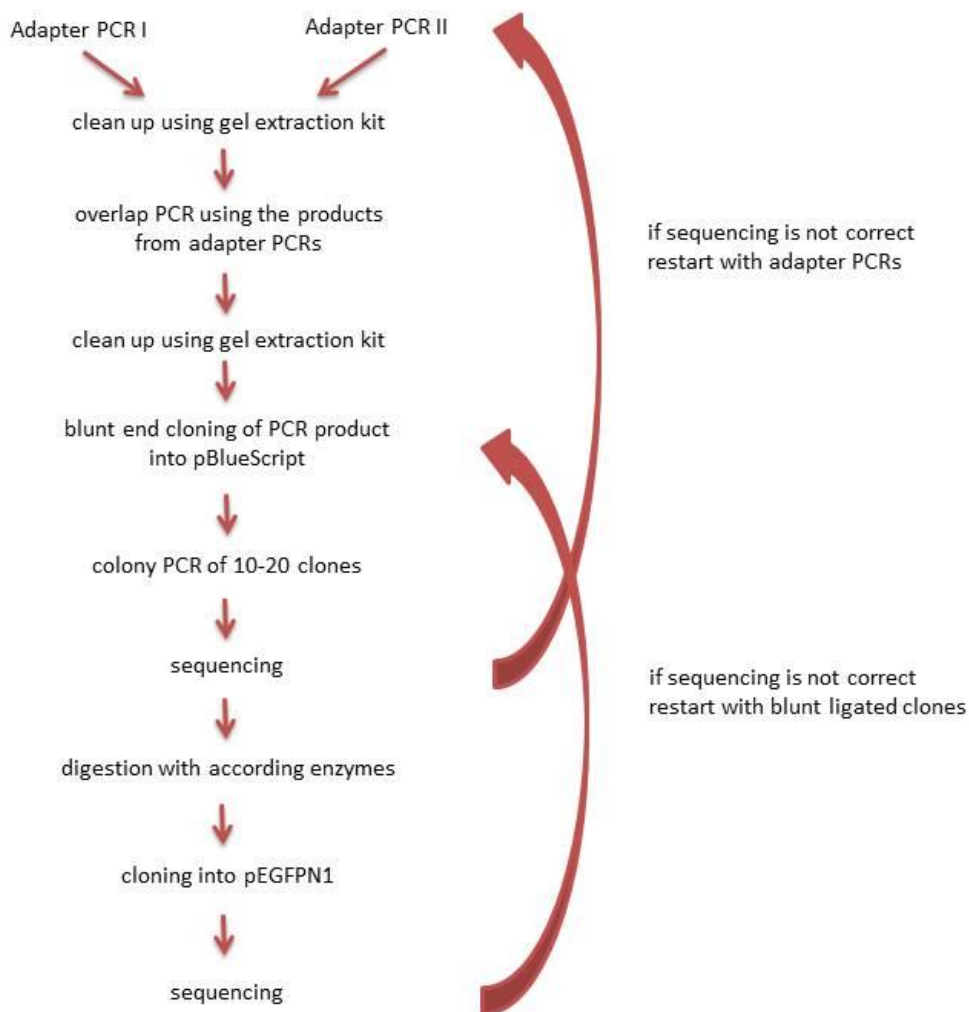


Figure 3.1: Overview of the used cloning strategy for obtaining mutated otoferlin constructs

Mixtures, programs and procedures which were used without change for the generation of all C₂ domain deletion constructs are mentioned below. All used enzymes and buffers were obtained from Thermo Scientific.

Constructs with otoferlin point mutations were cloned into pcDNA3mOtof vector. For the generation of constructs with an additional RXR motif pBlueScript mOtof vector was needed.

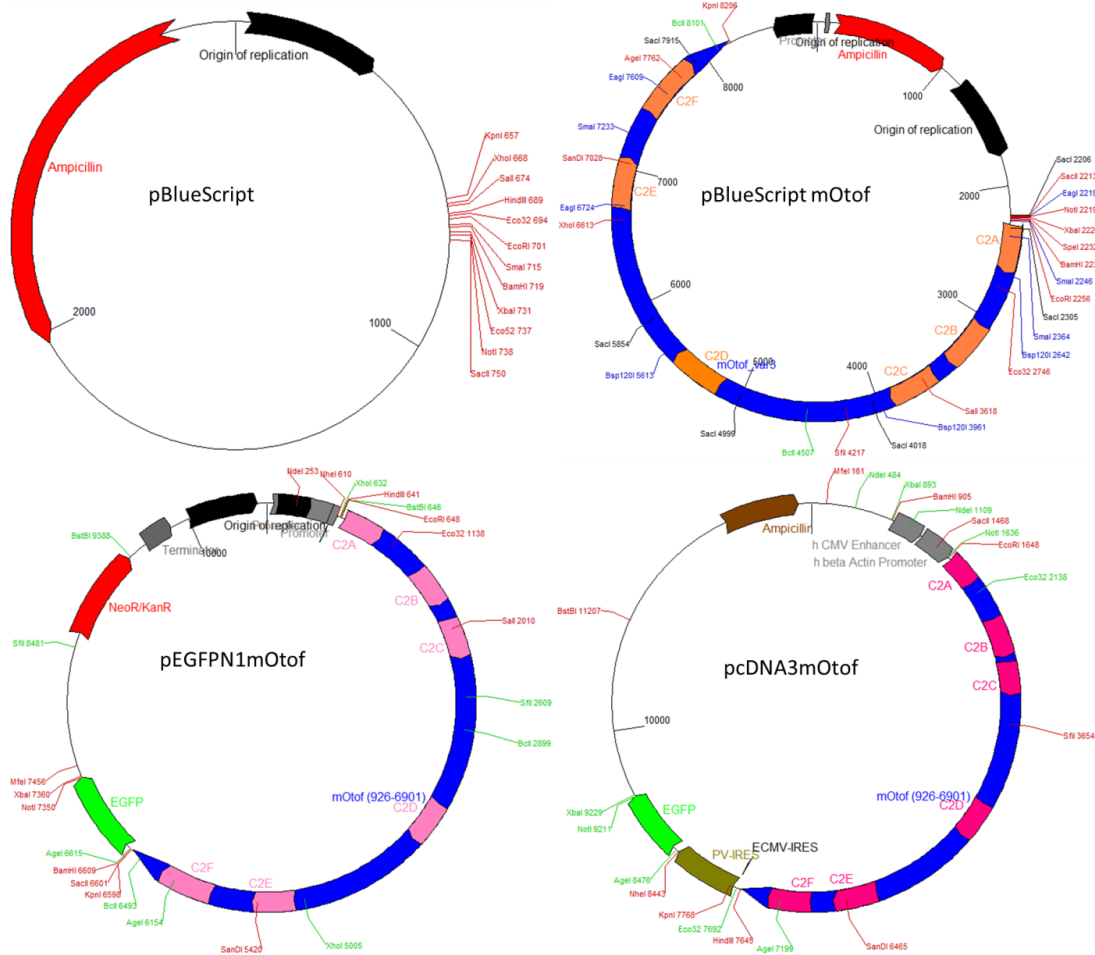


Figure 3.2: Depicted are the four used vectors, with the main enzyme restriction sites, for generation of used constructs in this work

Mixture of adapter PCR

- 0.5µl Pfu
 - 0.3µl DNA Template
 - 0.5µl Primer each
 - 4.5µl 11x Buffer
 - 2µl DMSO
 - 41.7µl H₂O_{dest}
-
- 50µl

Mixture of overlap PCR

0.5µl	Pfu
9µl	cleaned PCR product from PCR I
9µl	cleaned PCR product from PCR II
0.5µl	Primer each
4µl	11x Buffer
17.5µl	H ₂ O _{dest}
<hr/>	
40µl	

All used primers and their sequence for adapter PCRs as well as overlap PCRs are mentioned in tables A1 and A2. For performing an overlap PCR the mixture without primers was incubated for three cycles to allow the overlapping sites to already align.

Subcloning into pBlueScript and ethanol precipitation

PBlueScript vector was linearized using EcoRV. The following mixture without Fast AP was incubated for 45min at 37°C, then 1µl Fast AP was added and incubated for another 15min at same temperature.

2-3µg	pBlueScript vector
1µl	EcoRV
2µl	red buffer
1µl	Fast AP
<hr/>	
20µl	

The insert was phosphorylated for 30min at 37°C in the following mixture:

9µl	cleaned PCR product
1.5µl	10x T4 polynucleotid kinase buffer
1µl	10mM ATP
1.5µl	T4 polynucleotidekinase
2µl	H ₂ O _{dest}

15µl

Both insert and vector where loaded on an 1% or 2% agarose gel, depending on the size of the insert, the correct size was confirmed. The insert was purified using the gel extraction kit. The DNA was then resuspended in 10µl H₂O_{dest}.

For the ligation the following chemicals were mixed and incubated either for 2h at room temperature or overnight at 16°C.

1µl	linearized pBlueScript vector
2µl	10x ligation buffer
9µl	cleaned PCR product
1µl	T4 DNA ligase
7µl	H ₂ O _{dest}

20µl

After ligation the mixture was ethanol precipitated over night at -20°C using the following mixture. Before adding ethanol the solution was mixed by pipetting up and down a few times.

20µl	ligation mixture
1µl	Glycogen
2.1µl	3M sodium acetate
69.3µl	EtOH 100%

92.4µl

On the next day the precipitation was centrifuged (1h, 13300rpm, 4°C) and the supernatant was removed. The pellet was washed once in 70% EtOH (15min, 13300rpm, 4°C). After removing the supernatant the pellet was air dried and resuspended in 10µl H₂O_{dest}.

XL1Blue cells were electroporated with the whole mix and incubated over night at 37°C.

Identification of insert containing pBlueScript clones using colony PCR

The colonies on the agar plate were checked whether they contain an insert or not. For that one colony was picked using a pipette tip and shortly incubated in 10µl H₂O_{dest}. The pipette tip was transferred to an Eppendorf tube containing 1ml of LB media supplemented with Carbenicillin (Roth, 50µg/ml). The water containing the template was then mixed with the required chemicals, the primers where the same as used in PCR for amplifying the insert. Mixture of the PCR and program were as followed:

2µl	11x buffer	95°C	3min	} 30cycles
0.2µl	primer each	95°C	30sec	
1µl	Dream Taq polymerase	x	30sec	
6.6µl	H ₂ O _{dest}	72°C	x	
10µl	H ₂ O _{dest} containing DNA	72°C	3min	
<hr/>				
20µl		10°C	∞	

Variables in the PCR program, primer annealing and extension time, are marked by an x. The same temperature and time as in overlap PCRs was used, the extension time was adjusted to the length of the expected insert (30sec/1kbp). The whole PCR mixture was transferred to an agarose gel. Insert containing colonies were incubated overnight in 5ml LB medium supplemented with Carbenicillin (50mg/ml) at 37°C, mini preps were performed on the next day.

Final cloning into pEGFPN1

In case the sequence was correct pBlueScript vector with insert generated in the previous PCRs and pEGFPN1mOtof vector were digested using the chosen enzymes as mentioned below.

Insert		Vector	
3-6µl	buffer	3-6µl	buffer
1µl	enzyme each	1µl	enzyme each
2µl	pBlueScript del C ₂ A	2µl	pEGFPN1mOtof
17-20µl	H ₂ O _{dest}	20-23µl	H ₂ O
30µl		30µl	

The digested vector and the produced insert were then ligated together.

1µl	ligase buffer
0.6µl	backbone pEGFPN1mOtof
0.75µl	Ligase
7.65µl	insert (digested insert from pBlueScript)
<hr/>	
10µl	

3.1.2 Cloning of pEGFPN1mOtof del C₂A

In contrast to the generation of the remaining deletion constructs cloning of pEGFPN1mOtof del C₂A required only one adapter PCR instead of two and thus no overlap PCR. It was possible to choose the forward overlapping primer in a way that the enzyme cutting site of EcoRI was already located on the primer. The reverse primer was generated binding downstream of EcoRV restriction site. The PCR was performed using the previously mentioned mixture (see section 3.1.1) and the following program. Primers pEGFPN1mOtof del C₂A, for

(CTTCGAATTCGCCACCATGGCCGCCACAGATGGCACTGTGGGC) and pEGFPN1mOtof del C₂A, rev (ATCTTGTCTTTGGGGCTCCT) were used.

95°C	3min	}	30cycles
95°C	30sec		
60°C	30sec		
72°C	30sec		
72°C	3min		
10°C	∞		

The PCR product was loaded on a 2% agarose gel, the correct band (size 292bp) was cut out and the DNA was then purified using the Gel extraction kit. Following steps were performed as already mentioned in section 3.1.1. For digestion with EcoRI and EcoRV 2x Tango Buffer was used.

In Fig. 3.3 pEGFPN1mOtof vector before and after removal of the C₂A domain are shown.

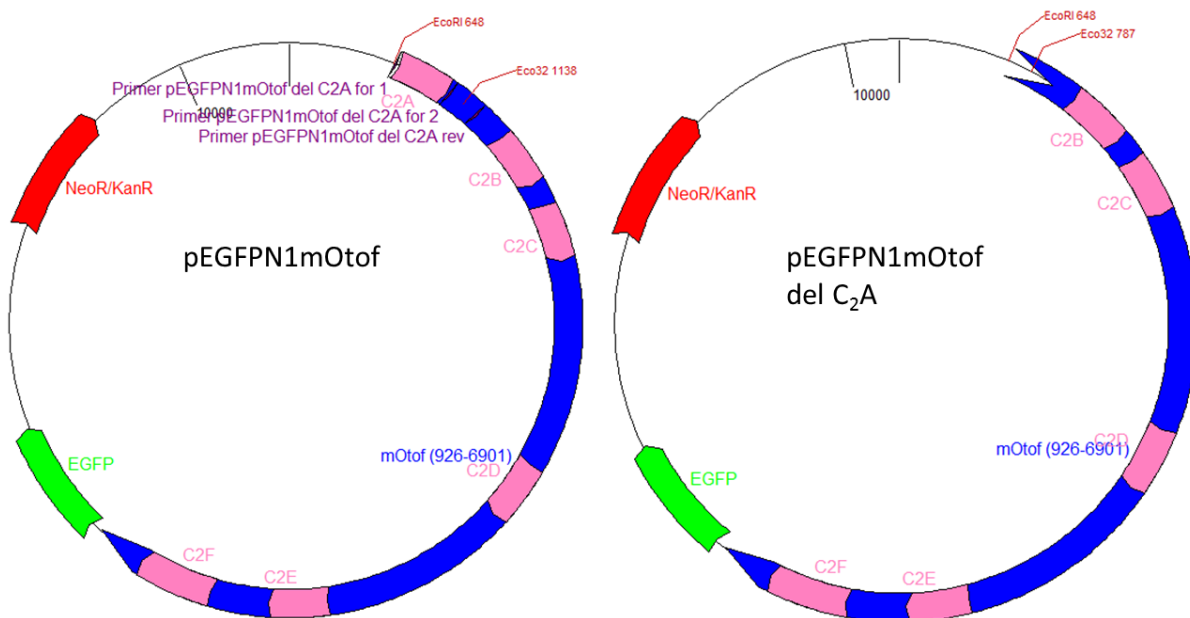


Figure 3.3: Depicted are vector maps of pEGFPN1mOtof vector before removing the C₂A domain (left) and afterwards (right). The used restriction enzymes as well as their location are shown in red; the

location of the used primers is indicated in purple. The overstretching primer is shown as two parts, indicating the part binding upstream and downstream of the C₂A domain. Eco32 = EcoRV

3.1.3 Cloning of pEGFPN1mOtof del C₂B

To obtain a deletion construct of mouse otoferlin with a missing C₂B domain in the pEGFPN1 vector the desired sequence was removed using two pairs of designed primers in two adapter PCRs followed by one overlap PCR, using both obtained products from the previous PCRs as templates (compare Fig. 3.1). The obtained product was amplified and subcloned into pBlueScript using blunt end ligation. The insert was sequenced and, in case of a correct sequence, digested with the enzymes EcoRV and Sall and finally cloned into pEGFPN1 mOtof.

Two adapter PCRs in a mixture as stated previously were performed as followed. For PCR1 and PCR2 primer pairs pEGFPN1mOtof del C₂B PCR1, for (AAGGACAGCCAGGAGACAGA) and pEGFPN1mOtof del C₂B PCR2, rev (TGCCCACCACCTGGTAATCCATGGGCCTTC) as well as for PCR2 pEGFPN1mOtof del C₂B PCR2, for (ATTACCAGGTGGTGGGCAAGGAGACAAC) and pEGFPN1mOtof del C₂B PCR2, rev (GCTGCTCTTCTGCACTGATG) were used, respectively.

Adapter PCR1		Adapter PCR2
95°C 3min	} 30cycles	95°C 3min
95°C 30sec		95°C 30sec
59°C 30sec		59°C 30sec
72°C 1min		72°C 1min
72°C 3min		72°C 3min
10°C ∞		10°C ∞

The expected sizes of PCR1 and PCR2 were 391bp and 293bp respectively. The PCR products were loaded on a 2% agarose gel, the correct band was cut out and the DNA was then purified using the Gel extraction kit. Overlap PCR was performed as stated before (see section 3.1.1).

Primers pEGFPN1mOtof del C₂B PCR1 for and pEGFPN1mOtof del C₂B PCR2 rev were used. The PCR program is mentioned below. Afterwards the PCR was again loaded on a 2% agarose gel and the correct band (size 666bp) was cut out and purified using the gel extraction kit.

95°C	5min	}	3 cycles
37°C	5min		
72°C	5min		
95°C	3min	}	25 cycles
95°C	30sec		
60°C	30sec		
72°C	2min		
72°C	5min		
10°C	∞		

Ligation procedure of overlap product and pBlueScript vector was conducted as previously stated. Both insert and vector were loaded on a 1% agarose gel where the correct size was confirmed and cleaned using the gel extraction kit. After ligation the whole mix was electroporated into XL1Blue cells and incubated over night at 37°C. Colony PCRs were done the next day.

In case the sequence was correct, pBlueScript vector with del C₂B insert and pEGFPN1mOtof vector were digested using EcoRV and Sall using 2x Tango Buffer as mentioned below.

Insert	Vector
6µl Tango buffer	6µl Tango Buffer
1µl enzyme each	1µl enzyme each
5µl pBlueScript del C ₂ B	2µl pEGFPN1mOtof
17µl H ₂ O _{dest}	20µl H ₂ O _{dest}
30µl	30µl

The digested vector and the produced insert were then ligated together.

In Fig. 3.4 pEGFPN1mOtof vector before and after removal of the C₂B domain are shown.

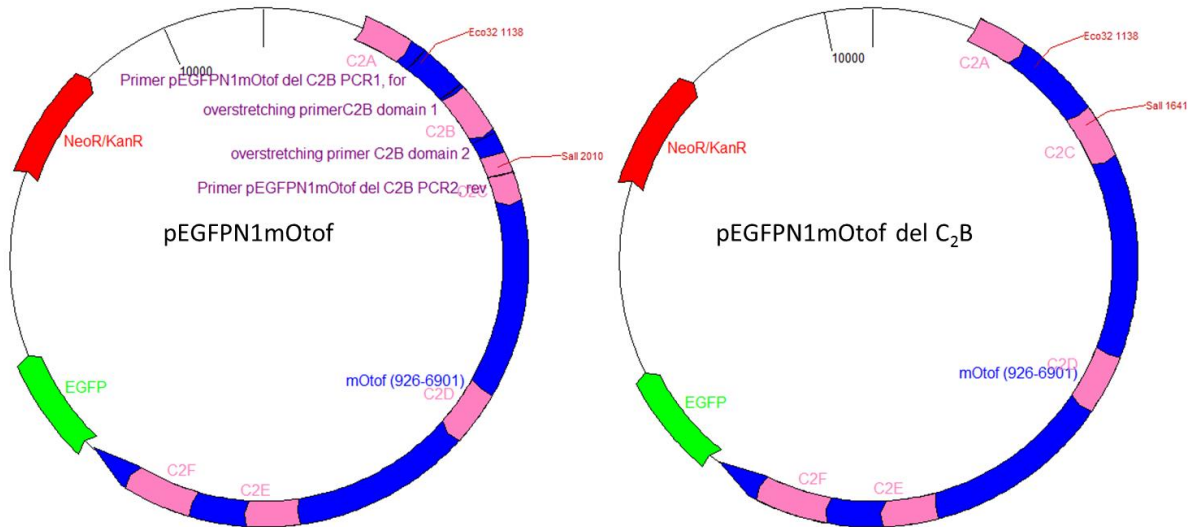


Figure 3.4: Depicted are vector maps of pEGFPN1mOtof vector before removing the C₂B domain (left) and afterwards (right). The used restriction enzymes as well as their location are shown in red; the location of the used primers is indicated in purple. The overstretching primer is shown as two parts, indicating the part binding upstream and downstream of the C₂B domain.

3.1.4 Cloning of pEGFPN1mOtof del C₂C

To obtain a deletion construct of mouse otoferlin with a missing C₂C domain in the pEGFPN1 vector, the desired sequence was removed using two pairs of primers in two adapter PCRs, followed by one overlap PCR, using the both obtained products from the previous PCRs as templates (compare Fig. 3.1). The obtained product was amplified and subcloned into pBlueScript using blunt end ligation. The insert was sequenced and, in case of a correct sequence, digested with the enzymes *San*DI and *Eco*RV and finally cloned into pEGFPN1 mOtof.

Two adapter PCRs in a mixture as stated previously were performed as followed. For PCR1 and PCR2 primer pairs pEGFPN1mOtof del C₂C PCR1, for (AAGGACAGCCAGGAGACAGA) and pEGFPN1mOtof del C₂C PCR2, rev (AGTTGCGCGTCCGTGCCCACTGCCGTTTC) as well as for PCR2

pEGFPN1mOtof del C₂C PCR2, for (GTGGGCACGGACGCGCAACTACACACTGCTG) and pEGFPN1mOtof del C₂C PCR2, rev (ACAGAGGCGTGTTCAGGATCT) were used, respectively.

Adapter PCR1		Adapter PCR2
95°C 3min		95°C 3min
95°C 30sec	} 30cycles	95°C 30sec
59°C 30sec		63°C 30sec
72°C 2min		72°C 6.30min
72°C 3min		72°C 3min
10°C ∞		10°C ∞

The expected sizes of PCR1 and PCR2 were 880bp and 3187bp respectively. The PCR products were loaded on a 1% agarose gel, the correct band was cut out and the DNA was then purified using the Gel extraction kit. Overlap PCR was performed as stated before (see section 3.1.1). Primers pEGFPN1mOtof del C₂C PCR1 for and pEGFPN1mOtof del C₂C PCR2 rev were used. The PCR program is mentioned below. Afterwards the PCR was again loaded on a 1% agarose gel and the correct band (size 4047bp) was cut out and purified using the gel extraction kit.

95°C 5min	} 3 cvcles
37°C 5min	
72°C 5min	
95°C 3min	} 30 cvcles
95°C 30sec	
63°C 30sec	
72°C 8.30min	
72°C 5min	
10°C ∞	

Ligation procedure of overlap product and pBlueScript vector was conducted as previously stated. After ligation the whole mix was electroporated into XL1Blue cells and incubated overnight at 37°C. Colony PCRs were done the next day.

In case the sequence was correct pBlueScript vector with del C₂C insert and pEGFPN1mOtof vector were digested using SanDI and EcoRV using 3µl fast digest buffer green as mentioned below. Since SanDI was only purchasable as a fast digest enzyme, a fast digest enzyme and a normal one were combined. A digestion mixture was prepared using the fast digest buffer green, which came with SanDI and had loading dye already included, including all ingredients except SanDI. Digestion with EcoRV only was performed for 50min; subsequently SanDI was added and incubated at 37°C for another 10-15min.

Insert		Vector	
3µl	Fast Digest Buffer green	3µl	Fast Digest Buffer green
1µl	enzyme each	1µl	enzyme each
5µl	pBlueScript del C ₂ B	2µl	pEGFPN1mOtof
20µl	H ₂ O _{dest}	23µl	H ₂ O _{dest}
<hr/>		<hr/>	
30µl		30µl	

The digested vector and the produced insert were then ligated together as stated previously.

In Fig. 3.5 pEGFPN1mOtof vector before and after removal of the C₂C domain are shown.

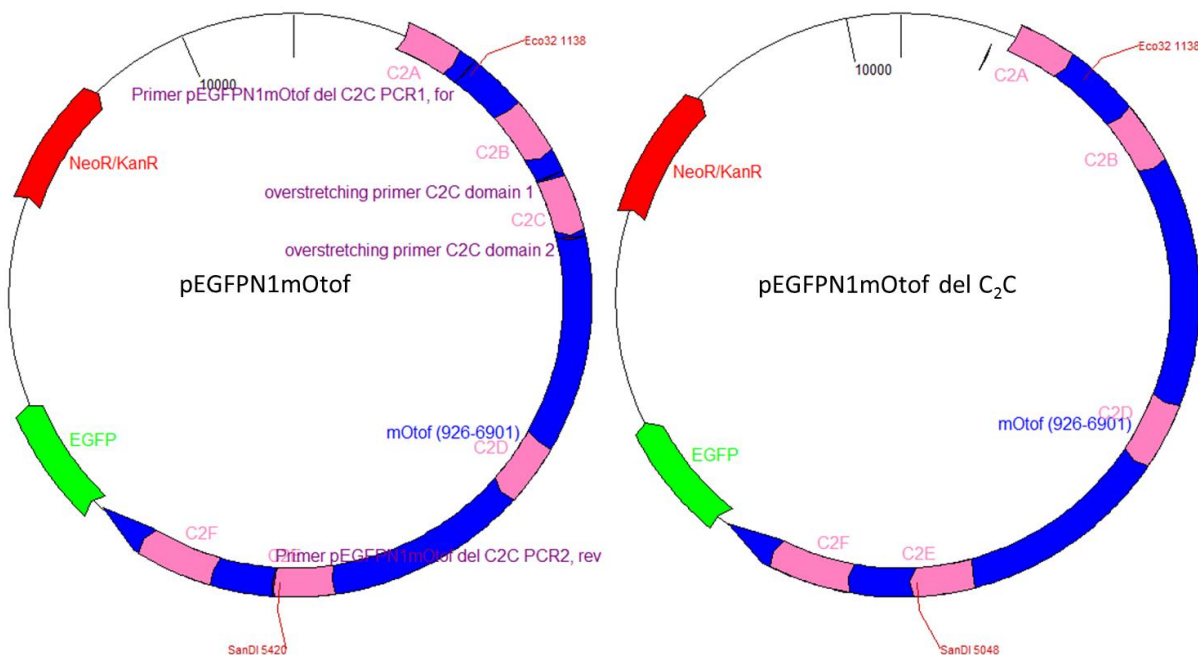


Figure 3.5: Depicted are vector maps of pEGFPN1mOtof vector before removing the C₂C domain (left) and afterwards (right). The used restriction enzymes as well as their location are shown in red; the location of the used primers is indicated in purple. The overstretcher primer is shown as two parts, indicating the part binding upstream and downstream of the C₂C domain.

3.1.5 Cloning of pEGFPN1mOtof del C₂F

To obtain a deletion construct of mouse otoferlin with a missing C₂F domain in the pEGFPN1 vector the desired sequence was removed using two pairs of designed primers in two adapter PCRs followed by one overlap PCR, using the both obtained products from the previous PCRs as templates (compare Fig. 3.1). The obtained product was amplified and subcloned into pBlueScript using blunt end ligation. The insert was sequenced and in case of a correct sequence digested with the enzymes KpnI and SanDI and finally cloned into pEGFPN1 mOtof.

Two adapter PCRs in a mixture as stated previously were performed as followed. For PCR1 and PCR2 primer pairs pEGFPN1mOtof del C₂F PCR1, for (ATGTTGACAGTGGCCGTGTA) and pEGFPN1mOtof del C₂F PCR2, rev (CATTCTCATTCTCGTACTTCTTGGGTTCC) as well as for PCR2

pEGFPN1mOtof del C₂F PCR2, for (GAAGTACGAGAATGAGAATGATGAGTTTGAGC) and pEGFPN1mOtof del C₂F PCR2, rev (GCTGAACTTGTGGCCGTTTACG) were used, respectively.

Adapter PCR1		Adapter PCR2
95°C 3min		95°C 3min
95°C 30sec	}	95°C 30sec
58°C 30sec		58°C 30sec
72°C 1.30min		72°C 1min
72°C 3min		72°C 3min
10°C ∞	30cycles	10°C ∞
		30cycles

The expected sizes of PCR1 and PCR2 were 544bp and 446bp respectively. The PCR products were loaded on a 2% agarose gel, the correct band was cut out and the DNA was then purified using the Gel extraction kit. An overlap PCR was conducted as already stated before (see section 3.1.1). The used program is mentioned below. Primers pEGFPN1mOtof del C₂F PCR1 for and pEGFPN1mOtof del C₂F PCR2 rev were used. The correct band size (964bp) was confirmed on a 1% agarose gel.

95°C 5min	}	3 cvcles
37°C 5min		
72°C 5min		
95°C 3min	}	25 cvcles
95°C 30sec		
60°C 30sec		
72°C 2min		
72°C 5min		
10°C ∞		

Ligation procedure of overlap product and pBlueScript vector was conducted as previously stated. After ligation the whole mix was electroporated into XL1Blue cells and incubated over night at 37°C. Colony PCRs were done the next day.

In case the sequence was correct pBlueScript vector with del C₂F insert and pEGFPN1mOtof vector were digested using KpnI and SanDI using 3µl fast digest buffer green as mentioned below. For digestion procedure using one normal and one fast digest enzyme see section 3.1.4.

Insert	Vector
3µl fast digest buffer green	3µl fast digest buffer green
1µl enzyme each	1µl enzyme each
5µl pBlueScript del C ₂ F	2µl pEGFPN1mOtof
20µl H ₂ O _{dest}	23µl H ₂ O _{dest}
<hr/> 30µl	<hr/> 30µl

The digested vector and the produced insert were then ligated together.

In Fig. 3.6 pEGFPN1mOtof vector before and after removal of the C₂F domain are shown.

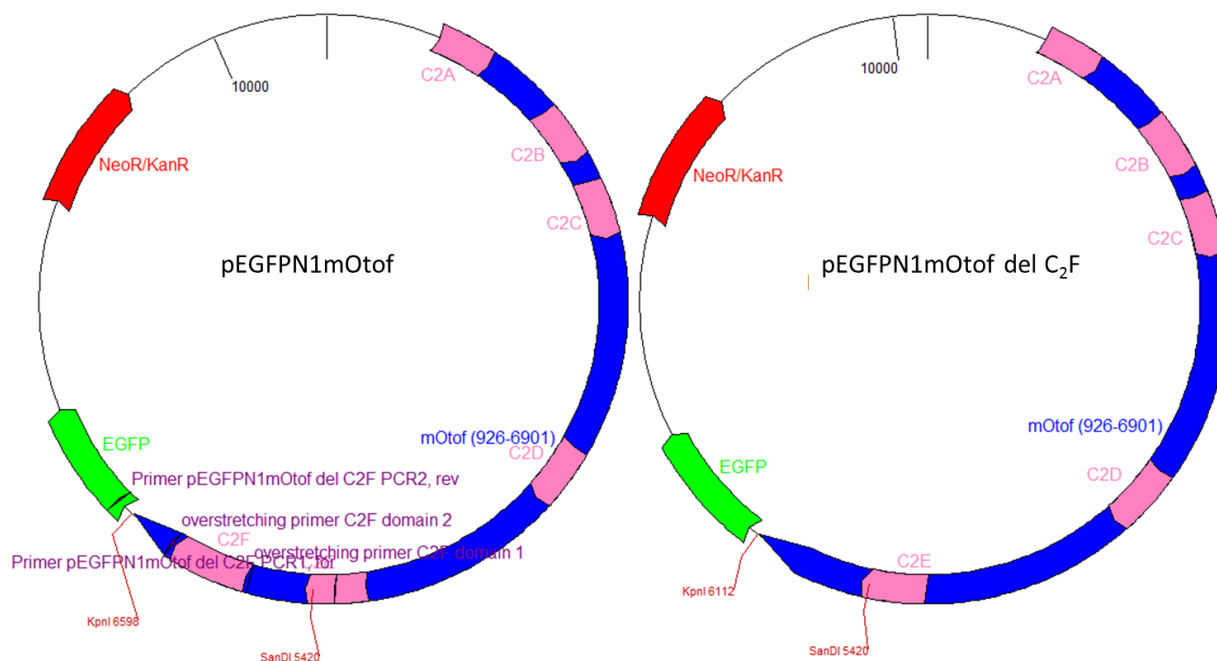


Figure 3.6: Depicted are vector maps of pEGFPN1mOtof vector before removing the C₂F domain (left) and afterwards (right). The used restriction enzymes as well as their location are shown in red; the location of the used primers is indicated in purple. The overstretching primer is shown as two parts, indicating the part binding upstream and downstream of the C₂F domain.

3.1.6 Cloning of constructs containing a point mutation in otoferlin

Generating of constructs with a single point mutation was performed similar to generation of C₂ deletion constructs. Using two pairs of primers in two adapter PCRs, an overlap PCR and subcloning steps, a point mutation in the amino acid sequence of otoferlin was inserted. All constructs were finally subcloned into pcDNA3 vector. For the generation of pcDNA3mOtof R1607W, similar to the generation of pEGFPN1mOtof del C₂A only one PCR was necessary. Used primers are mentioned in table A2. All constructs could be obtained using similar primers

For inserting the I515T as well as the G541S mutation two adapter PCRs each were performed which programs are shown below. For inserting I515T mutation primer pairs pEGFPN1mOtof I515T 1, for (CGTTCATCGGTGAGAACAAG) as well as pEGFPN1mOtof I515T 1, rev (GCGCAGGTCGGTGAAGTGGGTGCCGATGG) and pEGFPN1mOtof I515T 2, for

(ACCCACTTCACCGACCTGCGCAAGATTTCC) and pEGFPN1mOtof I515T 2, rev (ACAGAGGCGTGTTCAGGATC) were used; for inserting the G541S mutation primer combination pEGFPN1mOtof G541S 1, for (CGTTCATCGGTGAGAACAAG) and pEGFPN1mOtof G541S 1, rev (GCGTGGAGCTGTACATGTTCAACCAGGCTG) as well as pEGFPN1mOtof G541S 2, for (GAACATGTACAGCTCCACGCGCAACTACAC) and pEGFPN1mOtof G541S 2, rev (ACAGAGGCGTGTTCAGGATC) were used.

Adapter PCR1			Adapter PCR2	
95°C	3min		95°C	3min
95°C	30sec	} 30cycles	95°C	30sec
56°C	30sec		56°C	30sec
72°C	30sec		72°C	7.30min
72°C	3min		72°C	3min
10°C	∞		10°C	∞

The expected sizes of 220bp and 3329bp for I515T as well as 290bp and 3252bp for G541S were confirmed on an agarose gel. DNA was purified and used for following overlap PCR. Primers pEGFPN1mOtof I515T 1, for (CGTTCATCGGTGAGAACAAG) and pEGFPN1mOtof I515T 2, rev (ACAGAGGCGTGTTCAGGATC) were used.

95°C	5min	} 3 cycles
37°C	5min	
72°C	5min	
95°C	3min	
95°C	30sec	} 25 cycles
56°C	30sec	
72°C	7.30min	
72°C	5min	
10°C	∞	

The correct size of 3535bp was confirmed on a 1% agarose gel and the DNA was purified using gel extraction kit. For inserting the R1607W mutation no previous adapter PCRs were needed. PCR was performed using primers pEGFPN1mOtof R1607W, for (CGTTCATCGGTGAGAACAAG) and pEGFPN1mOtof R1607W, rev (TCATGGGGTCCCACCAGATATTGTAGCCATGTATG), mixture was as described earlier.

95°C	3min		
95°C	30sec	}	30cycles
60°C	30sec		
72°C	7.30min		
72°C	3min		
10°C	∞		

Ligation procedure of overlap product/R1607W product and pBlueScript vector was conducted as previously stated. After ligation the whole mix was electroporated into XL1Blue cells and incubated over night at 37°C. Colony PCRs were performed the next day.

In case the sequence was correct, pBlueScript vector with desired mutation and pEGFPN1mOtof vector were digested using SanDI and Sall utilizing 3µl fast digest buffer green as mentioned below. For digestion procedure using one normal and one fast digest enzyme see section 3.1.4.

The digested vector and the produced insert were then ligated together.

In Fig. 3.7 the obtained constructs are shown. The localization of the individual point mutations is indicated.

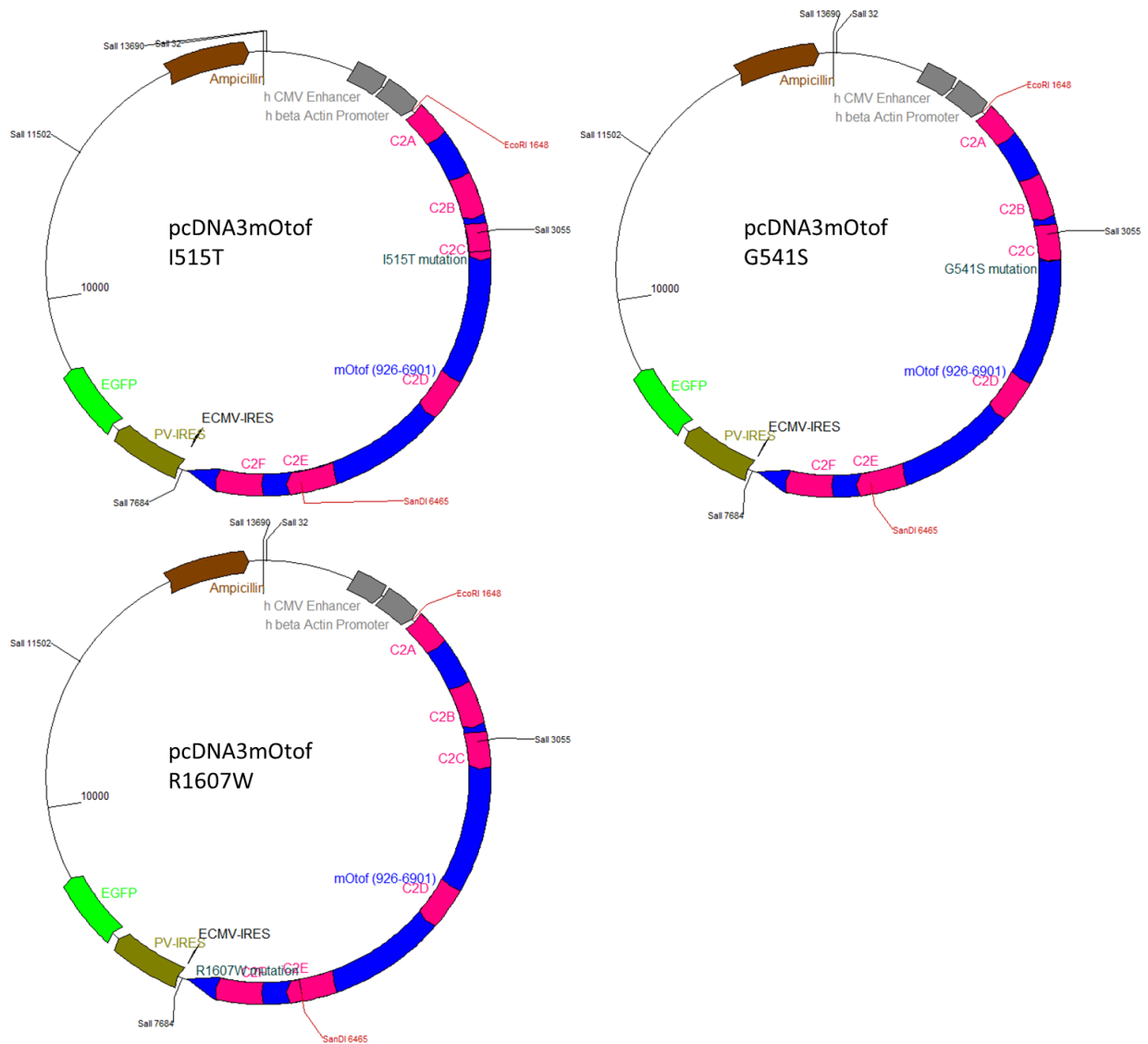


Fig. 3.7: Shown are the obtained constructs after inserting a point mutation as well as their locations in otoferlin.

3.1.7 Cloning of pEGFPN1mOtof RXR and pcDNA3mOtof RXR I515T

Inserting of the RXR motif into otoferlin was performed similar to previously explained generation of C₂ domain deletion constructs. Instead of deleting parts of the nucleotide sequence, nucleotides which will later form the RXR motif were inserted using the pair of partially complementary primers.

The RXR motif without the I515T mutation was first subcloned into pBlueScript mOtof using SfiI and SanDI. From the pBlueScript mOtof vector the insert was cut out using SanDI and Sall and cloned into pEGFPN1mOtof. The latter combination consisted of a fast digest and a normal enzyme whereas the other pair was composed of two fast digest enzymes. For digestion procedure using one normal and one fast digest enzyme see section 3.1.4.

Since a pcDNA3mOtof vector with the I515T mutation in otoferlin was already generated before, a sequence containing the RXR motif was removed from the generated pBlueScript mOtof RXR vector and inserted into this already existing construct using SanDI and SfiI.

For generating pEGFPN1mOtof RXR construct, two adapter PCRs followed by one overlap PCR were performed. Programs and mixture of the adapter PCR are shown below. Instead of Pfu DNA polymerase to amplify the sequence in PCRs Phusion polymerase was used. For PCR1 primers pEGFPN1mOtof RXR PCR1, for (CAATGATTGACCGGAAAAATGGGG) and pEGFPN1mOtof RXR PCR1, rev (CACAGCACACGGCAGCGCCGGAGAAGCCTGACCGTGGTGTTCAGCTGGGGGCTGAGCGGTCTGG) were chosen, for PCR2 primers pEGFPN1mOtof RXR PCR2, for (CGGCGTGCCGTGTGCTGTGCAATGGGGGCTCCTCCTCTCACTCCACAGGGGAGGTTGTAGTAAGC) and pEGFPN1mOtof RXR PCR2, rev (CTCTTTACAGAGGCGTGTTCAGG).

Adapter PCR1			Adapter PCR2				
95°C	3min	} 30cvcles	95°C	3min	} 30 cvcles	0,5µl	Pfusion
95°C	30sec		95°C	30sec		10µl	Phusion buffer GC
55°C	30sec		65°C	30sec		0.3µl	DNA template
72°C	1min		72°C	1min		0,5µl	Primer each
72°C	3min		72°C	3min		1.5µl	DMSO
10°C	∞		10°C	∞		1µl	dNTPs (25mM each)
				35.7µl	H ₂ O _{dest}		
				50µl			

The PCR products were loaded on a 1% agarose gel where the expected sizes of 1904bp for PCR1 and 1124bp for PCR2 were confirmed. The correct bands were cut out and the DNA was purified. An overlap PCR was conducted as mentioned below. Primers pEGFPN1mOtof RXR PCR1 for and pEGFPN1mOtof RXR PCR2 rev were used. The correct band size (3010bp) was confirmed on a 1% agarose gel.

95°C	3min	} 30 cvcles	9µl	cleaned PCR product each
95°C	30sec		8µl	Phusion buffer GC
60°C	30sec		0.8µl	dNTPs (0.25mM each)
72°C	1.35min		1.2µl	DMSO
72°C	3min		0.4µl	Phusion
10°C	∞		0.5µl	primer each
			10.6µl	H ₂ O
			40µl	

After subcloning of the overlap PCR product into pBlueScript mOtof vector, three constructs were sequenced. In case of correct sequence, the insert was cloned into pEGFPN1 mOtof or into the already existing pcDNA3mOtof I515T vector using the already mentioned enzymes.

After ligation the whole mix was electroporated into XL1Blue cells and incubated over night at 37°C. Colony PCRs were done the next day as already described.

3.2 Kits

Gel Extraction (Zymoclean™ Gel DNA Recovery Kit, Zymo Research)

The procedure was done according to the manual. The gel slice was incubated at 55°C until completely dissolved; the DNA was resuspended in 10µl H₂O_{dest}.

DNA Clean Up (DNA clean and concentrator™-5, Zymo Research)

The procedure was done according to the manual. The DNA was mixed at the ratio of 1:5 with DNA binding buffer and then resuspended in 10µl H₂O_{dest}.

Plasmid extraction peqGOLD Plasmid Miniprep Kit I (peqlab)

The procedure was done according to the manual. Plasmid was resuspended in 75µl elution buffer (included in kit).

NucleoBond® PC 100 (Machery-Nagel)

A single colony was transferred into 50ml LB media supplied with the according antibiotic and incubated at 37°C for 16h. The cells were pelleted (Beckmann Coulter® Avanti® J-30I) and resuspended in 4ml buffer S1. Buffer S2 was added and the mixture was incubated for 5min at RT, then buffer S3 was added and the mixture was incubated on ice for 5min. A column was equilibrated using 2.5ml buffer N2. The mix was filtrated; the eluate was transferred to the column and filtered. The column was washed using 10ml buffer N3. Using 5ml buffer N5 the plasmids were eluted. The eluate was mixed with 3.5ml isopropanol and incubated at least 1h

at 4°C. Plasmid was pelleted (1h, 4°C 4000g, Beckmann Coulter® Avanti® J-30I) and washed using 600µl 70% EtOH. Dried pellet was resuspended in 75µl elution buffer.

3.3 HEK cell culturing

HEK cells, which were kept in liquid nitrogen for longer storage, were thawed; when the pellet was nearly completely melted cells were poured into a 10cm petri dish containing 10ml HEK cell medium. The medium was replaced one day later and cells grew until 80-90% confluence. For culturing, HEK cells had to be splitted to avoid too high density. Firstly, media was removed and cells were washed with 3ml PBS, then treated with 2ml Trypsin and incubated for 5min at 37°C for detaching the cells. Trypsin containing the cells was transferred to a 15ml falcon tube and a few milliliters of medium were added, then the cells were pelleted (1500rpm, 5min). Cells were resuspended in amount of medium depending on the size of the pellet and splitted in new dishes at a ratio from 1:5 to 1:20.

In case a specific amount of cells was needed, cells were counted after centrifugation and removing the Trypsin solution. For that between 4ml and 8ml HEK cell medium, depending on the size of the pellet, was added and the pellet was resuspended by carefully pipetting up and down. Using a Neubauer Counting Chamber cell counted and the quantity of cells in 10µl was estimated. The appropriate amount of medium containing the cells was then transferred to a petri dish and distributed evenly by shaking movements.

Transfection procedure

HEK cells were transfected using Lipofectamine 2000. For cells incubated in a 6cm petri dish 8µg DNA and 20µl Lipofectamine 2000 were needed. Both DNA and transfection reagent were mixed with 500µl OptiMEM medium each and incubated for 5min. Both solutions were then

mixed and incubated for another 20min. HEK cell medium was replaced by 5ml DMEM medium without supplements and 1ml of the mixture was pipetted to the cells.

3.4 Cycloheximide procedure for HEK cells

Cells were splitted as described above. 1.000.000 cells per 6cm dish were incubated overnight for attaching to the surface. On the next day medium was replaced by DMEM medium without supplements and cells were transfected using Lipofectamine 2000 (see transfection procedure section 3.3), solution stayed with the cells overnight. 14h later cells were treated with Cycloheximide in a concentration of 100µg/ml and cells were incubated either at 37°C or at 38.5°C. Samples were taken at certain time points, namely 0min (control without Cycloheximide), 5min, 10min, 20min, 30min, 60min, 2h, 3h, 6h, 9h, 12h and 24h (extended time points longer than 2h only for otoferlin WT and otoferlin I515T). Therefore medium was removed and cells were washed carefully with 3ml PBS. After removing PBS 100µl Laemmli loading buffer was added directly and cells were removed using a cell scraper. The liquid was transferred into a 1.5ml tube and all tubes were stored at -20°C until all samples were taken. Then samples were thawed and sonified (Branson sonifier: 20% duty cycle, output control 2, Bandelin Sonopuls 40% power) for 3x20sec, in between the three steps the samples were cooled down to room temperature. After sonification, the samples were ready to load on a gel.

20µl of each sample were loaded on polyacrylamide gels (see section 3.11) and separated until bromophenol band left the gel. The gel was stained using Coomassie blue and destained using water until single bands were visible. The gel was then brought to mass spectrometry department (Research Group Mass Spectrometry) for further treatment.

Mass spectrometry data were analyzed using *Maxquant* program (version 1.5.2.8) by Kuan-Ting Pan (Research Group Mass Spectrometry). IBAQ values were determined and normalized to 4 stable background proteins (Sperm Associated Antigen 9 (Spag9), topoisomerase (DNA) II beta (Top2b), Bromodomain-containing protein 4 (Brd4), and Ubiquitin-60S ribosomal protein L40,

(Uba5)). Those background proteins were present in high abundance across all the samples and were stable over the chosen time range. IBAQ values were copied to Microsoft Excel and the values of the mutants were normalized to those of otoferlin wild type

3.5 Gene Gun

Generation of Gene Gun bullets

For the generation of Gene Gun bullets the protocols of Belyantseva, 2009 and Zhao et al., 2012 were modified. 25mg gold with a diameter of 1 μ m were mixed with 100 μ l 0.05M spermidine, vortexed for 15sec and sonified for 30sec. 50 μ g DNA diluted in 50 μ l H₂O were added and the solution was vortexed for 5sec. During vortexing, 100 μ l 1M CaCl were pipetted carefully to the mixture. Following was an incubation step of 10min including vortexing steps every 30secs for 5secs. For pelleting the particles the mix was centrifuged (2min, 1000g) and most of the supernatant was removed, the gold particles were resuspended in the remaining liquid. The gold particles were washed three times (10sec, 1000g) with 100% EtOH, after the last washing step most of the EtOH was fully removed. Gold particles were transferred into a 15ml falcon tube using 3ml 50 μ g/ml PVP, the mixture was vortexed for 15secs. The Tefzel tubing was dried at N₂ flow of 0.4l/min for at least 15min. After drying the gold particle solution was transferred into the Tefzel tubing using a syringe. The gold particles were distributed equally throughout the inside of the tubing by several turning steps using the tubing prep station. Using N₂ at 0.4-0.5l/min the Tefzel tubing was dried during constant rotation, afterwards the bullets were cut using the provided bullet cutter.

Transfection procedure

Mice at the age from p3 to p5 were decapitated using sharp scissors. The head was dipped into 70% EtOH for a few seconds to allow sterilization of the tissue. Afterwards the mice's head was

cut in halves from caudal to cranial and the brain was removed carefully using small scissors. The back part of each side of the head containing the cochlea and with that the organ of Corti was cut off and put into a petri dish with HEPES HANKS solution. Under the sterile bench the organ of Corti was removed using forceps of different sharpness and transferred into a culture dish with 1ml DMEM/F-12 media supplemented with 10% NBCS. In case the stria vascularis was already partially removed during the preparation procedure, it was removed completely. Before the Gene Gun transfection, the organ of Corti was flipped upside down with the basilar membrane facing up and carefully directed to the middle of the petri dish. The medium was removed cautiously and left in the pipette tip. The petri dish was removed from the sterile bench and placed under a tripod, two cell strainers with a mesh diameter of 40 μ m (BD Falcon) glued together on top of each other were placed over the organ of Corti (modified from Zhao et al., 2012). Using a helium pressure of 200-220psi the gold particles were transferred into the organ of Corti. The tissue was placed back under the sterile bench and two milliliters of medium were added. The organ of Corti was flipped back and separated into two to three parts. These parts were carefully attached to earlier with CellTak coated coverslips and incubated for 48h. After that the tissue underwent an immunostaining (see section 3.6, all washing steps were performed in petridishes, blocking and antibody incubation took place on coverslips).

3.6 Immunohistochemistry and Immunocytochemistry

Immunostaining procedure of organs of Corti

Mice at the age ranging from p14-p20 were used for immunostainings. After isolation of the cochlea, edge and top of it was removed carefully and a small opening was carved in by removing a bit of the cartilage. The cochlea was transferred into a 0.5ml tube and 500 μ l 4% formaldehyde were added for fixation, the tubes were incubated on ice for 1h. All following steps were performed under shaking. Several washing steps for at least 30min with PBS followed and the tissue was then blocked for 1h using either DSDB or GSDB depending on the

origin of the secondary antibodies. The primary antibodies diluted in either DSDB or GSDB were added and the cochlea was incubated overnight at 4°C. On the next day the preparation was washed several times with wash buffer, then according secondary antibodies in a ratio 1:200, diluted in GSDB or DSDB, were added. The cochlea was incubated in darkness for 1h and afterwards washed in wash buffer including several buffer replacements. After the last washing step the cochlea was transferred to a Petri dish containing PBS, the organ of Corti was removed carefully and transferred to an object slide. After removing most of the wash buffer, 100µl 5mM PB was carefully dribbled around the organ of Corti and incubated in darkness 1-5min. Afterwards, the liquid was removed and 10µl Mowiol Mounting Medium was dropped on the organ of Corti, then it was covered with a cover slip. The preparations were kept in the fridge until further study. Used antibodies are displayed in table A4 and Table A5.

3.7 Fluorescence Microscopy and image analysis

Stained organs of Corti were imaged on a Leica SP5 confocal microscope (63x Glycerol objective, NA = 1.3, imaging of z-stacks with 0.6-0.8µm step size) using 488nm argon laser and 594nm DPSS laser. For imaging of PLA and Gene Gun samples an additional 405nm laser was used. Distribution of proteins in the inner hair cell was analyzed by a *Matlab* routine implemented in *Imaris* by Gerhard Hoch (Institute for Auditory Neuroscience). Gene Gun cells were stained using α -otoferlin and α -VGlut3 antibodies. The fluorescence was normalized to the cellular fluorescence of each fluorophore. Five parallel line scans from apical to basal through the middle of the cells were performed. The most basal part of the membrane was set manually. It was determined as the most basal point of the cell that exceeds the threshold value for the summed fluorescence. The threshold for summed fluorescence was set to 5 for Gene Gun transfected cells to quantify the fractional membrane staining of otoferlin. The otoferlin-VGlut3 fluorescence value was read out. This value represents the fraction of membrane bound otoferlin (for an overview compare Fig. 3.8). Immunostainings were visualized using *ImageJ* software.

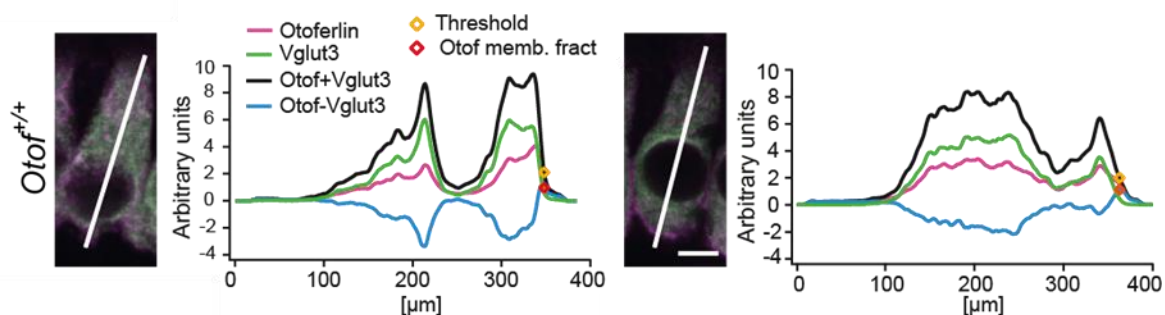


Figure 3.8: Shown is a maximum projection of a wild type inner hair cell to illustrate *Imaris* analysis. Cell is stained against otoferlin (magenta) and VGlut3 (green), scale bar is 5 μ m. Average of five parallel line scans of otoferlin is depicted magenta in the graph; average of VGlut3 is depicted in green. The sum of both fluorescences is shown as a black line, the blue line shows Otof fluorescence minus VGlut3 fluorescence. The most basal point is depicted as a yellow diamond, the orange diamond indicates read out of otoferlin minus VGlut3, modified from Strenzke et al., 2016).

3.8 Proximity Ligation Assay

To test for possible interaction partners of otoferlin, proximity ligation assay were performed. Promising candidates were dynamin and OPA1 since those two proteins were a result from pull down assays done by Sandra Meese (Molecular Structural Biology, Ralf Ficner) and Sunit Mandad (Bioanalytical Mass Spectrometry Group, Henning Urlaub)). After isolation of a mouse cochlea a small hole was cracked into its upper part to allow the solutions to reach the inner tissue. The organ of Corti was then fixed on ice for 1h in 4% formaldehyde and blocked in normal DSDB for 1h, interrupted by several washing steps with PBS. Antibodies for otoferlin in combination with either dynamin 1/2/3 or OPA1 were diluted in DSDB without Triton-X-100 and incubated shaking at 4°C overnight. In addition to the antibodies which should lead to a PLA signal, a co-staining with α -calbindin to stain the inner hair cells was performed. All following incubation steps were conducted under gentle shaking in a wet chamber at 37°C; following washing steps were performed under gentle shaking at room temperature.

On the next day the two PLA probes were diluted at a ratio of 1:6 in DSDB without Triton and incubated for 20min, then the mixture was pipetted in the tube containing the cochlea. During

the incubation time of the two PLA probes, samples were washed in provided Wash Buffer A, solution was changed at least four times. PLA solution on cochleae was incubated for 90min. Afterwards, PLA solution was removed and the samples were washed in Wash Buffer A for 20min. Subsequently ligase solution at a ratio of 1:5 in H_2O_{dest} was given to the samples and preparations were incubated for 1h. After incubation in ligase solution, samples were washed again for 30min in Wash Buffer A including several buffer replacements. The organ of Corti was isolated from the cochlea using Buffer A instead of HEPES HANKS. The tissue was transferred carefully into a well of a 24-well plate and treated with polymerase at a rate of 1:80 in diluted amplification stock at a ratio of 1:5. The mixture was incubated for 100min. After removing of amplification solution the organ of Corti was washed for 20min in Wash Buffer B and subsequently washed for up to 5min in 0,01x Wash Buffer B, all steps included several buffer replacements. Organs of Corti were then mounted on object slides using provided DAPI mounting medium, the edges of the cover slips were sealed with nail polish. The earliest after 15min the slides could be analyzed by fluorescence microscopy. For a short glimpse Axiovert 40 CFL with HBO 50 lamp from Zeiss was used, for a more intense analysis samples were imaged using SP5 microscope from Leica.

3.9 RNA-isolation and generation of cDNA from organs of Corti

Organs of Corti were isolated, beyond the age of p14 at least two mice were needed, at the age from p6-p8 one mouse was sufficient. The tissue was transferred into a 1.5ml reaction tube and incubated on ice until all organs were isolated. For the mentioned amount of tissue 800 μ l TRIZOL (Invitrogen) were added, the mixture was transferred into 1ml Wheaton homogenizer and homogenized carefully avoiding bubbles. Subsequently the homogenized liquid was transferred into a 1.5ml tube and incubated for 5min at RT. 160 μ l chloroform were added and the tubes were shaken by hand strongly. After another incubation step of 3min at RT the composition was centrifuged for 15min, 13300rpm and 4°C. After that step the upper phase was transferred into a new tube and mixed with 1 μ l glycogen and 400 μ l isopropanol. After

mixing carefully the tubes were incubated for at least two hours, better overnight, at -18°C to precipitate the RNA. After pelleting of RNA (45min, 13300rpm, 4°C) a washing step with freshly prepared 75% EtOH followed (12min, 13300rpm, 4°C). The pellet dried at RT nearly completely and was then resuspended in 13µl RNase free water. The mix was incubated for 10-15min at 55-60°C and, if needed, stored at -80°C.

For reverse transcription 13µl of RNA solution were used and incubated for 1min at 55°C. Following components were then added

0.65µl	oligo dT primers (50 pmol/µl)
0.4µl	Random Hexamers (biomers.net; 0.5 µg/µl)
1.3µl	dNTPs (10mM each)

and incubated for 5min at 65°C, samples were then kept on ice. The following components were added:

5.3µl	5x first strand buffer
5.6µl	0,1M DTT (final concentration 1 mM)
1.3µl	RNase out (1.8U)
1µl	SuperScript II (260 U)

The mix was then incubated for

10min	RT
30min	37°C
60min	42°C
5min	70°C

For precipitation of cDNA 1µl glycogen, 2.3µl 3M NaAc and 76µl 100% EtOH were added, gently mixed and incubated at -18°C overnight.

After precipitation the cDNA was pelleted (60min, 13300rpm, 4°C) and subsequently washed with 100µl 75% EtOH (10min, 13300rpm, 4°C). After drying the pellet was suspended in 25µl H₂O_{bidest}.

3.10 Real-Time PCR

Real-Time quantitative PCR was performed on cDNA of organs of Corti from p9 wild type and *Otof*^{f515T/1515T} mice, all pipetting steps were done using filter tips to avoid contamination. Taqman assays were used to perform Real-Time PCR, Mm00453306 (Applied Biosystems) for amplification of otoferlin, Mm00446873_m1 for TATA binding protein (TBP) and Mm00464451_m1 for bassoon on 2 µl of cDNA solution each. The cDNA is amplified comparable to a normal PCR; additionally the amount of cDNA is quantified after every cycle. The amount of otoferlin was compared to either TBP or bassoon. To ensure perfect mixing of all ingredients, two mastermixes were made.

Mastermix I		Mastermix II	
12.5µl	2x Taq-Man MasterMix	1.25µl	20x Primermix
2µl	Template	9.25µl	H ₂ O _{bidest}

Additionally to every sample, a negative control containing water instead of DNA was carried out. After pipetting both mixes in a well of a 96-well plate the top was covered with a self-sticking foil to avoid evaporation, subsequently the plate was shortly centrifuged (1000rpm, 3min). All experiments were performed in triplicates.

The mRNA level of *Otof*^{f515T/1515T} in comparison to wild type mice was analyzed by the $\Delta\Delta C_t$ -method. With that approach the amount of transcript is indicated as a multiple of the reference sample, here otoferlin cDNA from wild type mice. Firstly, different cDNA concentrations of the samples were normalized to an endogenous constantly expressed control gene, here either TBP

or bassoon as an inner hair cell protein. C_t values from experiments with same DNA and same primers were averaged by calculation of a linear value from C_t values from

$$\text{Lin}(C_t) = 2^{(42-C_t)}$$

This is based on the assumption that a single DNA molecule results in a C_t of 42 although deviations from 42 do not change the overall result. Values of $\text{Lin}(C_t)$ are averaged and back calculated, to “real” C_t values using the following form:

$$C_t = 42 - \text{LN}(\text{Lin}(C_t))/\text{LN}2$$

The value of 42 is eliminated. The now gotten averaged C_t values can now be used to calculate ΔC_t values for each tissue sample using

$$\Delta C_t = C_t(\text{Otof}) - C_t(\text{TBP}).$$

ΔC_t values from individual cDNA preparations were averaged by the calculation of a linear value of ΔC_t which was averaged and back calculated as above. Relative mRNA amount which compares to the amount of cDNA in wild type and *Otof*^{#515T/515T} mice is calculated by

$$\Delta\Delta C_t = \Delta C_t (\text{mutant}) - \Delta C_t (\text{wt})$$

and relative Otof mRNA amount = $2^{-\Delta\Delta C_t}$.

3.11 Polyacrylamide gels and Western Blot of HEK cell lysates

Western Blot procedure (according to Towbin et al., 1979)

To isolate and separate proteins from HEK cells, SDS PAGE and western blot were performed. HEK cells were harvested and processed as already described before (see section 3.4). Gels consisted of 6% acrylamide running gel and 5% acrylamide stacking gel (see section 2.7). The electrophoresis chamber was filled with running buffer and the combs used for generating the

slots were removed carefully. For experiments 20µl sample and 6µl of prestained marker were pipetted into the gel slots. The electrophoresis was performed at 80V until the bromophenol band was just leaving the gel. The stacking gel was removed and the proteins were subsequently blotted onto a nitrocellulose membrane. The blot chamber containing the blot sandwich and transfer buffer was placed inside a box filled with crushed ice to prevent too much heat and thus destroying the proteins. The procedure was optimized to a blotting time of 2h at 250mA. After the blotting procedure the membrane was stained using Ponceau S to control the protein transfer. The membrane was blocked for 30min in blocking solution with several changes of solution. Afterwards the primary antibodies (mOtof 1600, rb α - β -Actin 1:6000, rb α -Tubulin 1:2500, rb α -GFP 1:1000), were diluted in blocking solution and incubated over night at 4°C under shaking. Next day the membrane was washed with PBS to remove unbound primary antibody and subsequently treated with horse radish peroxidase coupled secondary antibody diluted in blocking solution (1:5000). The membrane was incubated for 1h under shaking. After several washing steps with PBST the membrane was developed using a two component system (Pierce® ECL Plus Western Blotting Substrate, Thermo Scientific). Developing time was 10min in total, a picture was taken every 30secs and the luminescence of every picture was summed up.

The intensity of each band, otoferlin as well as loading control bands, was analyzed using *ImageJ* software.

4 Results

4.1 The mRNA level in *Otof*^{A515T/I515T} mice is not reduced compared to wild type mice

A single point mutation changing isoleucine to threonine leads in humans to temperature sensitive hearing loss. At normal body temperature patients have already impaired speech recognition but almost normal pure tone hearing (Varga et al., 2006a). An increase in body temperature by as little as 1°C, for example during sports or fever, leads to severe to profound deafness. The reason for that phenotype is not yet understood. A mouse line was generated carrying the named mutation to investigate the reason for temperature dependent hearing loss (Strenzke et al., 2016). At normal body temperature otoferlin protein levels are reduced by 65% what made us wonder if a reduced mRNA level could be the reason. In combination with a maybe less stable version of the protein this could lead to an otoferlin amount below a certain threshold. First I checked whether the amount of RNA of both wildtype otoferlin and the mutated form differs. For that a quantitative Real-Time PCR was performed, using the organs of Corti from wild type and *Otof*^{A515T/I515T} mice. In the first run primers for otoferlin and for TBP were used, in the second run instead of TBP primers bassoon as an inner hair cell protein was measured. Amounts of otoferlin mRNA were normalized to either TBP or bassoon (compare Fig. 4.1). TBP is a stable housekeeping gene which is constantly expressed, bassoon is localized in the inner hair cells, its' expression should not be influenced by the alteration of otoferlin.

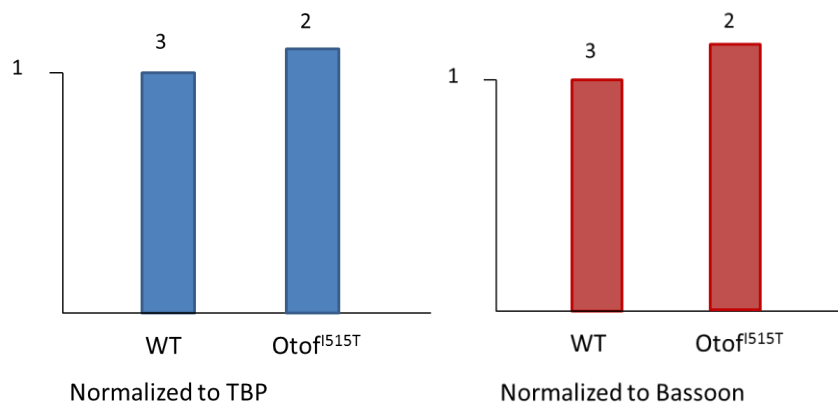


Figure 4.1: Results of quantitative Real-Time PCR. Numbers above bar graphs show count of used mice. Left in blue is otoferlin normalized to TATA-binding-protein, right in red is otoferlin normalized to Bassoon as an inner ear protein.

Although for *Otof*^{f515T/f515T} mice the organs of Corti of only two mice were used compared to three organs of Corti coming from wildtype mice the results are still useful. The amount of mutated otoferlin is not decreased as expected but in contrast slightly increased compared to wild type otoferlin.

4.2 HEK cells were transfected with otoferlin constructs

Transfected HEK cells express wild type otoferlin

HEK cells up to passage 25 were used for transfection experiments. Cells were either transfected with wildtype otoferlin or with a deletion construct with one C₂ domain missing. Cells transfected with wildtype otoferlin functioned as a control. Since the transfected vector in addition to otoferlin also contained GFP, that protein was also stained and functioned as a transfection control. For immunostainings N-terminal otoferlin antibody from Abcam and GFP antibody from Invitrogen were used. Fig. 4.2 shows two images of stained cells transfected with

an otoferlin/GFP fusion construct. The protein is expressed and distributed through the cell. Since otoferlin and GFP are not separated, the GFP staining excludes the nucleus.

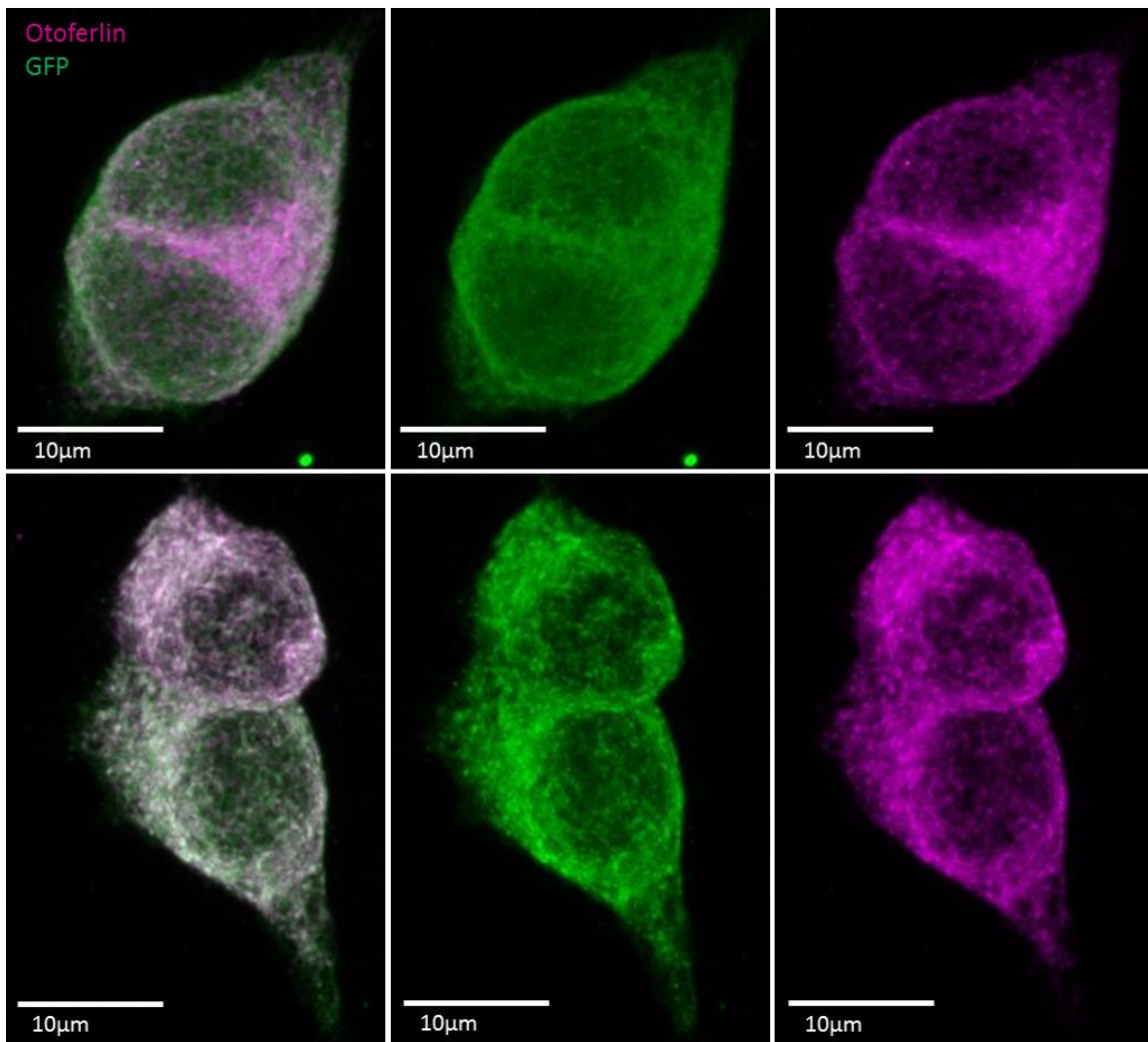


Figure 4.2: Staining of HEK cells transfected with wildtype otoferlin. Left row shows merged images, middle row shows control GFP staining, right row shows otoferlin staining.

Staining of cells transfected with otoferlin deletion constructs

Cells were transfected with different otoferlin deletion constructs and incubated until satisfying confluency was reached, which took between 24h to 48h (compare Fig. 4.3).

Disregarding from cells transfected with otoferlin del C₂C cells look comparable among each other. Also compared to cells transfected with otoferlin wildtype no severe difference is detectable.

For cells transfected with otoferlin del C₂C the GFP staining was normal but no otoferlin staining was detectable. It seems that the Abcam α -otoferlin antibody binds in the C₂C domain and could therefore not detect otoferlin when this domain was deleted.

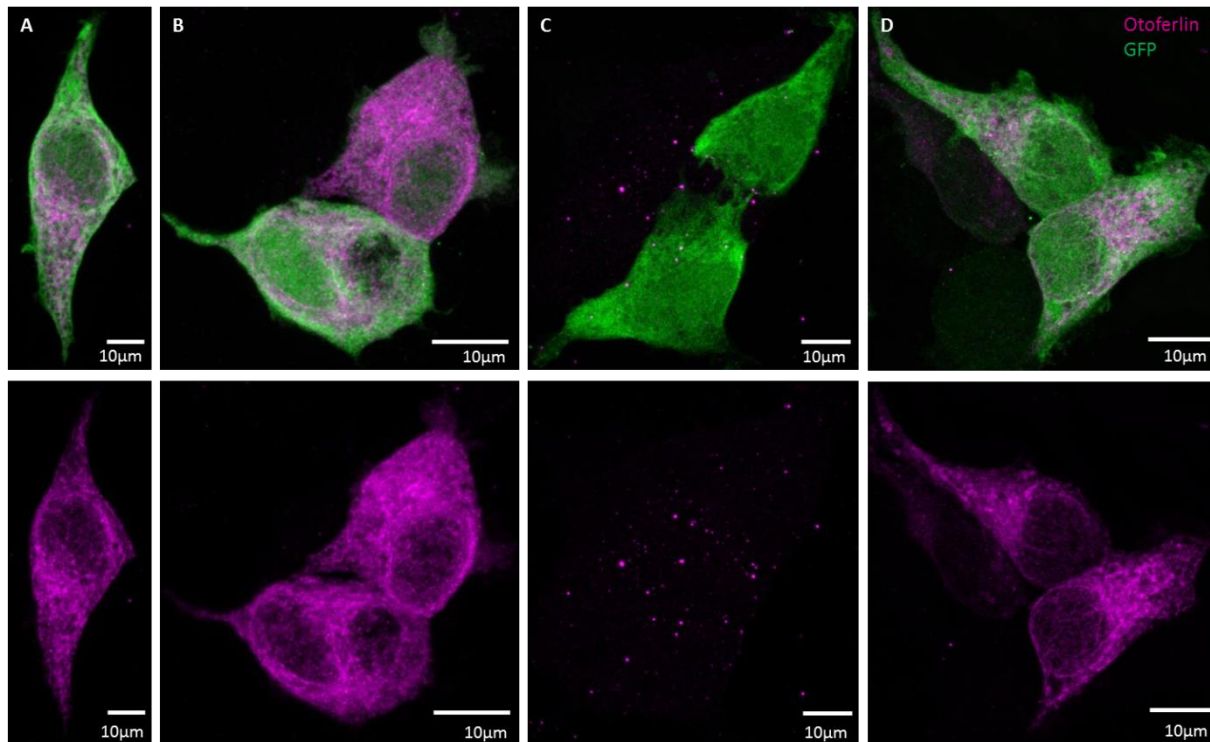


Figure 4.3: Pictures showing immunofluorescence stainings of HEK cells transfected with different otoferlin deletion constructs stained against otoferlin and GFP. Top row shows merged images, bottom row shows otoferlin staining alone. **A)** HEK cells transfected with otoferlin del C₂A **B)** HEK cells transfected with otoferlin C₂B **C)** HEK cells transfected with otoferlin C₂C **D)** HEK cells transfected with otoferlin C₂F

4.3 Western Blots with transfected HEK cell lysates

In addition to staining of transfected HEK cells an amount of 1.000.000 cells were used for generating cell lysates for Western Blot. Cells were transfected with wildtype otoferlin, either as a fusion construct between otoferlin and GFP (otoferlin w/o SC, compare also Fig. 4.2) or as a construct with a stop codon in between (otoferlin + SC), leading to two separated proteins. Furthermore, HEK cell lysates transfected with otoferlin constructs with a missing C₂ domain were used. After blotting, the membrane was treated with C-terminal otoferlin antibody (SynapticSystems) which did not show any signal. After treatment with N-terminal α -otoferlin (Abcam) and α -GFP antibody clear bands at the size of otoferlin (~230kDa) and fainter bands at the size of GFP (~55kDa) were visible. In the lane with cells transfected with otoferlin del C₂C no otoferlin band is visible but a band at the size of GFP (compare Fig 4.4).

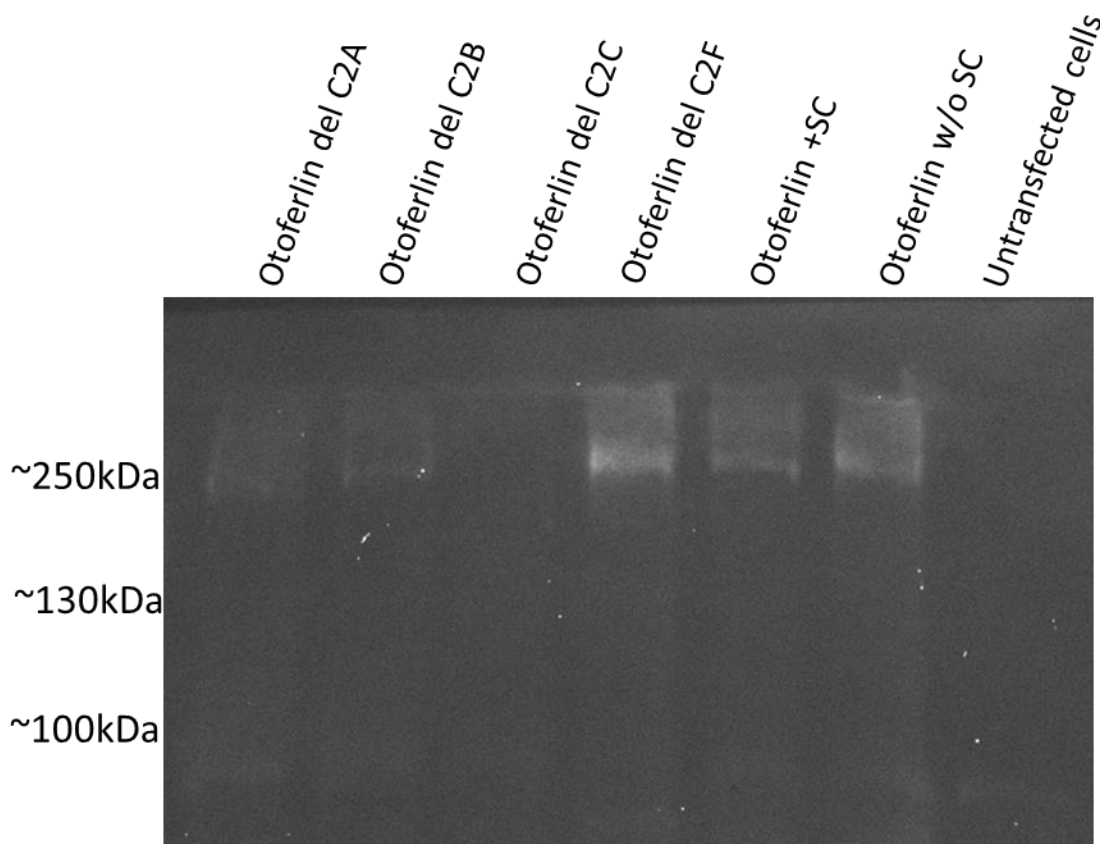


Figure 4.4: Western Blot of different HEK cell lysates.

4.4 Immunostainings of organs of Corti from HA sumo mice

An occurring mutation in the C₂F domain of otoferlin is the so called pachanga mutation which mutates a possible sumoylation site. For that reason I wanted to test whether otoferlin is sumoylated or not. I performed immunofluorescence stainings of *His₆-HA-SUMO1* (kind gift of Marilyn Tirard, Max-Planck-Institut für experimentelle Medizin, Göttingen) (compare Fig. 4.5). In this mouse line sumoylations have a hemagglutinin (HA) tag which makes it possible to check for them by simple immunostainings using an HA antibody.

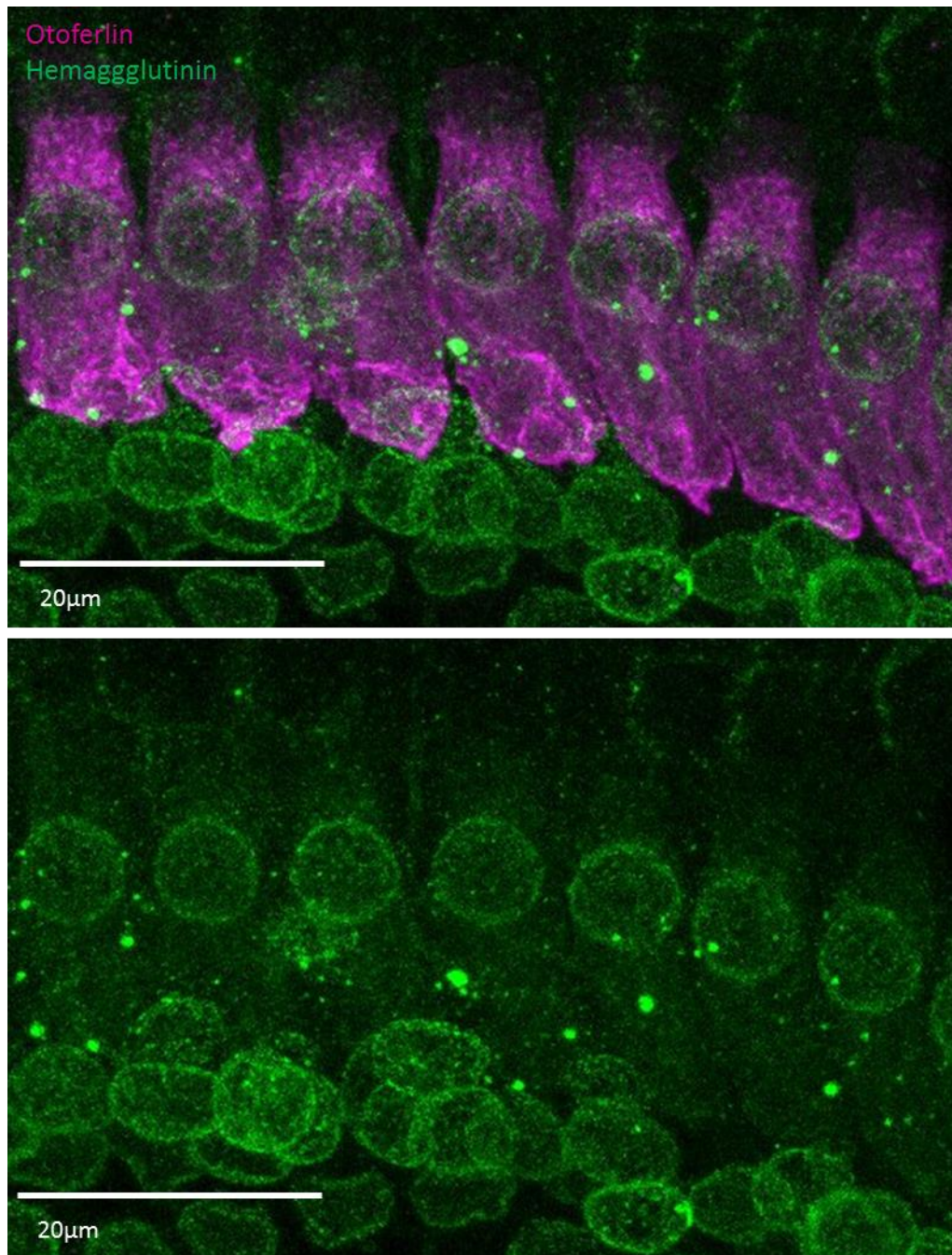


Figure 4.5: Projection of single slices of immunofluorescent stained inner hair cells from *His₆-HA-SUMO1*. Top stained against otoferlin and hemagglutinin, bottom hemagglutinin staining alone.

The stainings revealed that sumoylations can be found in the nuclei as expected but not distributed through the cell like it would be the case when otoferlin was sumoylated.

4.5 Proximity ligation assay to check for possible interaction partners of otoferlin

Not much is known about otoferlin interaction partners. To identify possible candidates a pull down assay using brain lysate and a His/Strep tagged C₂ABC protein was done (Sandra Meese, Department of Molecular Structural Biology, Göttingen and Sunit Mandad, Bioanalytical Mass Spectrometry, Göttingen) and revealed, amongst other proteins, dynamin and OPA1. To strengthen the hypothesis of an interaction partner I performed proximity ligation assays (PLA). This immune based assay results in a fluorescent signal when the two PLA probes, which are coupled to the secondary antibodies, bind in a distance of 40nm or less. To make it easier to find the inner hair cells in the mounted organ of Corti, Phalloidin or α -calbindin antibody was added. In the mounting medium DAPI was included which stains the nuclei. Different combinations of antibodies were used as well as otoferlin in combination with α -OPA1 and α -dynamin 1/2/3.

Those four antibody combinations bound to proteins which are either interacting, in a proximity closer than 40nm or are even the same protein (mCtBP2 + rbCtBP2, mOtof + rbOtof) and were for those reasons planned as positive controls. Since those proteins are only present in the cells it was anticipated that the signals will be restricted to the cells what is obviously not the case for every signal. Immunostainings of the tested controls are shown in Fig. 4.6.

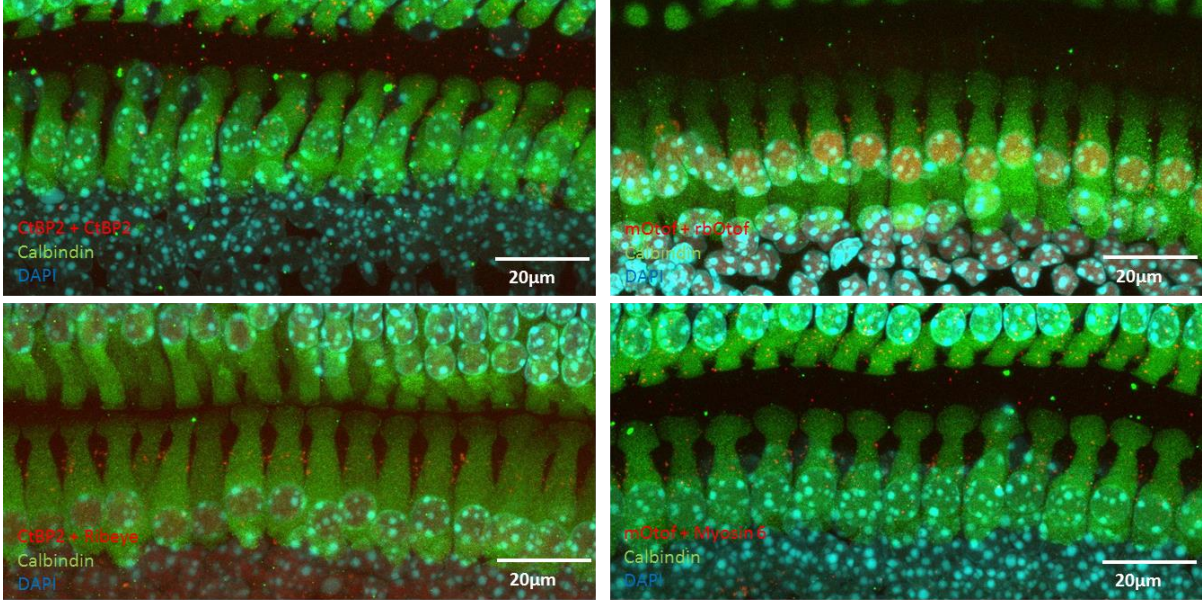


Figure 4.6: Shown are three different PLAs, each additionally stained with α -calbindin (green) and DAPI (blue), the antibody pair for a PLA signal is indicated in the pictures.

Nevertheless, in Fig. 4.7 it is shown that for every used antibody pair indeed signals can be found inside the cell. That we also have signals outside or between cells is maybe due to one poor of the two antibodies so that they are not always binding properly and not leading to a reliable signal.

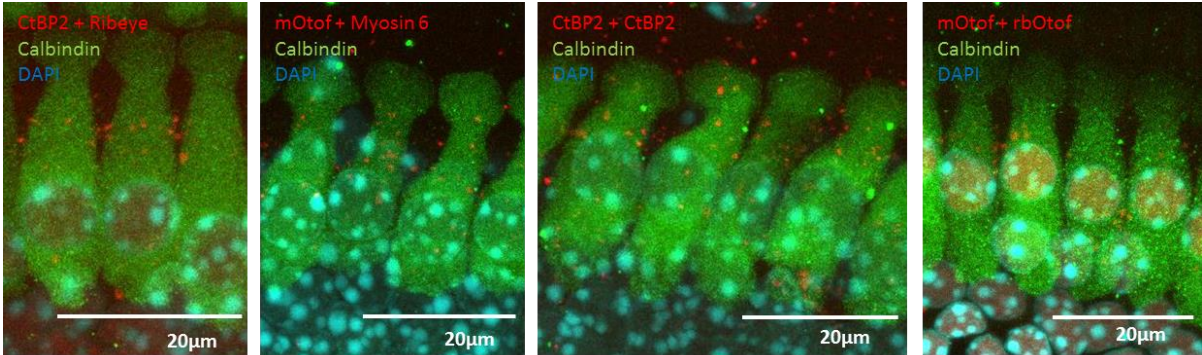


Figure 4.7: Enlarged cutouts from PLA control pictures showing that with every used antibody pair some signals are inside inner hair cells

Anyway, I felt positive about going on and using PLAs for finding possible interaction partners of otoferlin using α -OPA1 and α -dynamin 1/2/3 antibodies.

Proximity ligation assays with otoferlin and dynamin results in fluorescent spots disregarding the used K^+ -concentration and the incubation temperature

For otoferlin together with dynamin as well as otoferlin with OPA1 the hypothesis was that during stimulation of exocytosis of the sample more proteins interact which should lead to more fluorescent spots. So the sample was treated with three different solutions differing in their K^+ -concentration. The inhibitory solution contained fewest K^+ (5mM) whereas the long excitatory solution contained the most (50mM). In between these two values was the mild excitatory solution (40mM).

In all samples red signals indicating close proximity of otoferlin and dynamin are visible. The hypothesis was that the amount of signals differs according to the applied Ca^{2+} -concentration. Just looking at the pictures revealed that the number of fluorescent spots does not differ as much as expected. Instead of an antibody for Calbindin I used Phalloidin which is not staining the entire hair cell but only F-Actin rich regions. For that reason it cannot be said if the signals are restricted to inner hair cells or if they are also in between cells as it was in the controls. The results of those experiments are shown in Fig. 4.8.

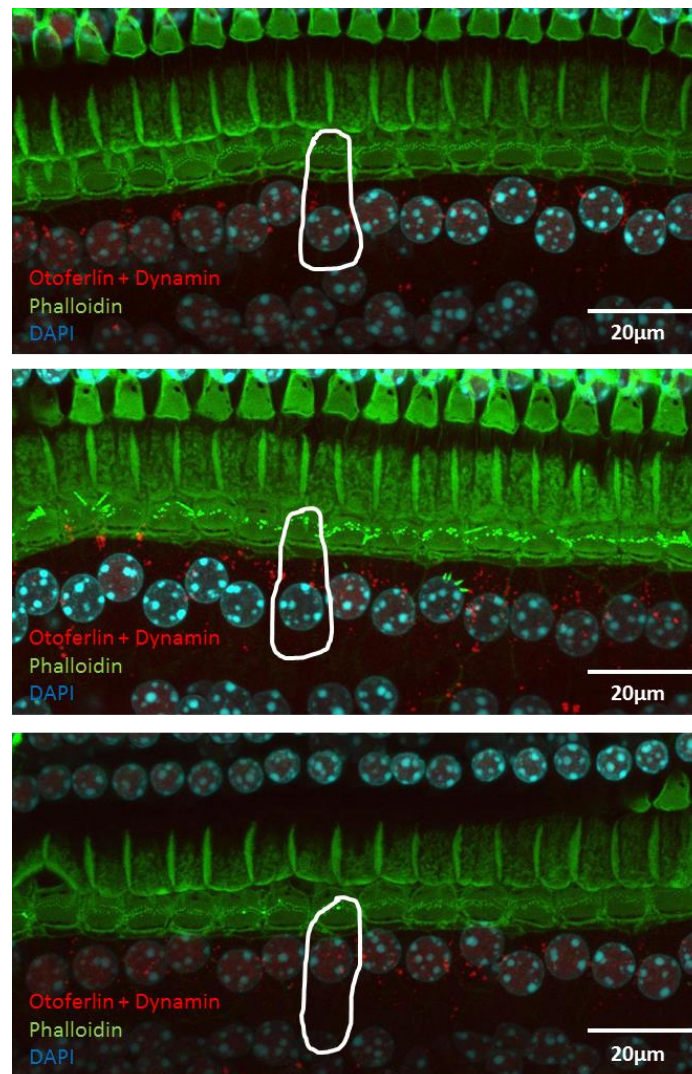


Figure 4.8: Shown are three PLAs performed in different solutions (from top to bottom 5mM K⁺, 40mM K⁺, 50mM K⁺). A single inner hair cell is circled in white.

Further I wanted to know if the incubation temperature has any influence on the proximity of otoferlin and dynamin, so I incubated samples in 40K⁺-solution at room temperature as well as 37°C. The most spots were expected for 37°C in combination with the mild stimulation solution, the fewest when organ of Corti was treated with inhibitory solution. By looking at the different pictures it is visible that signals are not equally distributed through the sample, at some spots a lot signals seem to cluster together whereas at other parts no spots could be detected. This is the same for all used conditions (compare Fig. 4.9). This, taken together with results from

experiments with different solutions (compare Fig. 4.8), made me decide that this antibody combination will not lead to reliable results. That's why I decided to go on with PLAs using otoferlin and OPA1.

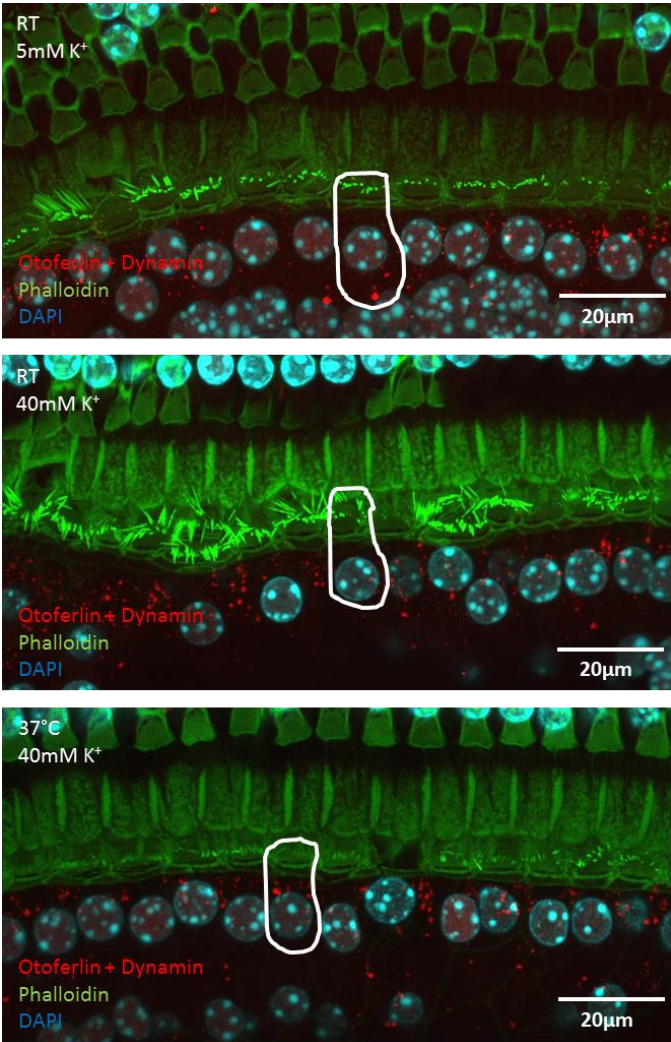


Figure 4.9: Shown are three PLAs performed in inhibitory or mild stimulation solution and either at room temperature or at 37°C (see indications in pictures)

Proximity ligation assay of otoferlin and OPA1 results in fluorescent spots

PLAs performed in the inhibitory solution lead to only very few signals which are mostly not inside the cells but between them. However, more signals can be found in cells stimulated with the mild excitatory solution. Again, some signals are inside the cells and some are in between them.

PLAs were performed with an α -Calbindin staining additionally and in inhibitory as well as in mild excitatory stimulation solution. Results of those experiments are shown in Fig. 4.10.

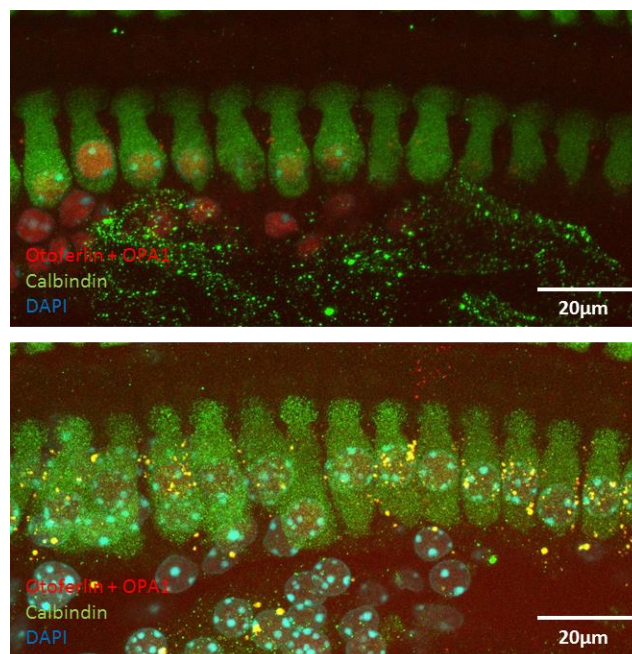


Figure 4.10: Shown are two PLAs of otoferlin and OPA1 performed in different solutions (5K⁺ on top, 40K⁺ on the bottom).

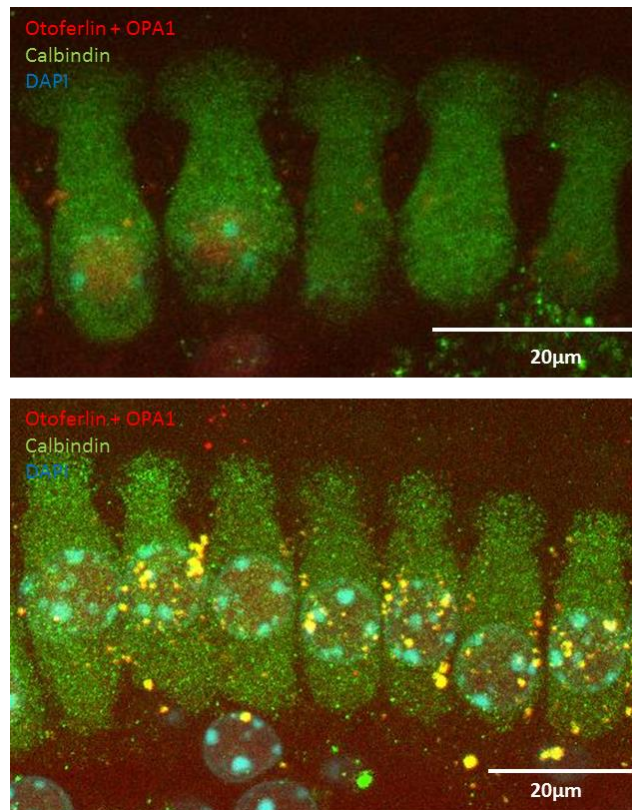


Figure 4.11: Enlarged cutout of PLAs performed with α -otofelin and α -OPA1 antibodies. Signals can be found in the cells as well as between them.

Same as already seen in the controls, signals could be observed in the cells as well as between them.

Since PLAs did not show reliable results and it turned out in the meantime by yeast two-hybrid experiments (performed by Sarah Helfmann, InnerEarLab, Molecular Biology of Cochlear Neurotransmission), that neither OPA1 nor any dynamin seemed to interact with otoferlin I gave up on those experiments.

4.6 Measuring the reduction of wild type and mutated otoferlin protein over 2h via mass spectrometry showed little difference

A few point mutation in otoferlin, namely I515T, G541S, G614E, R1080P, R1607W and E1804del, lead to temperature sensitive hearing loss. The reason for deafness occurring with elevated body temperature is not yet clear and since every mutation is located throughout the whole protein it is very unlikely that all have the same cause. One hypothesis was that the mutation makes one or more of the mutated proteins instable and it is degraded faster over time. I blocked the protein biosynthesis using Cycloheximide so that no new protein could be synthesized. Because of the reason that patients with any of those mutations become deaf within a very short time span as soon as the body temperature rises I decided to examine degradation over 2h at 37°C and 38.5°C using mass spectrometry. The amount of otoferlin was compared to stable background proteins, namely Spag9, Top2b, Brd4, and Uba52, which were chosen in cooperation with Kuan-Ting Pan (Research Group Mass Spectrometry, Max Plank Institute for biophysical chemistry, Göttingen). In addition to the mentioned mutations I also analyzed otoferlin with the pachanga mutation which results in lesser protein compared to the wildtype and complete deafness. Although it was planned to also investigate cells transfected with cDNA of otoferlin E1804del this did not work out due to transfection problems. After transfecting HEK cells with that cDNA cells tended to die or grew very slow. The mutations G614E and R1080P were not tested at all.

Shown in Fig. 4.12 is the amount of wildtype otoferlin either at 37°C or at 38.5°C. Higher temperature in this figure as well as in the next is always displayed in darker red. After two hours of incubation the amount did hardly change which shows that otoferlin seems to be more stable than expected. At every measured time point the amount of wildtype otoferlin at 37°C is comparable to the amount at elevated temperature.

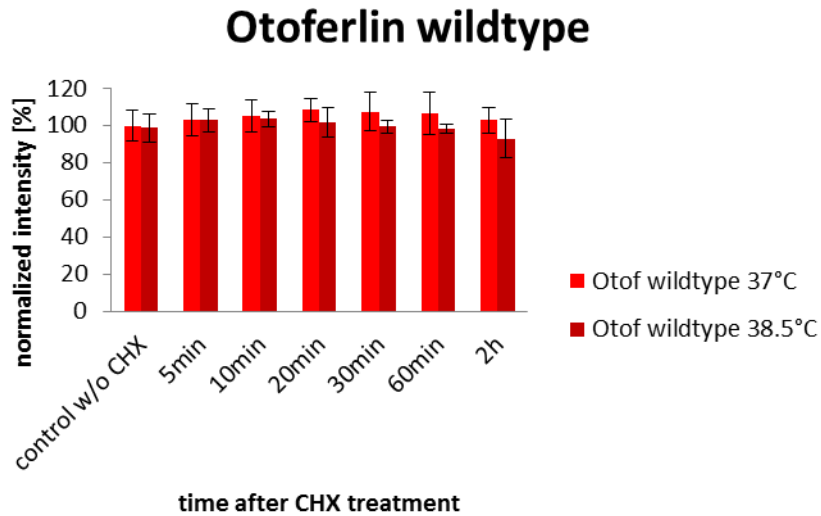


Figure 4.12: Degradation of wildtype otoferlin at 37°C and 38.5°C over 2h after CHX treatment

In Fig. 4.13 the protein quantity of the four used muted forms of otoferlin is shown always compared to wildtype otoferlin in red at 37°C and darker red at elevated temperature (same color code as Fig. 4.12). The amount of protein in all mutants was normalized to the amount of wildtype otoferlin incubated at 37°C.

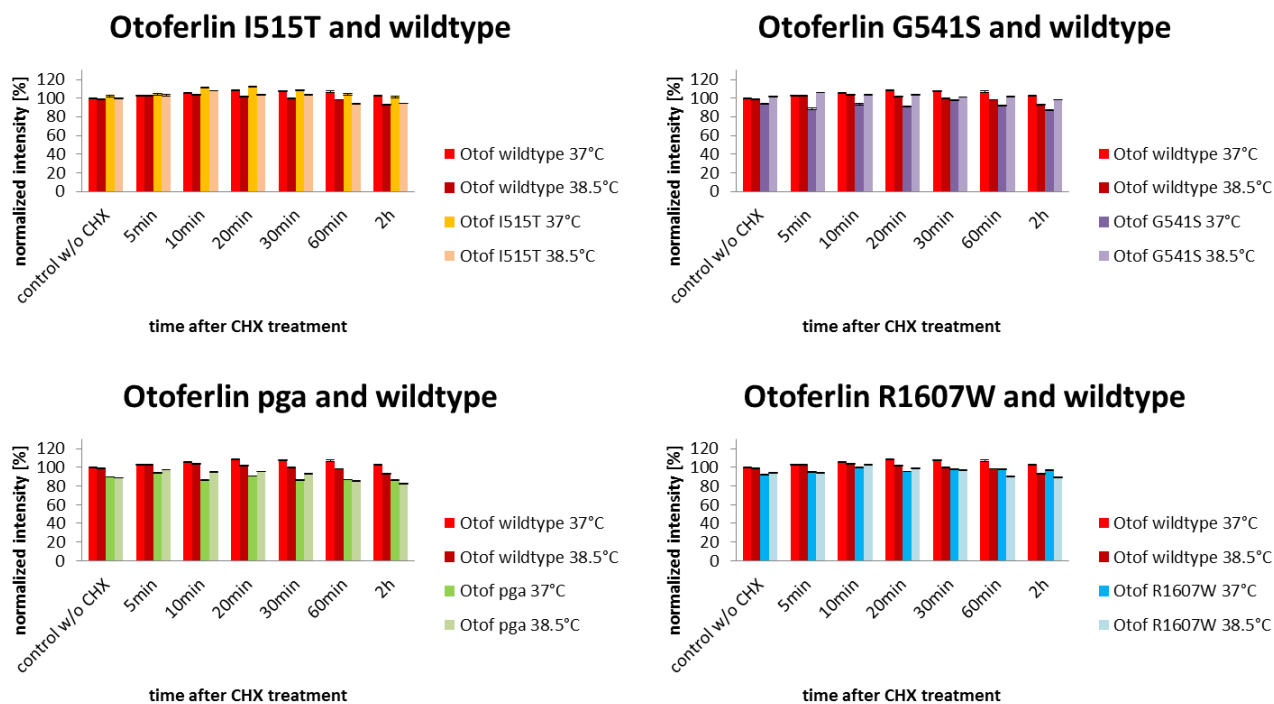


Figure 4.13: Displayed are the results of mass spectrometry data over 2h in four bar graph charts, each showing the normalized intensity of wildtype otofelin (in red) and one temperature sensitive (I515T, G541S, R1607W) or pachanga mutation. Error bars show SEM, n=3

The amount of otofelin carrying the I515T mutation, shown in yellow colors, does neither change much in the investigated time range nor is it lower compared to levels of not mutated otofelin. Anyway, the amount of this mutated otofelin form is always comparable to wild type otofelin. A trend to a decreased level after two hours can be adumbrated. The normalized intensity after 2h for 37°C and 38.5°C is 101.2 and 94.1 respectively.

Shown in purple colors is the amount of otofelin protein with the G541S mutation. A trend towards slightly lower levels at 37°C compared to elevated temperature could be seen but taking the error bars into count it cannot be proven. Comparing the amount to wild type otofelin levels no drastic change could be observed. The normalized intensity after two hours for 37°C and 38.5°C is 87.1 and 98.2.

The amount of protein carrying the pachanga mutation is shown in green colors. Same as for otoferlin with the G541S mutation, the quantity of protein with the pachanga mutation seems to be lower without looking at the error bars. But giving consideration to those the change is not drastically and the amount of mutated otoferlin is again comparable to the wild type form. The normalized intensity after two hours of incubation is 85.9 and 82.4 for 37°C and 38.5°C respectively.

The amount of otoferlin carrying the R1607W mutation is displayed in blue colors. The amount of mutated otoferlin at 38.5°C is over the investigated time comparable to those at 37°C. In addition the amounts of otoferlin with the R1607W mutation is comparable to wild type otoferlin over the two hours of incubation. The normalized intensity after two hours of incubation is 96.4 and 89.2 for 37°C and 38.5°C respectively.

Taken together I showed that none of the tested mutated forms of otoferlin degrades rapidly, hinting that fast degradation at elevated temperature does not seem to be the reason for temperature sensitive hearing loss. Nevertheless I was interested on the behavior of mutated forms of otoferlin at elevated temperature, so I performed another set of HEK cell transfection with cDNA of wild type otoferlin and carrying the I515T mutation with incubation time over 24h.

4.7 Measuring the reduction of wildtype otoferlin and otoferlin I515T protein over 24h using mass spectrometry showed little difference

Since otoferlin was not drastically degraded after 2h of incubation, I decided to incubate wildtype and otoferlin I515T transfected cells for up to 24h to have a good hint on possible degradation mechanisms as well as half life time. The other mutations were left out because the I515T mutation was the most interesting one to study and to compare with recent data.

Experiments were conducted as previously, medium of HEK cells with satisfying confluency was supplemented with 100 μ g/ml Cycloheximide and cells were incubated at either 37°C or 38.5°C. The results (see Fig. 4.14) show that after 24h incubation protein levels neither of otoferlin wildtype nor of otoferlin I515T changed as we expected.

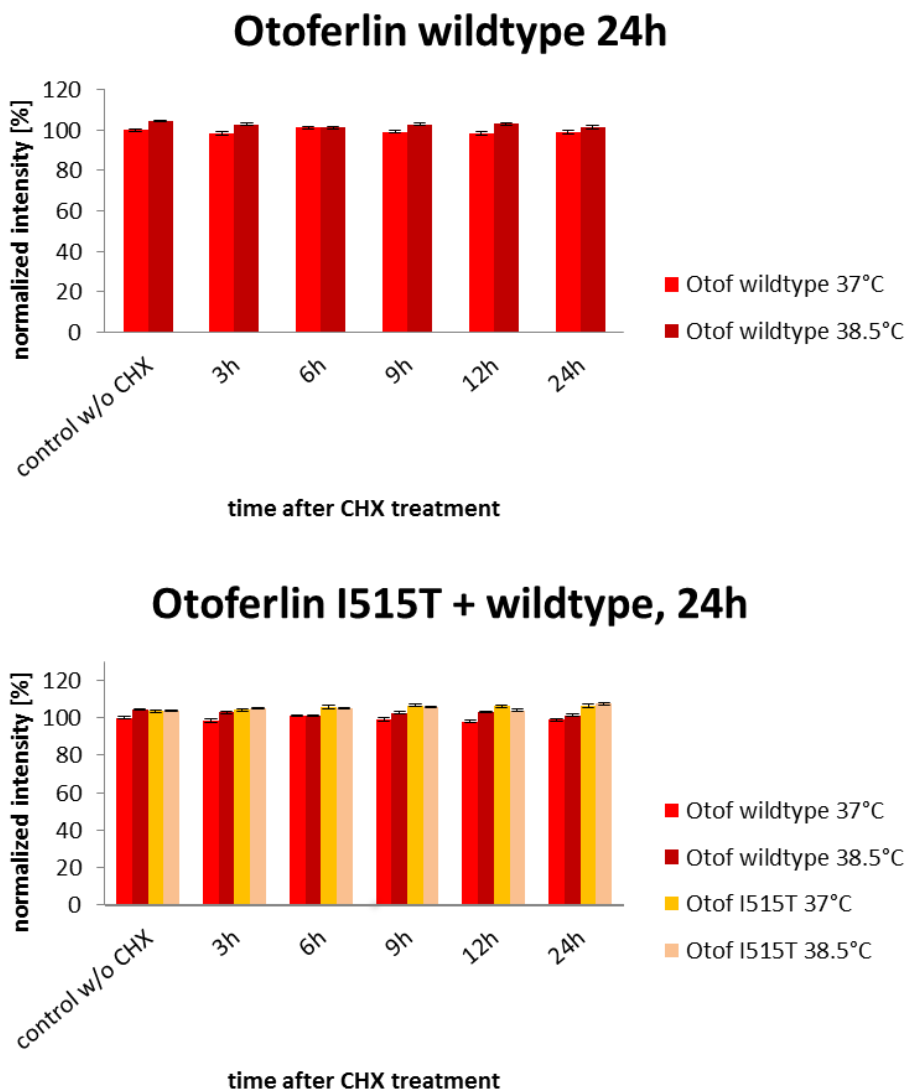


Figure 4.14: Results of mass spectrometry analysis of otoferlin wildtype and otoferlin I515T mutation showing normalized intensity. Error bars show SEM, n=3

Protein levels of otoferlin wildtype incubated at elevated temperature comparably to otoferlin protein levels from 37°C, if anything showing a slight trend towards higher levels. Otoferlin I515T protein levels also did not show great reduction and only irrelevant differences between different temperatures could be determined. Compared to wildtype otoferlin protein levels, protein levels of the mutated form are comparable as well.

4.8 Differences between mouse and human otoferlin

Verification of the otoferlin form present in mouse organs of Corti

So far it was never checked for the otoferlin sequence in mouse organs of Corti by experiments. In public databases several sequences could be found like RefSeqs (reference sequence) variant 1, variant 2 or several computed mRNA sequence of predicted otoferlin isoforms, one of those was congruent with the otoferlin cDNA subcloned in our lab from organ of Corti cDNA. Alignment of the two RefSeq variants and our lab clone showed that in variant 1 a short amino acid stretch is present whereas it is absent in the other two isoforms (compare Fig. 4.15 A). I generated cDNA from mouse organs of Corti and performed a PCR using primers which bind upstream and downstream of amino acid 168, the sequence under question. After agarose gel electrophoresis (compare Fig. 4.15 C) I expected a band either of the product size of 155bp for transcript variants 2 and cochlear otoferlin or 200bp for variant 1. The PCR reveals an intense band at the size of the smaller product.

Mouse otoferlin lacks one amino acid stretch which is present in humans

Patients carrying the otoferlin I515T mutation already have a severe hearing phenotype at normal body temperature and become deaf rapidly when the body temperature rises. However, mice having the same mutation in otoferlin are not deaf at elevated body temperature. This fact made us wonder whether there is a difference in the sequence of mouse

and human otoferlin explaining that. A *CLUSTAL 2.1* alignment was made including otoferlin of different species and three variants of mouse otoferlin (compare Fig. 4.15 B). Using cDNA of mouse organs of Corti a PCR was performed using primers binding upstream and downstream of amino acid 1242 in mouse variant 4. This results either in a product size of 148bp for variants 1 and 4 or 208bp for transcript variant 2. The PCR reveals an intense band at the size of the smaller product (compare Fig. 4.15 C).

A

```

human      163 PGEKSFR-----RAGRSVFSAMKLGKNRSHKEEPQRPDEPAVLEMED 204
bos        163 SGEKSFR-----RAGRSVFSAMKLGKNRPHKEEPQQRQDEPAVLEMED 204
rat        163 PGEKSFR-----RAGRSVFSAMKLGKTRSHKEEPQQRQDEPAVLEMED 204
mouse var2 162 SGEKSFR-----RAGRSVFSAMKLGKTRSHKEEPQQRQDEPAVLEMED 203
mouse var4 162 SGEKSFR-----RAGRSVFSAMKLGKTRSHKEEPQQRQDEPAVLEMED 203
mouse var1 162 SGEKSFRSKGREKTKGGRDGEHKAGRSVFSAMKLGKTRSHKEEPQQRQDEPAVLEMED 218
Xenopus    173 SGERAFK-----RVGKGVFSAMKLGKTRPPKDESQRQDEPAVLETED 215
gallus     172 STERSFR-----RAGKGVFSAMKLGKARPTKDDHRKQDEPAVLEAED 214
          . *::*:          :*::***** * . *:: : : *****

```

B

```

human      1234 PDRSAPSWNTTVRLLRRCRVLCNNGSSSHSTGEVVVTMEPEVPPIKKLETMVKLD 1287
bos        1234 PDRSAPNWNTSGRLLQGRRLYSGGSSSRLTGEVVVSMEPEVPPIKKLETMVKLD 1287
rat        1234 PDRSAANWNTTVRLLRGYHMLCNGGSSSPTGEVVVSMEPEVPVKKLETIVKLD 1287
mouse var2 1233 PDRSAPNWNTTVRLLRGCHRLRNGGSSSRPTGEVVVSMEPEEPVKKLETMVKLD 1286
mouse var4 1233 PDRSAPNWNT-----TGEVVVSMEPEEPVKKLETMVKLD 1266
mouse var1 1248 PDRSAPNWNT-----TGEVVVSMEPEEPVKKLETMVKLD 1281
Xenopus    1246 PDKNSQQWTTAAKLMNGYLAMTNGRPRSRTTGEIVINMEPEAPVKKMETMVKLE 1299
gallus     1245 PDKKAQHWNT-----MTGEIIVNMEPEVPPIKKMETMVKLE 1278
          **::: * .          ***** : ***** *::*:*****:

```

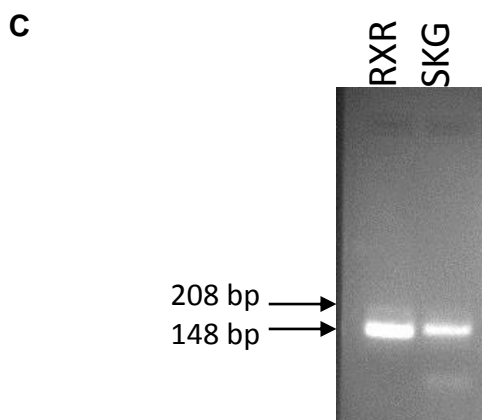


Figure 4.15: Shown are sequence variations of otoferlin across different species and three different mouse variants (Human otoferlin, NP_001274418.1; *Bos Taurus*, NP_001137579.1; *Mus musculus* transcript variant 4, NM_001313767.1 (cDNA used in our experiments); *Mus musculus* transcript variant 1, NP_001093865.1; *Mus musculus* transcript variant 2, NP_114081.2; *Xenopus*, XP_012826776.1, *Gallus gallus*, XP_004935917.1)(Strenzke et al., 2016). **A**) The presence of the amino acid stretch

SKGREKTKGGRDGEH was tested via PCR and agarose gel electrophoresis (compare **C**). For amplification of the SKG-sequence primers pEGFPN1mOtof del C₂B PCR1, for and pEGFPN1mOtof del C₂A rev were used. **B**) The sequence between C₂D and C₂E was tested for presence or absence of an arginine-rich domain including a RXR-motif using PCR and agarose gel electrophoresis (compare **C**). Primers TCATCTACCGACCTCCAGACC and CACATCCACCTTGACCACAGC were used. **C**) Agarose gel of mentioned PCRs with mouse organ of Corti cDNA from **A** and **B**.

Taken the results of the two PCRs together it seems that mouse cochlear otoferlin misses an amino acid stretch around amino acid 168 (SKGREKTKGGRDGEH) (compare Fig. 4.15 A) as well as a stretch present in human (compare Fig. 4.15 B). Based on these results a new entry to public DNA databases was generated which was named mouse variant 4 (NM_001313767.1).

4.9 Biolistic transfection of inner hair cells using different forms of otoferlin

Optimizing Gene Gun transfection

Regarding age of used mice, diameter of used gold particles (0.6µm, 1µm, 1.6µm), time of incubation after transfection, used pressure and orientation of organ of Corti the whole procedure had to be optimized. For the optimizing procedure I transfected wildtype mice with a construct containing GFP alone. It turned out that transfection with the smallest gold particles lead to very stable but only very few transfected cells and transfecting with particles of 1.6µm in diameter lead to a lot transfected cells of which unfortunately a lot died within a day. Transfecting cells with gold particles of 1µm in diameter lead to results in between which was the reason why that size was chosen for further experiments.

To find the perfect age of mice for transfection it was started with young mice ranging between p2 and p8. It was anticipated that younger mice are easier to transfect and that more tissue could be removed from the cochlea. It turned out that mice at the age of p5 and older were hard to transfect and showed very few transfected cells, same was for the young mice at p3.

However, p4 mice showed more transfected cells than the other mice tested, the fluorescent was in addition stable for up to four days and cells seem to be less destroyed. All the further transfection experiments were conducted with p4 mice.

Transfected organs of Corti were incubated for up to four days to ensure stability of GFP signals in the transfected cells. Daily a few organs of Corti were fixed and stained against GFP and VGlut3. Although not all cells survived the transfection even after four days of incubation cells in a good condition were visible. In the end it was decided to incubate cells for two days, if cells after immunofluorescence staining did not look healthy they were not taken into count for the analysis.

In the first time of the optimizing procedure I tried to transfect inner hair cells by applying the shooting pressure from above. It turned out that most of the gold particles at low pressure (20-50psi) were not able to pass the tectorial membrane and according to that were not able to transfect the cells. The few transfected cells were no inner hair cells and even increasing the pressure rather lead to a damaged organ of Corti than to a sufficient amount of transfected cells. It was tried if flipping the organ of Corti after isolation and before transfection would lead to sufficient results. It turned out, that after increasing the pressure to ~210psi a satisfying amount of inner hair cells was transfected.

To ensure always the same distance between Gene Gun and tissue a self-made tripod with expendable legs was used. The distance between Gene Gun nozzle and organ of Corti could be adjusted to 4cm, 3cm, or 2cm. To keep the stress as low as possible and because it lead to transfected cells I decided to use a distance of 4cm.

The last optimizing step was performed together with Hanan Al-Moyed (Molecular biology of cochlear neurotransmission group). We tried to reduce the effective pressure on the tissue but ensure enough gold particles to transfect the cells. For that we tested different combinations of cell strainers with varying diameters or also single cell strainers (BD Falcon). It turned out that two 40 μ m cell strainers, one glued on top of the other, resulted in the best results. We observed healthy organs of Corti and still transfected cells which express the cDNA very stable.

To sum it all up I used for all my Gene Gun experiments gold particles with a diameter of $1\mu\text{m}$, mice at four days of age and two days of incubation at 37°C after transfection. Cells were transfected after flipping the organ of Corti and using a pressure of $\sim 210\text{psi}$, the distance between tissue and Gene Gun nozzle was ensured by using a tripod, the pressure was minimized by using two $40\mu\text{m}$ meshes. For a better understanding of the experimental set up compare Fig. 4.16.

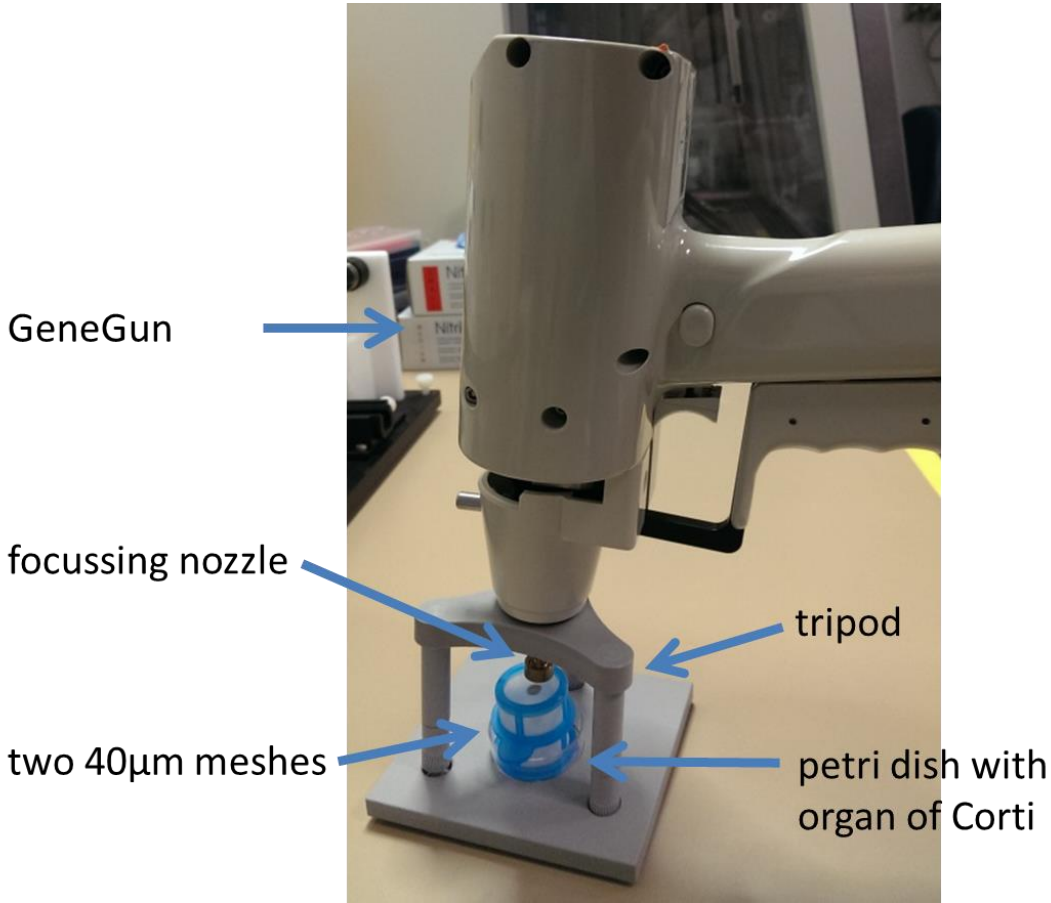


Figure 4.16: Experimental set up for transfecting organs of Corti using Gene Gun

Comparing cells of wild type mice and *Otof*^{-/-} transfected mice shows comparable distribution of otoferlin

After optimizing of the whole transfection procedure regarding age of mice, size of gold particles, time of incubation after transfection, orientation of organ of Corti for the transfection process and incubation duration after transfection, I first started by transfecting organs of Corti of *Otof*^{-/-} mice with cDNA of unaltered otoferlin and compared the protein distribution to those of wild type mice.

Transfected organs of Corti as well as tissue from wild type mice were incubated for two days after transfection or isolation respectively to allow on the one hand transfected cells the expression of the new cDNA and on the other hand attaching of the tissue to the cover slips. After that, immunostainings for VGlut3 and otoferlin were performed and the distribution was distinguished using *Imaris* software implemented by Gerhard Hoch (Institute for Auditory Neuroscience). *Imaris* is a MATLAB based routine which allows it to measure the distribution of fluorescence through an inner hair cell. The routine for that analysis was developed by Gerhard Hoch (Institute for Auditory Neuroscience) and Hanan Al-Moyed (Molecular Biology of Cochlear Neurotransmission) and adapted by me for my experiments. The cell was encircled and the nucleus as well as the most basal part of the cell was marked manually. Subsequently a vector was drawn, bisecting the cell into half from apical to basal. Along that vector five parallel line scans were performed. The marked basal point was determined as the most basal point of the cell that exceeds the threshold value for the summed fluorescence. The threshold for summed fluorescence was set to 5 to quantify the fractional membrane staining of otoferlin. The otoferlin-VGlut3 fluorescence value was then read out and represents the fraction of membrane bound otoferlin (compare section 3.7)

In wildtype cells it is clearly visible that otoferlin is localized in the membrane whereas VGlut3 is not. This was the distribution I was expecting for Gene Gun transfection as well. Staining and comparison of transfected and wild type cells showed that the distribution is a little different (compare Fig. 4.17). Otoferlin membrane staining in transfected cells is not as strong as in wildtype cells but nevertheless comparable regarding the method I was using which made me

go on with further transfection experiments with modified otoferlin cDNA. For exemplary immunofluorescence staining compare Fig. 4.17. *Imaris* analysis is shown in Fig. 4.18.

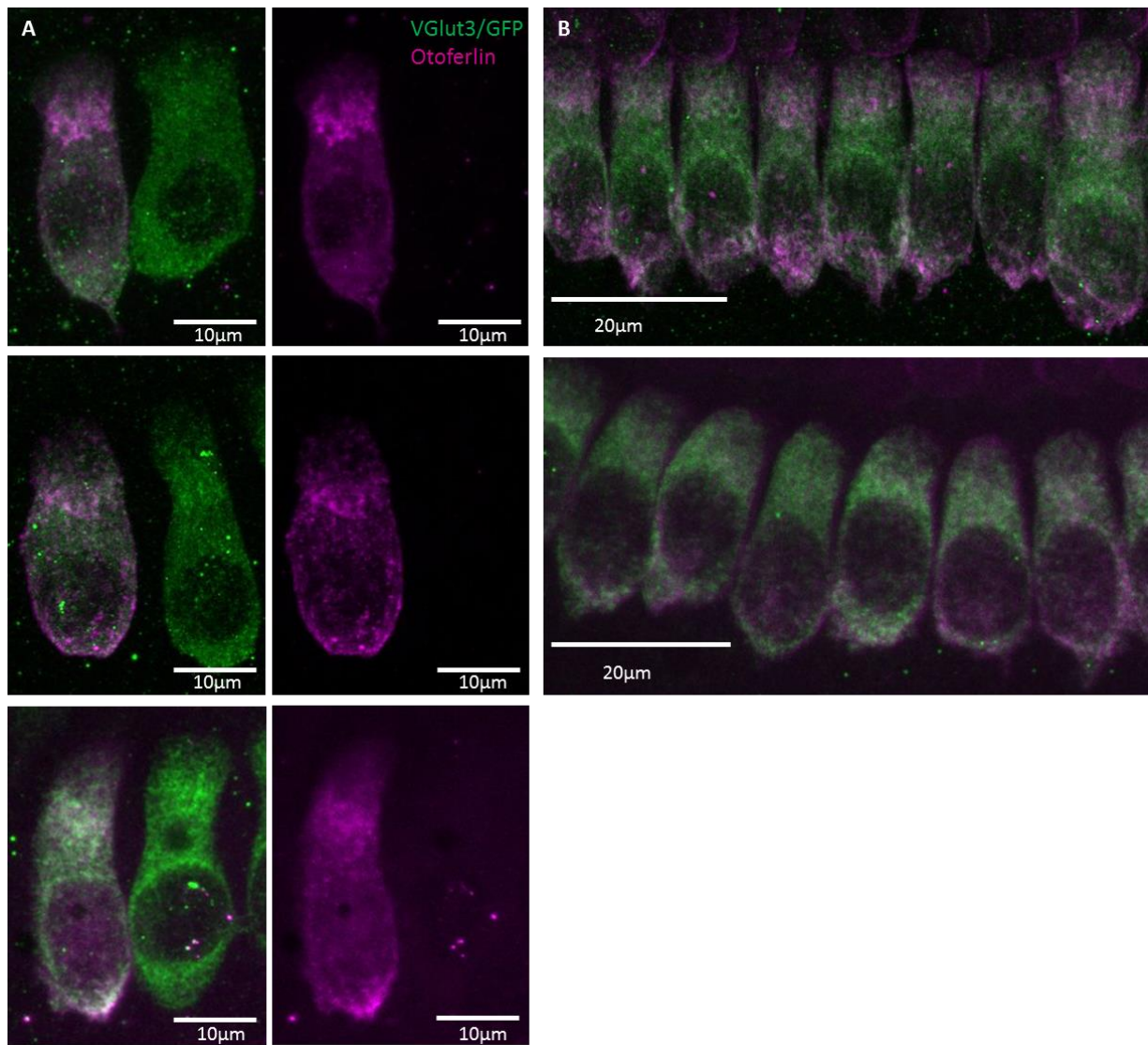
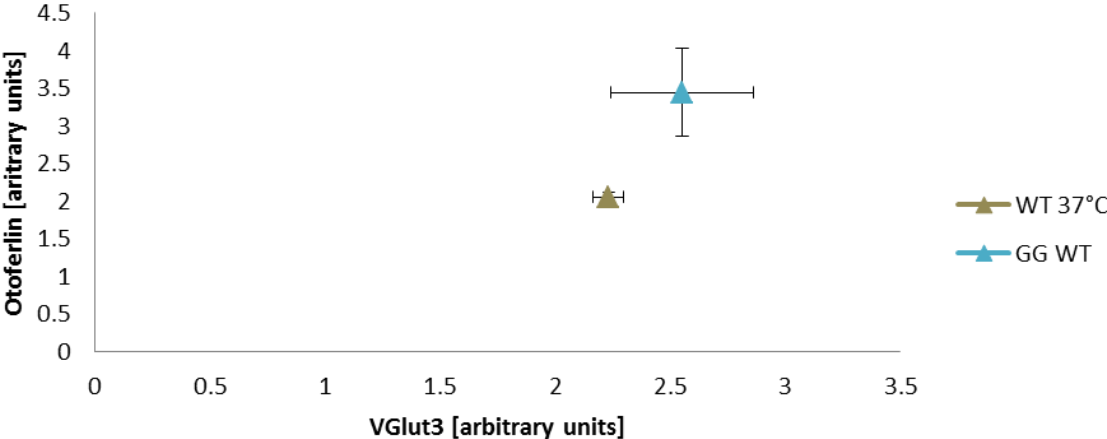


Figure 4.17: Comparison of wild type inner hair cells and with otoferlin cDNA transfected *Otof*^{-/-} cells via Gene Gun. **A)** Organs of Corti were transfected with wild type cDNA of otoferlin and GFP by Gene Gun. Left images show merge of both channels, left shows otoferlin staining alone (**B**) stained inner hair cells from wild type mice, merge of both channels is shown. Gene Gun: n=6, wild type n=213

Ration of apical/basal distribution



Otoferlin membrane distribution

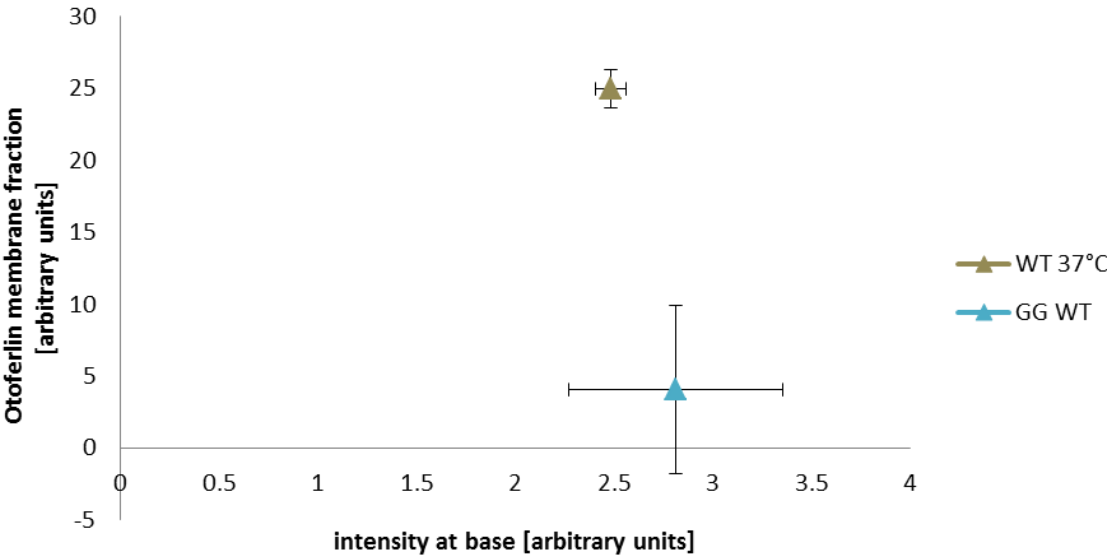


Figure 4.18: Different graphs showing the results of *Imaris* analysis, comparing wild type otoferlin transfected cells and cells from wildtype mice. Error bars show SEM. WT=wildtype, GG=Gene Gun. n=6 (GG WT), n=213 (WT)

***Otof*^{-/-} cells transfected with otoferlin RXR still show otoferlin membrane staining disregarding the incubation temperature**

Because of the difference in sequence between mouse and human otoferlin, mouse otoferlin is missing the arginine rich amino acid stretch containing an RXR motif (compare section 4.8), we wanted to know whether this stretch leads to a difference in membrane localization of otoferlin. For that we transfected organs of Corti and incubated them either at 37°C or additionally at 38.5°C for 30min feigning elevated body temperature. No matter at which temperature the cells were incubated, we did not observe an influence on the membrane localization of otoferlin in immunofluorescence stainings. Same as in *Otof*^{-/-} transfected cells membrane staining is still visible (compare Fig. 4.19).

Evaluation of the *Imaris* analysis (compare Fig. 4.20) revealed that otoferlin is equally distributed, only a slight trend towards lesser otoferlin membrane staining from wildtype transfected cells over otoferlin RXR transfected cells at 37°C and then incubated at elevated temperature could be observed. In addition less otoferlin is present compared to the wild type transfected cells but comparable levels could be seen if cells transfected with mutated otoferlin are compared.

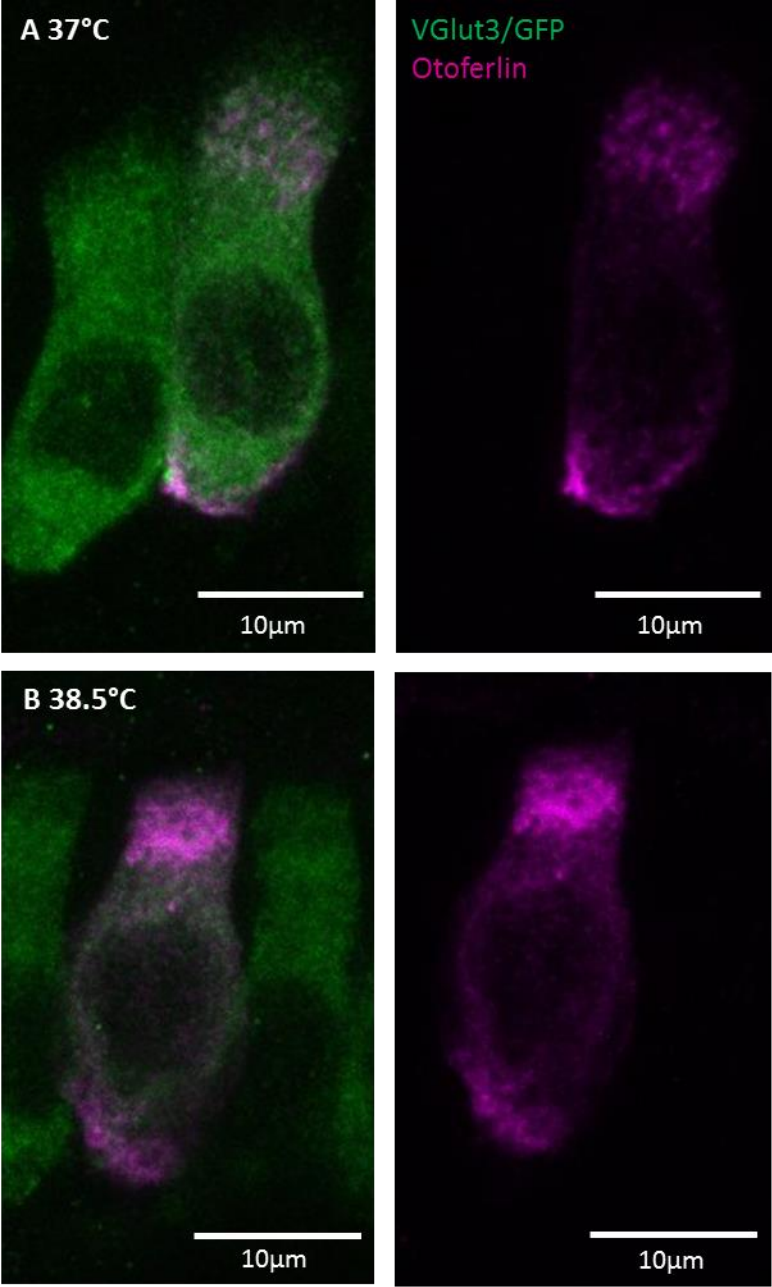


Figure 4.19: Staining of *Otof*^{-/-} transfected inner hair cells with cDNA of otoferlin RXR at different temperatures. **A)** Incubated at 37°C, left merge of both channels, right otoferlin staining. **B)** Incubated at 38.5°C, merge of both channels on the left and otoferlin staining on the right. 37°C n=4, 38.5°C n=4

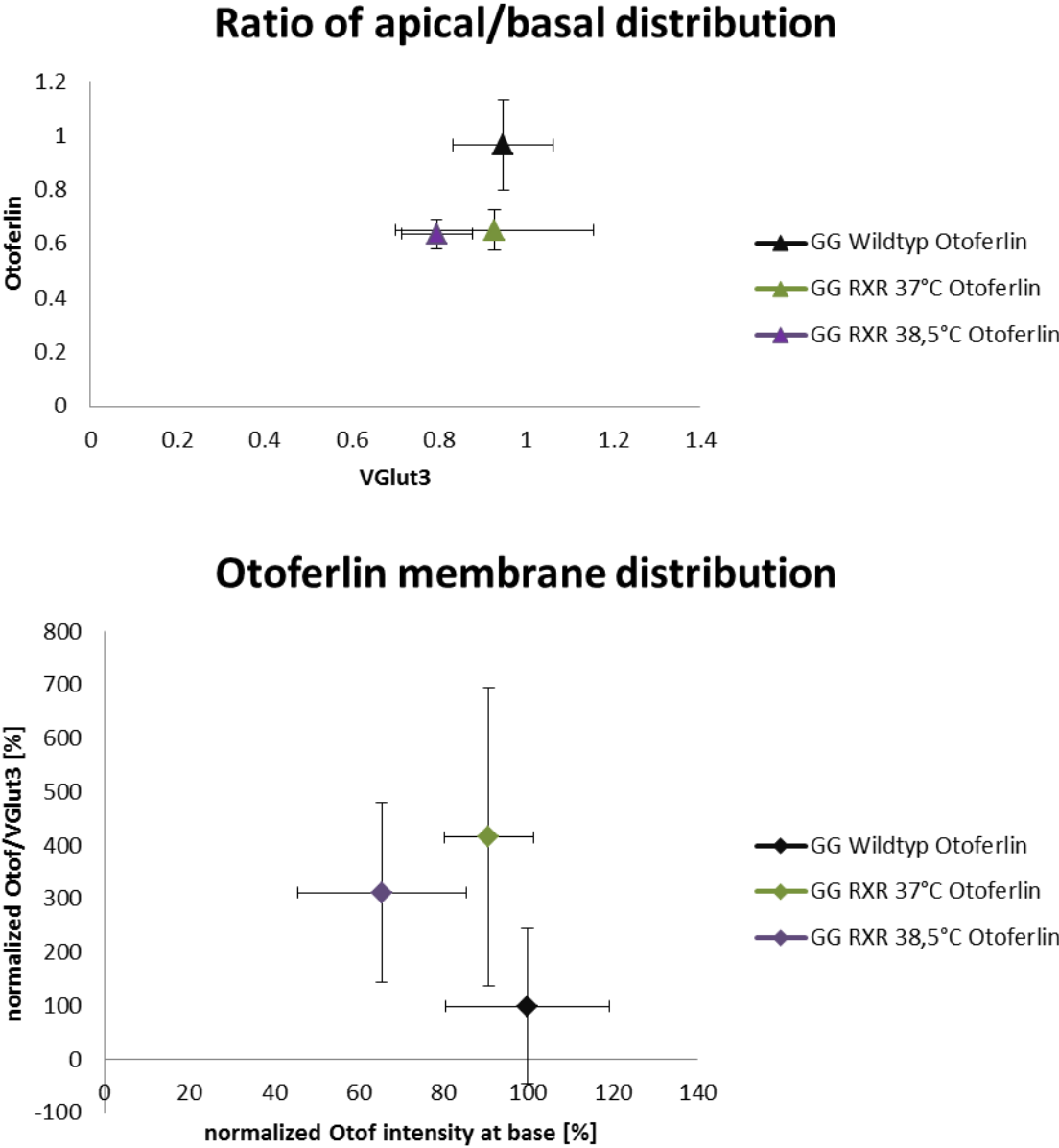


Figure 4.20: Different graphs showing the results of *Imaris* analysis, comparing wild type otoferlin transfected cells and otoferlin RXR transfected cells at 37°C at 38.5°C. Error bars show SEM. GG=Gene Gun, RXR=otoferlin containing RXR motif. n=6 (GG WT), n=4 (RXR 37°C), n=4 (RXR 38.5°C)

After those experiments I cloned another vector containing, in addition to the RXR motif, also the I515T mutation. Inner hair cells of *Otof*^{-/-} mice were again biolistically transfected,

incubated at 37°C and elevated temperature and after immunofluorescence staining analyzed using *Imaris* software.

***Otof*^{-/-} cells transfected with otoferlin I515T RXR show reduced otoferlin membrane staining**

After transfection of *Otof*^{-/-} cells with otoferlin RXR I515T cDNA via Gene Gun, cells were stained after incubation at different temperatures (compare Fig. 4.21), performed accordingly to cells transfected with otoferlin RXR. This revealed that the cells do not show any membrane staining.

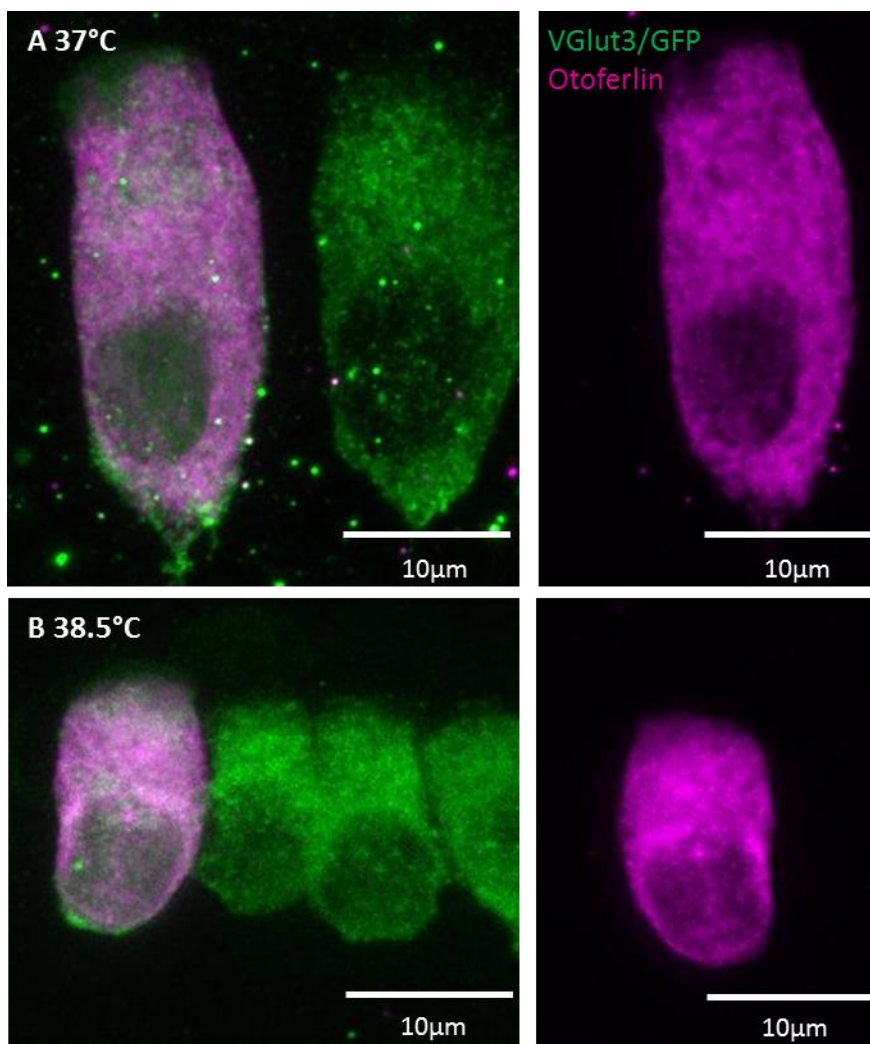


Figure 4.21: Staining of *Otof*^{-/-} transfected inner hair cells with cDNA of otoferlin RXR I515T at different temperatures. **A)** Incubated at 37°C, left merge of both channels, right otoferlin staining. **B)** Incubated at 38.5°C, merge of both channels on the left and otoferlin staining on the right. 37°C n=14, 38.5°C n=7

Analyzing these cells using *Imaris* software confirmed the observation. Having a look at the ratio of apical/basal distribution the amount of with otoferlin RXR I515T mutation transfected cells is lower. Additionally, when looking at the otoferlin membrane distribution the values for transfected cells with mutated otoferlin display negative numbers, showing that no membrane staining could be detected (compare Fig. 4.22).

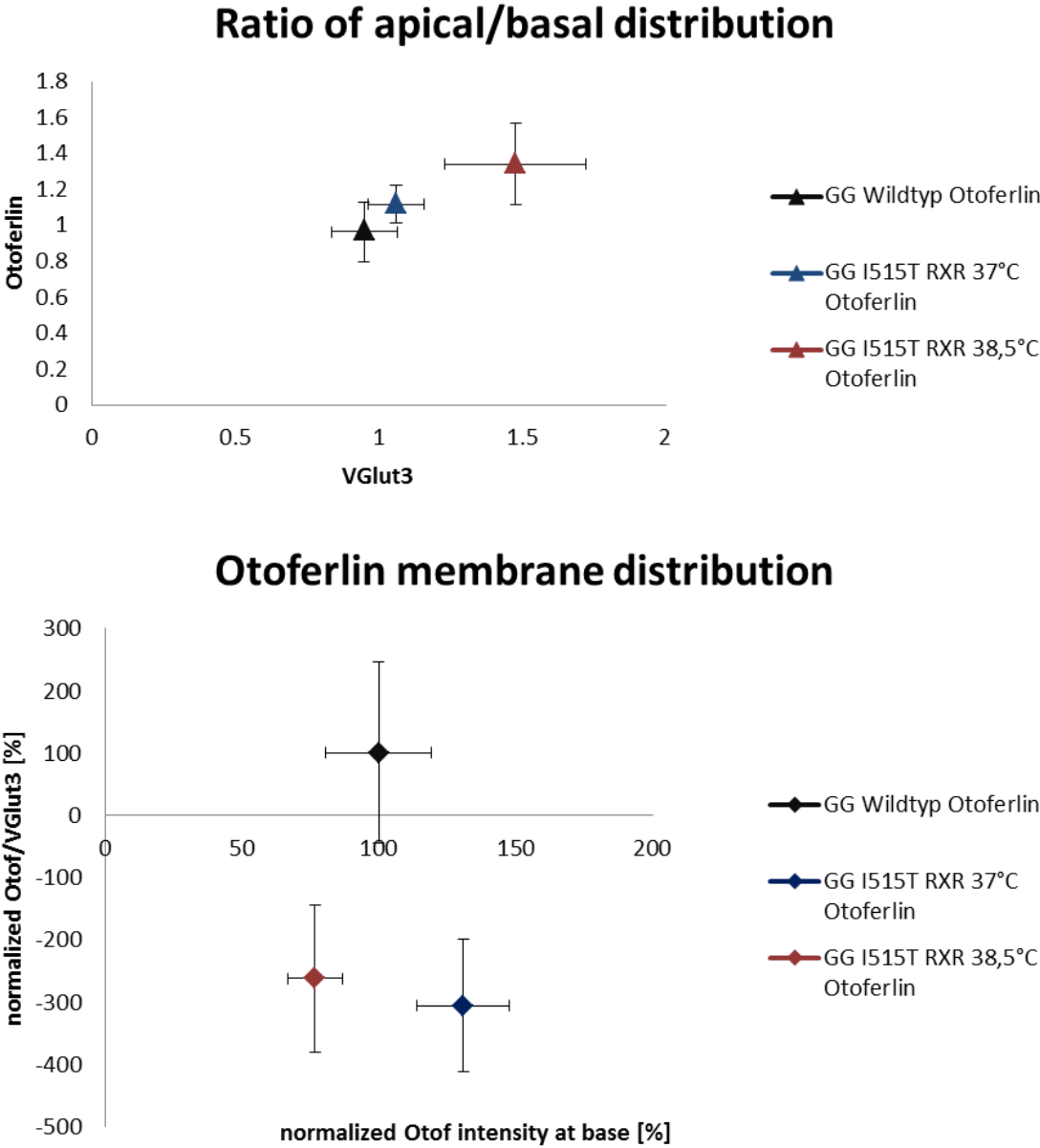


Figure 4.22: Different graphs showing the results of *Imaris* analysis, comparing wild type otoferlin transfected cells and otoferlin RXR I515T transfected cells at 37°C at 38.5°C. Error bars show SEM. GG=Gene Gun, RXR I515T=otoferlin containing RXR motif and I515T mutation. n=6 (GG WT), n=14 (RXR IT 37°C), n=7 (RXR I515T 38.5°C)

For cells incubated at higher temperature we expected an even lower membrane staining compared to cells incubated at 37°C. It turned out that cells incubated at 37°C already did not

show any membrane staining. With the method I was using it is apparently not possible to quantify that.

Transfection of *Otof*^{-/-} cells with otoferlin del C₂F cDNA results in reduced otoferlin membrane staining

Apart from the temperature sensitive mutations in otoferlin another one is the so called pachanga mutation, which is localized in the C₂F domain. Immunofluorescence stainings of mice with this mutation showed a greatly reduced amount of otoferlin (Pangrsic et al., 2010), which is even lower than the one seen in *Otof*^{#515T/1515T}. I was interested how otoferlin is distributed in the cell if the whole C₂F domain is removed and if it is comparable to the distribution observed in inner hair cells of pachanga mice.

After transfection of *Otof*^{-/-} cells with otoferlin del C₂F cDNA cells were incubated for 2 days and then immunostained against otoferlin and VGlut3 (compare Fig. 4.23). After analyzing the cells using *Imaris* software (compare Fig. 4.24) it was revealed, as it can also be seen on the pictures, that only very less membrane staining is visible.

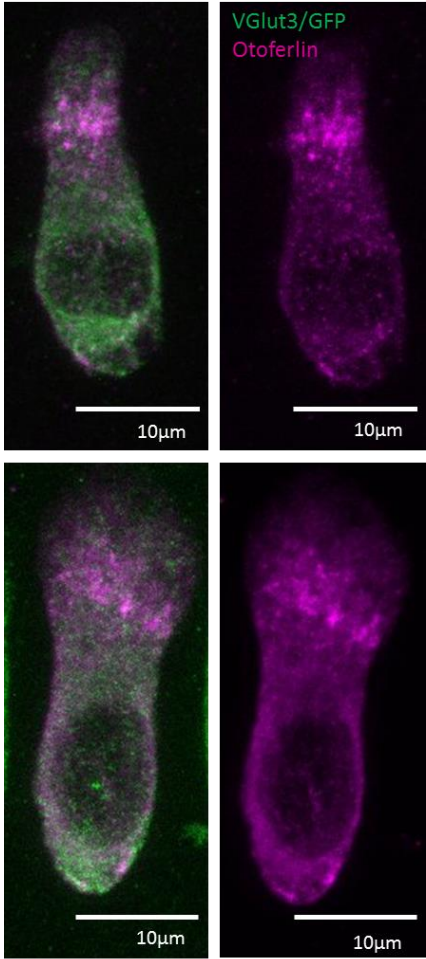


Figure 4.23: Two *Otof*^{-/-} cells transfected with otofferlin del C₂F. Left merge of both channels, right otofferlin staining alone. n=10

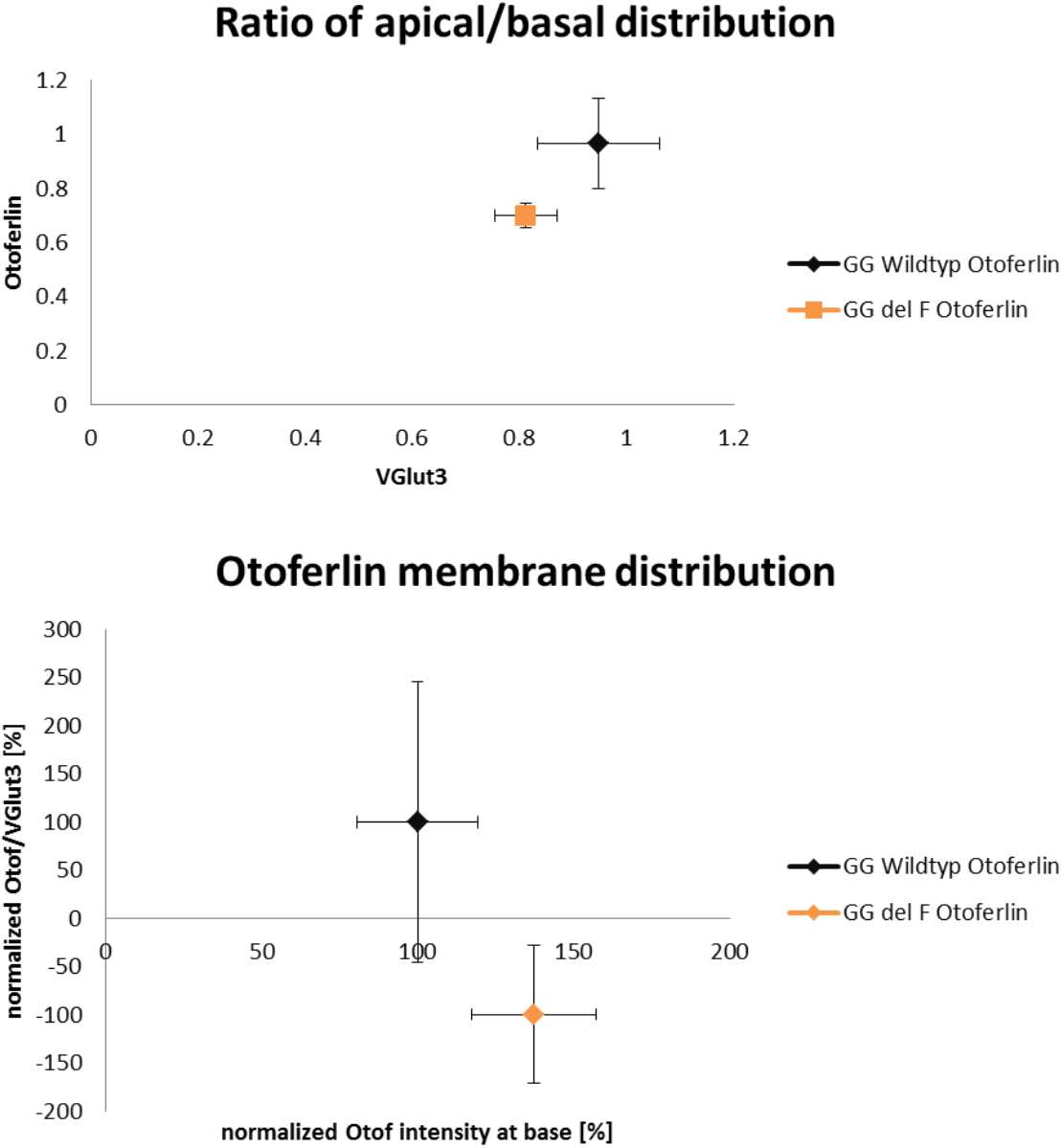


Figure 4.24: Different graphs showing the results of *Imaris* analysis, comparing wild type otoferlin transfected cells and otoferlin del C₂F transfected cells. Error bars show SEM. GG=Gene Gun, del F=otoferlin without C₂F domain. n=6 (GG WT), n=10 (del F)

5 Discussion

Otoferlin has been subject of many studies after it was discovered in 1999 (Yasunaga et al., 1999). It was proposed that otoferlin plays a role in the late step of exocytosis (Roux et al., 2006) as well as in endocytosis-exocytosis coupling via an interaction with the clathrin adapter protein 2 (AP2) (Duncker et al., 2013; Jung et al., 2015) and vesicle priming (Pangrsic et al., 2010). Since otoferlin knock out mice are profoundly deaf it is for sure essential for the hearing process. Recently, the hypothesis of otoferlin playing a role in vesicle priming was supported by a publication showing a reduced number of short tethers which connect synaptic vesicles with the active zone membrane in *Otof*^{-/-} mice (Vogl et al., 2015).

One of the aims of this study was to investigate the I515T mutation which occurs in human same as in mice, but interestingly only leads to deafness in humans at elevated body temperature. A mouse line for this mutation is available and was the subject of intensive studies (Strenzke et al., 2016).

Additionally, I was interested in the characterization of otoferlin constructs missing single C₂ domains. Since another well studied mutation called “pachanga” is localized in the C₂F domain (Pangrsic et al., 2010), I focused on investigation of otoferlin missing this domain.

Third, I tried to strengthen the evidence for dynamin and OPA1 as possible otoferlin interaction partners using proximity ligation assay and tested the stability of wildtype otoferlin and otoferlin mutants using a Cycloheximide assay and mass spectrometry analysis.

5.1 Determined mRNA levels in organs of Corti from *Otof*^{I515T/I515T} mice show no reduction in comparison to mRNA of wild type mice

One speculated mechanism for the I515T phenotype was that there may be reduced otoferlin mRNA levels in *Otof*^{I515T/I515T} inner hair cells. This can either originate from lower expression as well as accelerated degradation of mRNA. The latter can occur when the mRNA is for example recognized as defective. Additionally, different mRNAs can vary in their half-life times and are not present for a very long time. I found no statistic reduction when otoferlin mRNA levels of wild type mice and of *Otof*^{I515T/I515T} mice were compared to each other, neither normalized to TBP nor bassoon as an inner hair cell control. Thus, a lower mRNA level seems not to be the reason for the lower protein levels in otoferlin mutant mice. Similar experiments were conducted in the deaf *Otof*^{ppga/ppga} mice (Pangrsic et al., 2010). It was shown that those mice, comparable to *Otof*^{I515T/I515T} mice, also have a trend towards higher mRNA level compared to those of wild type mice. We concluded, that reduced amounts of mRNA levels were not the reason for both, the I515T as well as the pachanga phenotype. The next possible mechanism we had in mind was increased degradation of otoferlin protein carrying a temperature sensitive mutation.

5.2 Otoferlin protein as well as the temperature sensitive forms are not degraded by a proteasomal mechanism

Small changes in an amino acid sequence, as it is the case with temperature sensitive mutations in otoferlin, can already lead to defects regarding folding or stability (Lascu et al., 1997). To test this hypothesis, I performed Cycloheximide experiments with transfected HEK cells, blocking the protein biosynthesis and observing the protein degradation. Cells were transfected with a

distinct cDNA of wild type or a mutated form of otoferlin and incubated at 37°C or 38.5°C for two hours, a time range in which patients carrying the I515T mutation were already deaf (Varga et al., 2006b).

Our first attempt of analyzing those samples was Western Blot analysis. This method of blocking the protein biosynthesis with Cycloheximide, loading the samples on a polyacrylamide gel and blot the protein to a membrane was successfully conducted with small proteins such as Heat shock 70kDa protein 1A (Jiang et al., 2004) or zinc-finger-containing transcriptional repressor (Slug) (Kao et al., 2014). This raised hope for a larger protein like otoferlin (~230kDa) as well assuming that we use a proper working antibody. Unfortunately, I came across several problems. First the α -otoferlin antibody binding in the C₂C domain (Abcam) was not working reliably, sometimes showing protein bands of expected size in Western Blots, sometimes leading to several, unspecific bands on the blot and sometimes not binding at all. Variation of the blotting procedure regarding blotting time, current and detection reagent did not yield in consistent data. In addition, the intensity of the putative otoferlin band as well as of the loading control band was not only based on the amount of protein itself but seemed to be influenced by the position on the membrane, a phenomenon which was observed by loading same sample and same amount on one gel and blotting it. All this taken together made me give up on that method because it was not reproducible and not reliable. Since we expected minor changes of the otoferlin protein levels the technique of comparing the intensity of Western Blot bands is maybe not sensitive enough to determine such small differences, but this can only be ruled out by overcoming the mentioned problems. However, the approach of half-life-time determination using Western Blots was not completely useless because I optimized sample preparation and storage which came in handy for the next procedure. I observed that lysed HEK cells are better frozen directly and kept at -20°C until further treatment instead of keeping them only on ice. Importantly it turned out, that otoferlin seems to aggregate when it is heated in Laemmli buffer which is a common procedure for polyacrylamide samples. It was proofed that sonificating the samples three times for 20sec each works best.

Since we needed a method to determine the change in otoferlin protein levels and examine protein degradation we switched from Western Blot to mass spectrometry. Several proteins were analyzed regarding their half-life-time so far (Sandoval et al., 2013; Chen et al., 2016) which motivated us to perform similar experiments for otoferlin as well. It turned out that wild type otoferlin as well as the mutated forms in HEK cells are more stable than expected and the protein level is not significantly reduced after an incubation time of two hours. Extending the incubation time to 24h and analyzing the protein amount in transfected cells with either wild type otoferlin or *Otof*^{f515T/515T} still showed that even until this extended time span otoferlin levels still do not significantly decrease, neither wild type otoferlin but more interestingly nor *Otof*^{f515T/515T} protein levels.

My results indicate that fast proteosomal degradation is not the reason for temperature sensitive hearing loss. Another possible explanation for the temperature dependent hearing phenotype was that mutated otoferlin protein levels could originally be a little lower and drop below a certain threshold as soon as the body temperature rises, leading to deafness. At least in HEK cells the protein levels of mutated otoferlin were comparable to those of non-mutated otoferlin, showing if anything even a small trend towards higher levels. This might be an artefact of the organism properties, as by studying the mutant mouse lines *Otof*^{f515T/515T} and *Otof*^{pga/pga} it was shown that otoferlin protein levels are in contrast decreased to those in HEK cells (Pangrsic et al., 2010; Strenzke et al., 2016),

However, it cannot be excluded that the protein unfolds within a short time period at elevated temperatures and is no longer functional. The protein might then fold back to its normal structure when the body temperature is back at a normal level. This unfortunately cannot be investigated using mass spectrometry analysis since even unfolded protein would remain inside the cell and would then be processed as normally folded protein. Nevertheless it cannot be excluded that mutated otoferlin is degraded faster than wild type otoferlin although the degradation is not as fast as expected. However, due to the fact that HEK cells would not endure the used Cycloheximide concentration for a time span longer than 24h it is not possible to observe protein degradation of otoferlin with this assay for a longer period.

Modelling the C₂C domain (compare Fig. 5.1) of otoferlin with the I515T mutation (model kindly provided by Piotr Neumann) could show a possible explanation for the temperature sensitive hearing loss related to the I515T mutation. Here, the I515T points towards the center of the C₂C domain. Since the hydrophobic inner core strongly contributes to the protein domain stability by hydrophobic interaction of the non-polar side chains, the exchange from a hydrophobic (isoleucine) to a hydrophilic (threonine) amino acid is likely to render the protein less stable which could be an explanation for the I515T phenotype.

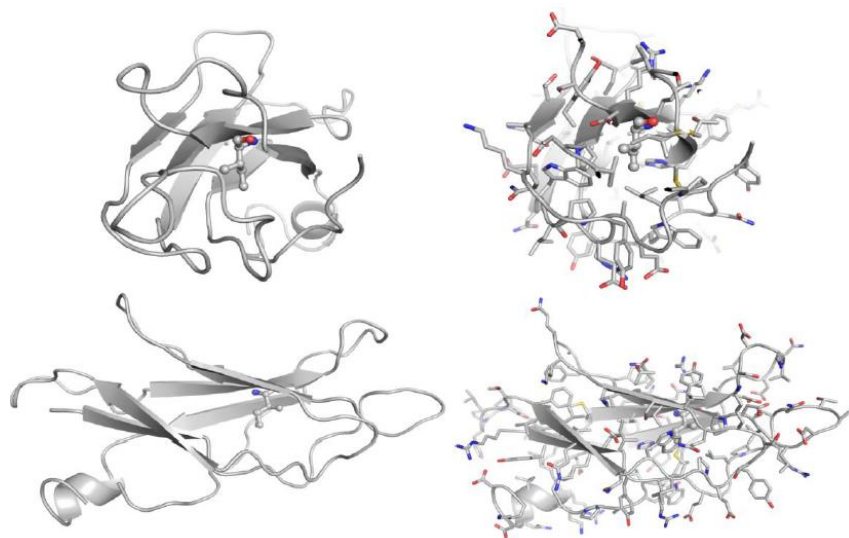


Figure 5.1: Model of the C₂C domain of otoferlin with I515T mutation. The domain is shown either without (left) or with (right) amino acid sidechains. Kind gift of Piotr Neumann, figure taken from (Strenzke et al., 2016)

5.3 Otoferlin is unlikely to be sumoylated

Different posttranslational modification forms like ubiquitylation or acetylation exist, which have an influence on interaction and localization as well as stability. Another important form of covalent modification takes place at specific lysine residues by small ubiquitin-like modifiers (SUMO). Sumoylation also plays an essential role in the regulation of different biological processes like DNA repair or cellular signaling (Hay, 2005; Geiss-Friedlander and Melchior,

2007). Interestingly it was predicted that the pachanga mutation D1767G destroys a possible sumoylation site (predicted using <http://sumosp.biocuckoo.org>). Thus, sumoylation of otoferlin would be a possible mechanism for the degradation or the regulation of cellular localization. Using His₆-HA-SUMO1 knock-in mice (kind gift of Marilyn Tirard, see also Tirard et al., 2012) it turned out that sumoylated proteins can be found inside and around the nucleus of inner hair cells but not in the remaining cell. Since otoferlin is distributed through the cell and is present at the membrane as well, a HA-signal should be detectable in the whole cell or at least in the region of active zones in case of an otoferlin sumoylation. This is not the case for inner hair cells, suggesting that neither otoferlin nor other synaptic inner hair cell proteins are sumoylated. In vitro experiments by R. Geiss-Friedländer further revealed no sumoylation of the otoferlin C₂F domain, supporting my immunohistochemical findings.

5.4 Gene Gun transfection could be successfully established for inner hair cells in our lab

Transfection of inner hair cells turned out to be more challenging than expected because of their orientation in the organ of Corti. Hair cells are protected by the cuticular plate and the tectorial membrane above and the basilar membrane below them. The cuticular plate especially made it very difficult to transfect inner hair cells when tried to transfect cells with tectorial membrane facing upwards and basilar membrane facing to the surface of the petri dish. To overcome the tectorial membrane high transfection pressure (200-250psi) was needed which lead to damaged or dead cells. Too high pressure combined with lack of space between tissue and Gene Gun nozzle can lead to increased tissue damage, which was already mentioned in 2001 by O'Brien and colleagues who successfully transfected HeLa and HEK cells (O'Brien et al., 2001). They also stated that transfection with a transfection pressure lower than 100psi was not effective which was also the case for us. They reduced the incoming pressure burst by using a 70nm mesh which still allowed the gold particles to pass and maintain enough pressure to

transfect cells. In another publication using the Helios Gene Gun, larvae of *Bombyx mori* were transfected using a focusing nozzle (Thomas et al., 2001). Thomas and colleagues were able to shoot dried particles as well as wet ones. With their modifications their shooting was always centered. We also tried transfecting inner hair cells using a focusing nozzle and lower pressure (20-60psi) since higher pressure destroyed inner hair cells or led to blown-away tissue. Unfortunately this did not yield in success for mouse inner hair cells. The most interesting modifications of this method were released in a publication in 2012 (Zhao et al., 2012) working mainly with bullfrog saccule hair cells but also with hair cells of chicken and mouse. They focused on reducing the shockwave on the tissue but maintained penetrating power which was also an important component for our transfection. Since the mentioned modification of O'Brian and colleagues as well as Thomas and colleagues did not work for them they built a semi-air dry chamber mostly out of common lab equipment like the cap of a falcon tube. In addition, to reduce the pressure, they were using a mesh with a diameter of 74 μ m. Based on those modifications, my colleague Hanan Al-Moyed and I started using meshes, either one or two in different combinations of 40 μ m and 70 μ m. It turned out that two meshes with 70 μ m in diameter, glued on top of each other, gave the best transfection results. To maintain the distance between nozzle and tissue, a self-build tripod was used (adapted from Michael Leitner and Dominik Oliver, Marburg), (for an overview of the setting compare Fig. 4.16). Finally we tried to increase the pressure and amount of transfected inner hair cells in the organ of Corti by flipping the tissue and having the basilar membrane facing up. Although the amount varied between different shooting experiments, it most of the times led to successfully transfected inner hair cells. Since it turned out that only with p4 mice transfection led to fluorescent inner hair cells it can now be speculated whether the mice were always precisely of that indicated age. Maturation happens quickly in the first days, so when a litter was not always discovered on the day of birth which can happen since the female mice tend to hide their pups, mice could be little older than p4 what makes it nearly impossible to transfect cells but anyway greatly decreases transfection efficiency.

5.5 It seems that a small amino acid stretch including a RXR motif is the reason for the I515T phenotype

The *Otof*^{I515T/I515T} mutant is a suitable mouse model which has been studied for a long time and produced a high amount of data (Strenzke et al., 2016). However, it appeared strange that those mice do not become deaf at elevated body temperature but humans carrying the same mutation become rapidly deaf indeed as soon as their body temperature rises. This made us wonder if a difference in the amino acid sequence of mouse and human otoferlin could be the reason. It turned out that indeed, apart from a few minor differences, a short amino acid stretch of twenty amino acids including an RXR motif is missing in the mouse sequence but existing in the human as well as in rat and *Xenopus* (Strenzke et al., 2016).

Earlier studies investigating the function of α_{2c} -adrenergic receptor (AR) revealed that this receptor also has a strange temperature dependent localization pattern (Filipeanu, 2015). The α_{2c} -AR plays an important role in a disease called Raynaud's phenomenon, first described by Maurice Raynaud in 1862. Patients having Raynaud's phenomenon observe a strong response when exposed to cold, the following effects appear one after another. First, because of local perfusion, the affected skin turns from normal color to white. Second, the affected skin turns from white to blue because of hypoxia. At last, after a short time span, the blood flow is restored and the skin turns red accompanied by great pain (Brand et al., 1997; Prete et al., 2014). It turned out that the mentioned receptor includes several putative RXR motifs which in other proteins prevents the protein from transport to the cell surface but in contrast supports the retention in the endoplasmic reticulum (Michelsen et al., 2005; Stepanchick et al., 2010). Comparison of α_{2c} -AR and α_{2B} -AR, the latter is missing these RXR motifs, showed that α_{2B} -AR is not transported to the membrane at decreased temperatures (Filipeanu et al., 2011). It was found that the plasma membrane levels of α_{2c} -AR were increased in HEK cells transfected with cDNA of human, mouse or rat when cells were exposed to lower temperature (30°C), since Raynaud's phenomenon occurs at decreased temperatures. The three mentioned species contain several RXR motifs in the investigated α_{2c} -AR protein. In addition, cells were also

transfected with cDNA of α_{2c} -AR from opossum, having less arginine clusters. It turned out that the membrane localization of opossum protein at reduced temperature was not statistically increased whereas it was for the other three species though.

Indeed, it seems that also in otoferlin the RXR motif might be one explanation why humans having the I515T phenotype become deaf at elevated temperatures whereas mice do not. At normal body temperature of 37°C, a remarkable fraction of I515T-otoferlin is localized at the plasma membrane of inner hair cells but when the body temperature is increased the fraction of protein at the plasma membrane is reduced (observation from Hanan Al-Moyed, Strenzke et al., 2016). Since the localization at normal body temperature is different, for the α_{2c} -AR in the endoplasmic reticulum and for otoferlin at the plasma membrane, the RXR motif seems to trigger relocation towards the plasma membrane at decreased temperature in the case of α_{2c} -AR and towards intracellular membranes at elevated body temperature in the case of otoferlin. Thus, the relocation due to the RXR motif in both cases reduces plasma membrane levels with increasing temperature.

In 2015 Redpath and colleagues conducted a study where they investigated the expression and localization of the six mammalian ferlins in three different cell lines including HEK cells (Redpath et al., 2015). They claim that in the tested cell lines myoferlin and dysferlin are expressed in the plasma membrane and support the endo-lysosomal pathway whereas otoferlin is localized to the trans-golgi and recycling networks and is localized at the membrane only in very low amounts. This is in stark contrast to what we observed in inner hair cells of wild type mice where we see a strong membrane staining. The staining, and with that the amount of otoferlin protein, is indeed reduced in the two investigated otoferlin mouse mutants *Otof*^{ppga/ppga} and *Otof*^{I515T/I515T}, by 65% in the latter (Pangrsic et al., 2010, Strenzke et al., 2016), but still detectable. However, the localization to the trans golgi compartment is in line with supposed roles of otoferlin that include recycling of synaptic vesicles (Strenzke et al., 2016) as well as synaptic exocytosis (Roux et al., 2006). One explanation for the varying results regarding the membrane localization of otoferlin could be that our results were obtained in mouse inner hair cells with mouse otoferlin while the data from Redpath and colleagues were gained in three

different cell lines, HEK293, Cos-7 and C2C12 myoblasts, by overexpression of the different human proteins. It seems that at least for otoferlin, the localization differs depending on the cell type. Regarding the weak membrane localization the authors suggested a closely coupled endocytosis and exocytosis. This results in otoferlin being only transiently at the membrane, which is also in line with the endocytosis-exocytosis coupling via an interaction with the clathrin adapter protein 2 (AP2) (Duncker et al., 2013; Jung et al., 2015). In addition, Redpath and colleagues mentioned that overexpression of proteins does not always lead to reliable results but was the only possible method for their study since no antibodies binding the lumina/extracellular domains of the human ferlins antibodies were available.

5.6 Proximity ligation assay could not be established for use in inner hair cells

A few interaction partners of otoferlin have been verified using different approaches like yeast two-hybrid, surface plasmon resonance or pull-down assays. However, to date the identified interaction were never reviewed if they really interact in inner hair cells. Proximity ligation assay seemed to be a useful tool to check the already existing interactions and also identify new ones.

Since I had two promising interaction partners of otoferlin, identified by pull down assays performed by Sandra Meese (Molecular Structural Biology, Ralf Ficner) and Sunit Mandad (Bioanalytical Mass Spectrometry Group), dynamin and OPA1, I wanted to strengthen the interaction hypothesis using proximity ligation assay. This assay leads to a fluorescent spot if the two secondary antibodies, which bind to the primary antibody detecting the proteins, are in proximity of 40nm or less. By staining the inner hair cells with α -calbindin antibody, it was easily visible if signals were inside or outside the cells and where exactly in the cell they are located. It turned out that in four positive controls the fluorescent spots were not restricted to inner hair cells. Another publication using proximity ligation assay as one of their methods shows the use of different cell types. Thymiakou and Episkopou used PLA to prove the interaction of P-

Smad1/5/8 and Smad4 in Neuro2a cells after treatment with bone morphogenetic protein 4 (Thymiakou and Episkopou, 2011). As negative controls, cells were incubated with just one primary antibody, no positive control was performed. After PLA they observed signals which were restricted to the cells, no other signals have been detected. In the negative control no fluorescent spots were visible. In another publication no interaction could be proven. It was tested whether transferrin receptor 2 (Trf2) and hemochromatosis protein (Hfe) are in close proximity which was not the case (Rishi et al., 2013). The study was conducted in Hepa 1-6 cells stably expressing Hfe or Trf2. Same as Thymiakou and Episkopou, negative controls with just one antibody were used. However, it was shown that Trf1 and Trf2 are leading to a fluorescent signal, indicating the formation of heterodimers whereas Hfe did interact with Trf1 but not Trf2. Their negative controls are clearly negative and their experiments show clear signals for Hfe and Trf1 but not Trf2 as well as Trf1 and Trf2.

Although in both publications no positive control is included, both researchers went for negative controls. Unfortunately, even our negative control, which was conducted in *Otof*^{-/-} mice using α -otoferlin and α -OPA1 antibody ended up in fluorescent spots, most of them between cells but a few inside the cells as well. It turned out they looked similar in the positive controls, where I observed fluorescent signals inside the cells where they were supposed to be, as well as in between inner hair cells, no matter which antibody combination was used as a positive control. To my knowledge, so far no scientific publication exists which includes successful proximity ligation assay results and show a close proximity of two cochlear inner hair cell proteins. Although immunofluorescence staining for many inner hair cell proteins can be easily performed, their epitope binding may not be strong enough for proximity ligation assays. In addition, in both publications blocking solution and antibody diluent were used which come together with the used PLA probes. Because using those for our antibodies did not work in inner hair cells at all, I switched to the common immunofluorescence solution used in our laboratory. For blocking donkey serum (DSDB) supplemented with Triton-X-100 was used, for diluting primary antibodies as well as PLA probes I used DSDB without Triton because Triton seemed to hinder the enzymes from their work. Both could be the reason why PLAs did not lead to a reliable result in inner hair cells. However, it can also be the case that the assay has to

be further optimized. Since it turned out during my studies that otoferlin and dynamin or OPA1 were not interacting using yeast two-hybrid assay (Sarah Helfmann, Molecular biology of cochlear neurotransmission group) and PLAs did not show convincing results, I did not proceed with that method.

5.7 The otoferlin C₂F domain apparently plays a role for plasma membrane localization

Inner hair cells were biolistically transfected with otoferlin del C₂F cDNA and stained after two days in culture using α -otoferlin and α -VGlut3 antibodies. It turned out that the otoferlin plasma membrane staining in those cells is nearly completely vanished. Inner hair cells with similar low fraction of plasma localized otoferlin can be observed in *Otof^{ppga/ppga}* mice (Pangrsic et al., 2010). Those mice seem to have normal inner hair cell mechano-electrical transduction as well as normal basolateral Ca²⁺ conductance and a normal readily releasable pool. Interestingly, the change in membrane capacity rose more slowly in those mutants when cells were depolarized longer, indicating that the sustained exocytosis is not working properly. Increasing the Ca²⁺-concentration enhanced the sustained exocytosis in those mutants. The pachanga mutation is caused by a missense mutation in the C₂F domain of otoferlin (D1767G in *mus musculus* otoferlin variant 1, NP_001093865). It was predicted earlier that the last four C₂ domains of otoferlin, meaning C₂C to C₂F, are critical for Ca²⁺-binding and thus for protein function and hearing (Yasunaga et al., 2000). Later it was stated in another publication, that only C₂D, C₂E and C₂F have the five aspartates needed for Ca²⁺ binding (Jiménez and Bashir, 2007). This was confirmed by Ca²⁺ binding experiments performed by Sandra Meese (Molecular Structural Biology, Ralf Ficner). For the C₂F domain of otoferlin it was shown, that it binds Phosphatidylinositol 4,5-bisphosphate (PIP₂) in a Ca²⁺ independent manner (Padmanarayana et al., 2014). PIP₂ is a phospholipid component of cell membranes. In my biolistically transfected cells with otoferlin del C₂F cDNA the plasma membrane staining is completely gone, indicating

that the C₂F domain is important for plasma membrane binding, maybe by an interaction with PIP₂.

It can be hypothesized, based on my experiments, that the deletion of the C₂F domain might have an influence on the function. Since I can now only make a statement regarding the distribution of otoferlin in inner hair cells, it cannot be said if the hearing phenotype would be comparable to pachanga phenotype. However, the pachanga mutation consists of only an exchange of one amino acid and already has severe influences on hearing, leading to complete deafness of those mice. It is possible, that deleting the whole domain would lead to a similar phenotype, also indicated by the comparable protein distribution in immunofluorescence stainings.

In addition, cells transfected with otoferlin RXR I515T cDNA incubated at 38.5°C are also missing otoferlin membrane staining and patients carrying this mutation become deaf at elevated body temperature. It seems that otoferlin being correctly localized in the plasma membrane is required for a proper hearing.

5.8 Summary

Deafness is an interesting and intensely studied topic and can be caused by different, genetic as well as environmental, factors. One important cause of deafness are mutations in the otoferlin gene leading to non-syndromic deafness DFNB9. Interestingly, some mutations lead to temperature induced hearing loss where patients have normal to impaired hearing when their body temperature is normal but become deaf as soon as they become febrile. We analyzed three temperature sensitive mutations by mass spectrometry to investigate their protein stability. It turned out that wildtype otoferlin as well as the mutated forms are stable over a time range of 24h although rapid unfolding cannot be excluded.

Since mice carrying the I515T mutation show lower protein levels, we checked whether these levels depend on a lower amount of mRNA. We isolated RNA from organs of Corti from wildtype and *Otof*^{I515T/I515T} mice and conducted Real-Time PCRs. It turned out that in both mice mRNA levels were comparable.

To test the hypotheses if dynamin-1 as well as OPA1 are interaction partners of otoferlin it was tried to establish proximity ligation assays. Because it was shown using yeast two-hybrid assays, that otoferlin neither interacts with dynamin nor with OPA1 it was no longer focused on that.

Biolistic transfection of inner hair cells using the Gene Gun could be successfully established in our lab. We analyzed, with different modified cDNA, transfected cells regarding their protein distribution and membrane bound fraction of otoferlin. It could be shown that otoferlin with a missing C₂F domain is no longer localized to the membrane indicating an important role for this domain.

Cells biolistically transfected with otoferlin RXR did not lead to a reduction in otoferlin membrane staining whereas those with an additional I515T mutation show no membrane staining. It could be shown that cochlear mouse otoferlin is missing the RXR motif present in human as well as another amino acid stretch. This finding resulted in a new NCBI database entry.

References

- Achanzar WE, Ward S (1997) A nematode gene required for sperm vesicle fusion. *J Cell Sci* 110:1073–1081.
- Baldarelli RM, Lengyel JA (1990) Transient expression of DNA after ballistic introduction into *Drosophila* embryos. *Nucleic Acids Res* 18:5903–5904.
- Bedrosian JC, Gratton MA, Brigande JV, Tang W, Landau J, Bennett J (2006) In Vivo Delivery of Recombinant Viruses to the Fetal Murine Cochlea: Transduction Characteristics and Long-Term Effects on Auditory Function. *Mol Ther* 14:328–335.
- Belyantseva I (2009) Helios® Gene Gun–Mediated Transfection of the Inner Ear Sensory Epithelium. In: *Auditory and Vestibular Research* (Sokolowski B, ed), pp 103–124 *Methods in Molecular Biology™*. Humana Press. Available at: http://dx.doi.org/10.1007/978-1-59745-523-7_7 [Accessed February 9, 2016].
- Bernatchez PN, Sharma A, Kodaman P, Sessa WC (2009) Myoferlin is critical for endocytosis in endothelial cells. *Am J Physiol - Cell Physiol* 297:C484–C492.
- Beurg M, Safieddine S, Roux I, Bouleau Y, Petit C, Dulon D (2008) Calcium- and otoferlin-dependent exocytosis by immature outer hair cells. *J Neurosci Off J Soc Neurosci* 28:1798–1803.
- Brand FN, Larson MG, Kannel WB, McGuirk JM (1997) The Occurrence of Raynaud's Phenomenon in a General Population: The Framingham Study. *Vasc Med* 2:296–301.
- Chen W, Smeekens JM, Wu R (2016) Systematic study of the dynamics and half-lives of newly synthesized proteins in human cells. *Chem Sci* 7:1393–1400.
- Dallos P (1992) The active cochlea. *J Neurosci* 12:4575–4585.
- Dulon D, Safieddine S, Jones SM, Petit C (2009) Otoferlin Is Critical for a Highly Sensitive and Linear Calcium-Dependent Exocytosis at Vestibular Hair Cell Ribbon Synapses. *J Neurosci* 29:10474–10487.
- Duncker SV, Franz C, Kuhn S, Schulte U, Campanelli D, Brandt N, Hirt B, Fakler B, Blin N, Ruth P, Engel J, Marcotti W, Zimmermann U, Knipper M (2013) Otoferlin Couples to Clathrin-Mediated Endocytosis in Mature Cochlear Inner Hair Cells. *J Neurosci* 33:9508–9519.
- Evesson FJ, Peat RA, Lek A, Brilot F, Lo HP, Dale RC, Parton RG, North KN, Cooper ST (2010) Reduced Plasma Membrane Expression of Dysferlin Mutants Is Attributed to

- Accelerated Endocytosis via a Syntaxin-4-associated Pathway. *J Biol Chem* 285:28529–28539.
- Fettiplace R, Hackney CM (2006) The sensory and motor roles of auditory hair cells. *Nat Rev Neurosci* 7:19–29.
- Filipeanu CM (2015) Chapter Eleven - Temperature-Sensitive Intracellular Traffic of α_{2C} -Adrenergic Receptor. In: *Progress in Molecular Biology and Translational Science* (Wu G, ed), pp 245–265 *Trafficking of GPCRs*. Academic Press. Available at: <http://www.sciencedirect.com/science/article/pii/S187711731500037X> [Accessed July 7, 2015].
- Filipeanu CM, de Vries R, Danser AHJ, Kapusta DR (2011) Modulation of α_{2C} adrenergic receptor temperature-sensitive trafficking by HSP90. *Biochim Biophys Acta* 1813:346–357.
- Geiss-Friedländer R, Melchior F (2007) Concepts in sumoylation: a decade on. *Nat Rev Mol Cell Biol* 8:947–956.
- Geppert M, Goda Y, Hammer RE, Li C, Rosahl TW, Stevens CF, Südhof TC (1994) Synaptotagmin I: A major Ca^{2+} sensor for transmitter release at a central synapse. *Cell* 79:717–727.
- Hay RT (2005) SUMO: A History of Modification. *Mol Cell* 18:1–12.
- Heffner HE, Heffner RS (2008) High-Frequency Hearing. In: *The Senses: A Comprehensive Reference*, pp 55–60. New York: Academic Press. Available at: <http://www.sciencedirect.com/science/article/B8SV0-4RD4KNB-X/2/4f5c26aed9c6204c019136aa242f69d7> [Accessed May 17, 2011].
- Heidrych P, Zimmermann U, Breß A, Pusch CM, Ruth P, Pfister M, Knipper M, Blin N (2008) Rab8b GTPase, a protein transport regulator, is an interacting partner of otoferlin, defective in a human autosomal recessive deafness form. *Hum Mol Genet* 17:3814–3821.
- Heidrych P, Zimmermann U, Kuhn S, Franz C, Engel J, Duncker SV, Hirt B, Pusch CM, Ruth P, Pfister M, Marcotti W, Blin N, Knipper M (2009) Otoferlin interacts with myosin VI: implications for maintenance of the basolateral synaptic structure of the inner hair cell. *Hum Mol Genet* 18:2779–2790.
- Helfmann S, Neumann P, Tittmann K, Moser T, Ficner R, Reisinger E (2011) The crystal structure of the C₂A domain of otoferlin reveals an unconventional top loop region. *J Mol Biol* 406:479–490.
- Ho SN, Hunt HD, Horton RM, Pullen JK, Pease LR (1989) Site-directed mutagenesis by overlap extension using the polymerase chain reaction. *Gene* 77:51–59.

- Jiang X, Coffino P, Li X (2004) Development of a method for screening short-lived proteins using green fluorescent protein. *Genome Biol* 5:R81.
- Jiménez JL, Bashir R (2007) In silico functional and structural characterisation of ferlin proteins by mapping disease-causing mutations and evolutionary information onto three-dimensional models of their C₂ domains. *J Neurol Sci* 260:114–123.
- Johnson CP, Chapman ER (2010) Otoferlin is a calcium sensor that directly regulates SNARE-mediated membrane fusion. *J Cell Biol* 191:187–197.
- Jung S, Maritzen T, Wichmann C, Jing Z, Neef A, Revelo NH, Al-Moyed H, Meese S, Wojcik SM, Panou I, Bulut H, Schu P, Ficner R, Reisinger E, Rizzoli SO, Neef J, Strenzke N, Haucke V, Moser T (2015) Disruption of adaptor protein 2 μ (AP-2 μ) in cochlear hair cells impairs vesicle reloading of synaptic release sites and hearing. *EMBO J* 34:2686–2702.
- Kachar B, Brownell WE, Altschuler R, Fex J (1986) Electrokinetic shape changes of cochlear outer hair cells. *Nature* 322:365–368.
- Kao S-H, Wang W-L, Chen C-Y, Chang Y-L, Wu Y-Y, Wang Y-T, Wang S-P, Nesvizhskii AI, Chen Y-J, Hong T-M, Yang P-C (2014) GSK3 β controls epithelial–mesenchymal transition and tumor metastasis by CHIP-mediated degradation of Slug. *Oncogene* 33:3172–3182.
- Keyel PA, Thieman JR, Roth R, Erkan E, Everett ET, Watkins SC, Heuser JE, Traub LM (2008) The AP-2 adaptor beta2 appendage scaffolds alternate cargo endocytosis. *Mol Biol Cell* 19:5309–5326.
- Klein TM, Wolf ED, Wu R, Sanford JC (1987) High-velocity microprojectiles for delivering nucleic acids into living cells. *Nature* 327:70–73.
- Lascu I, Schaertl S, Wang C, Sarger C, Giartosio A, Briand G, Lacombe M-L, Konrad M (1997) A Point Mutation of Human Nucleoside Diphosphate Kinase A Found in Aggressive Neuroblastoma Affects Protein Folding. *J Biol Chem* 272:15599–15602.
- Lek A, Lek M, North KN, Cooper ST (2010) Phylogenetic analysis of ferlin genes reveals ancient eukaryotic origins. *BMC Evol Biol* 10:231.
- Liberman MC, Gao J, He DZZ, Wu X, Jia S, Zuo J (2002) Prestin is required for electromotility of the outer hair cell and for the cochlear amplifier. *Nature* 419:300–304.
- Liu J et al. (1998) Dysferlin, a novel skeletal muscle gene, is mutated in Miyoshi myopathy and limb girdle muscular dystrophy. *Nat Genet* 20:31–36.
- Luebke AE, Steiger JD, Hodges BL, Amalfitano A (2001) A modified adenovirus can transfect cochlear hair cells in vivo without compromising cochlear function. *Gene Ther* 8:789–794.

- Marlin S, Feldmann D, Nguyen Y, Rouillon I, Loundon N, Jonard L, Bonnet C, Couderc R, Garabedian EN, Petit C, Denoyelle F (2010) Temperature-sensitive auditory neuropathy associated with an otoferlin mutation: Deafening fever! *Biochem Biophys Res Commun* 394:737–742.
- Matsunaga T, Mutai H, Kunishima S, Namba K, Morimoto N, Shinjo Y, Arimoto Y, Kataoka Y, Shintani T, Morita N, Sugiuchi T, Masuda S, Nakano A, Taiji H, Kaga K (2012) A prevalent founder mutation and genotype-phenotype correlations of OTOF in Japanese patients with auditory neuropathy. *Clin Genet* 82:425–432.
- Michelsen K, Yuan H, Schwappach B (2005) Hide and run. *EMBO Rep* 6:717–722.
- Migliosi V, Modamio-Hoybjor S, Moreno-Pelayo MA, Rodriguez-Ballesteros M, Villamar M, Telleria D, Menendez I, Moreno F, Del Castillo I (2002) Q829X, a novel mutation in the gene encoding otoferlin (OTOF), is frequently found in Spanish patients with prelingual non-syndromic hearing loss. *J Med Genet* 39:502.
- Morton NE (1991) Genetic Epidemiology of Hearing Impairment. *Ann N Y Acad Sci* 630:16–31.
- Neef J, Jung S, Wong AB, Reuter K, Pangrsic T, Chakrabarti R, Kugler S, Lenz C, Nouvian R, Boumil RM, Frankel WN, Wichmann C, Moser T (2014) Modes and Regulation of Endocytic Membrane Retrieval in Mouse Auditory Hair Cells. *J Neurosci* 34:705–716.
- Nouvian R, Neef J, Bulankina AV, Reisinger E, Pangršič T, Frank T, Sikorra S, Brose N, Binz T, Moser T (2011) Exocytosis at the hair cell ribbon synapse apparently operates without neuronal SNARE proteins. *Nat Neurosci* 14:411–413.
- O'Brien JA, Holt M, Whiteside G, Lummis SCR, Hastings MH (2001) Modifications to the hand-held Gene Gun: improvements for in vitro Biolistic transfection of organotypic neuronal tissue. *J Neurosci Methods* 112:57–64.
- Ohsako T, Hirai K, Yamamoto M-T (2003) The *Drosophila misfire* gene has an essential role in sperm activation during fertilization. *Genes Genet Syst* 78:253–266.
- Oliver D, He DZZ, Klöcker N, Ludwig J, Schulte U, Waldegger S, Ruppertsberg JP, Dallos P, Fakler B (2001) Intracellular Anions as the Voltage Sensor of Prestin, the Outer Hair Cell Motor Protein. *Science* 292:2340–2343.
- Padmanarayana M, Hams N, Speight LC, Petersson EJ, Mehl RA, Johnson CP (2014) Characterization of the lipid binding properties of Otoferlin reveals specific interactions between PI(4,5)P2 and the C₂C and C₂F domains. *Biochemistry (Mosc)* 53:5023–5033.
- Pangrsic T, Lasarow L, Reuter K, Takago H, Schwander M, Riedel D, Frank T, Tarantino LM, Bailey JS, Strenzke N, Brose N, Müller U, Reisinger E, Moser T (2010) Hearing requires otoferlin-dependent efficient replenishment of synaptic vesicles in hair cells. *Nat Neurosci* 13:869–876.

- Pangršič T, Reisinger E, Moser T (2012) Otoferlin: a multi-C₂ domain protein essential for hearing. *Trends Neurosci* 35:671–680.
- Patel P, Harris R, Geddes SM, Strehle E-M, Watson JD, Bashir R, Bushby K, Driscoll PC, Keep NH (2008) Solution Structure of the Inner DysF Domain of Myoferlin and Implications for Limb Girdle Muscular Dystrophy Type 2B. *J Mol Biol* 379:981–990.
- Prete M, Fatone MC, Favoino E, Perosa F (2014) Raynaud's phenomenon: From molecular pathogenesis to therapy. *Autoimmun Rev* 13:655–667.
- Ramakrishnan NA, Drescher MJ, Drescher DG (2009) Direct interaction of otoferlin with syntaxin 1A, SNAP-25, and the L-type voltage-gated calcium channel Ca_v1.3. *J Biol Chem* 284:1364–1372.
- Rappoport JZ (2008) Focusing on clathrin-mediated endocytosis. *Biochem J* 412:415–423.
- Redpath GMI, Sophocleous RA, Turnbull L, Whitchurch CB, Cooper ST (2015) Ferlins show tissue-specific expression and segregate as plasma membrane/late endosomal or trans-Golgi/recycling ferlins. *Traffic*:n/a – n/a.
- Reisinger E, Bresee C, Neef J, Nair R, Reuter K, Bulankina A, Nouvian R, Koch M, Bückers J, Kastrup L, Roux I, Petit C, Hell SW, Brose N, Rhee J-S, Kügler S, Brigande JV, Moser T (2011) Probing the functional equivalence of otoferlin and synaptotagmin 1 in exocytosis. *J Neurosci Off J Soc Neurosci* 31:4886–4895.
- Rishi G, Crampton EM, Wallace DF, Subramaniam VN (2013) In Situ Proximity Ligation Assays Indicate That Hemochromatosis Proteins Hfe and Transferrin Receptor 2 (Tfr2) Do Not Interact. *PLoS ONE* 8:e77267.
- Romanos J, Kimura L, Fávero ML, Izarra FAR, de Mello Auricchio MTB, Batisso AC, Lezirovitz K, Abreu-Silva RS, Mingroni-Netto RC (2009) Novel OTOF mutations in Brazilian patients with auditory neuropathy. *J Hum Genet* 54:382–385.
- Roux I, Hosie S, Johnson SL, Bahloul A, Cayet N, Nouaille S, Kros CJ, Petit C, Safieddine S (2009) Myosin VI is required for the proper maturation and function of inner hair cell ribbon synapses. *Hum Mol Genet* 18:4615–4628.
- Roux I, Safieddine S, Nouvian R, Grati M 'hamed, Simmler M-C, Bahloul A, Perfettini I, Le Gall M, Rostaing P, Hamard G, Triller A, Avan P, Moser T, Petit C (2006) Otoferlin, defective in a human deafness form, is essential for exocytosis at the auditory ribbon synapse. *Cell* 127:277–289.
- Safieddine S, Wenthold RJ (1999) SNARE complex at the ribbon synapses of cochlear hair cells: analysis of synaptic vesicle- and synaptic membrane-associated proteins. *Eur J Neurosci* 11:803–812.

- Sandoval PC, Slentz DH, Pisitkun T, Saeed F, Hoffert JD, Knepper MA (2013) Proteome-Wide Measurement of Protein Half-Lives and Translation Rates in Vasopressin-Sensitive Collecting Duct Cells. *J Am Soc Nephrol* 24:1793–1805.
- Sanford JC, Klein TM, Wolf ED, Allen N (1987) Delivery of Substances into Cells and Tissues Using a Particle Bombardment Process. *Part Sci Technol* 5:27–37.
- Santarelli R, Rossi R, Scimemi P, Cama E, Valentino ML, La Morgia C, Caporali L, Liguori R, Magnavita V, Monteleone A, Biscaro A, Arslan E, Carelli V (2015) OPA1-related auditory neuropathy: site of lesion and outcome of cochlear implantation. *Brain* 138:563–576.
- Schmidt/Thews: *Physiologie des Menschen*; 27. Auflage 1997
- Schmitz F, Königstorfer A, Südhof TC (2000) RIBEYE, a component of synaptic ribbons: a protein's journey through evolution provides insight into synaptic ribbon function. *Neuron* 28:857–872.
- Schwander M, Sczaniecka A, Grillet N, Bailey JS, Avenarius M, Najmabadi H, Steffy BM, Federe GC, Lagler EA, Banan R, Hice R, Grabowski-Boase L, Keithley EM, Ryan AF, Housley GD, Wiltshire T, Smith RJH, Tarantino LM, Müller U (2007) A Forward Genetics Screen in Mice Identifies Recessive Deafness Traits and Reveals That Pejvakin Is Essential for Outer Hair Cell Function. *J Neurosci* 27:2163–2175.
- Smith MK, Wakimoto BT (2007) Complex regulation and multiple developmental functions of misfire, the *Drosophila melanogaster* ferlin gene. *BMC Dev Biol* 7:21.
- Starr A, Sininger Y, Winter M, Derebery MJ, Oba S, Michalewski HJ (1998) Transient deafness due to temperature-sensitive auditory neuropathy. *Ear Hear* 19:169–179.
- Stepanchick A, McKenna J, McGovern O, Huang Y, Breitwieser GE (2010) Calcium Sensing Receptor Mutations Implicated in Pancreatitis and Idiopathic Epilepsy Syndrome Disrupt an Arginine-rich Retention Motif. *Cell Physiol Biochem* 26:363–374.
- Strenzke N, Chakrabarti R, Al-Moyed H, Müller A, Hoch G, Pangrsic T, Yamanbaeva G, Lenz C, Pan K-T, Auge E, Geiss-Friedlander R, Urlaub H, Brose N, Moser T, Wichmann C, Reisinger E (2016) Hair cell synaptic dysfunction, auditory fatigue and thermal sensitivity in otoferlin Ile515Thr mutants. *EMBO J* 35 (23):2519–2535
- Sula A, Cole AR, Yeats C, Orengo C, Keep NH (2014) Crystal structures of the human Dysferlin inner DysF domain. *BMC Struct Biol* 14:3.
- Thomas J-L, Bardou J, L'hoste S, Mauchamp B, Chavancy G (2001) A helium burst biolistic device adapted to penetrate fragile insect tissues. *J Insect Sci* 1 Available at: <http://www.ncbi.nlm.nih.gov/pmc/articles/PMC355893/> [Accessed February 3, 2016].

- Thymiakou E, Episkopou V (2011) Detection of Signaling Effector-Complexes Downstream of BMP4 Using *in situ* PLA, a Proximity Ligation Assay. J Vis Exp Available at: <http://www.jove.com/index/Details.stp?ID=2631> [Accessed February 3, 2016].
- Tirard M, Hsiao H-H, Nikolov M, Urlaub H, Melchior F, Brose N (2012) In vivo localization and identification of SUMOylated proteins in the brain of His6-HA-SUMO1 knock-in mice. Proc Natl Acad Sci U S A 109:21122–21127.
- Towbin H, Staehelin T, Gordon J (1979) Electrophoretic transfer of proteins from polyacrylamide gels to nitrocellulose sheets: procedure and some applications. Proc Natl Acad Sci U S A 76:4350–4354.
- Varga R, Avenarius MR, Kelley PM, Keats BJ, Berlin CI, Hood LJ, Morlet TG, Brashears SM, Starr A, Cohn ES, others (2006a) OTOF mutations revealed by genetic analysis of hearing loss families including a potential temperature sensitive auditory neuropathy allele. J Med Genet 43:576.
- Varga R, Avenarius MR, Kelley PM, Keats BJ, Berlin CI, Hood LJ, Morlet TG, Brashears SM, Starr A, Cohn ES, Smith RJH, Kimberling WJ (2006b) OTOF mutations revealed by genetic analysis of hearing loss families including a potential temperature sensitive auditory neuropathy allele. J Med Genet 43:576–581.
- Vogl C, Cooper BH, Neef J, Wojcik SM, Reim K, Reisinger E, Brose N, Rhee J-S, Moser T, Wichmann C (2015) Unconventional molecular regulation of synaptic vesicle replenishment in cochlear inner hair cells. J Cell Sci 128:638–644.
- Wang D-Y, Wang Y-C, Weil D, Zhao Y-L, Rao S-Q, Zong L, Ji Y-B, Liu Q, Li J-Q, Yang H-M, Shen Y, Benedict-Alderfer C, Zheng Q-Y, Petit C, Wang Q-J (2010) Screening mutations of OTOF gene in Chinese patients with auditory neuropathy, including a familial case of temperature-sensitive auditory neuropathy. BMC Med Genet 11:79.
- Yasunaga Shin 'ichiro, Grati M 'hamed, Chardenoux S, Smith TN, Friedman TB, Lalwani AK, Wilcox ER, Petit C (2000) OTOF Encodes Multiple Long and Short Isoforms: Genetic Evidence That the Long Ones Underlie Recessive Deafness DFNB9. Am J Hum Genet 67:591–600.
- Yasunaga S, Grati M, Cohen-Salmon M, El-Amraoui A, Mustapha M, Salem N, El-Zir E, Loiselet J, Petit C (1999) A mutation in OTOF, encoding otoferlin, a FER-1-like protein, causes DFNB9, a nonsyndromic form of deafness. Nat Genet 21:363–369.
- Zak M, Breß A, Brandt N, Franz C, Ruth P, Pfister M, Knipper M, Blin N (2012) Ergic2, a brain specific interacting partner of otoferlin. Cell Physiol Biochem Int J Exp Cell Physiol Biochem Pharmacol 29:941–948.

Zhao H, Avenarius MR, Gillespie PG (2012) Improved Biolistic Transfection of Hair Cells. PLoS ONE 7 Available at: <http://www.ncbi.nlm.nih.gov/pmc/articles/PMC3462194/> [Accessed December 14, 2012].

Appendix

Table A1: Used primers for obtaining C₂ domain deletion constructs or constructs with an additional RXR domain. For better clarity recurrent primers are highlighted.

Name of primer	Sequence of primer 5' -> 3'
pEGFPN1mOtof del C ₂ A, for	CTTCGAATTCGCCACCATGGCCGCCACAGATGGCACTGT GGGC
pEGFPN1mOtof del C ₂ A, rev	ATCTTGTCTTTGGGGCTCCT
pEGFPN1mOtof del C ₂ B PCR1, for	AAGGACAGCCAGGAGACAGA
pEGFPN1mOtof del C ₂ B PCR1, rev	TGCCACCACCTGGTAATCCATGGGCCTTC
pEGFPN1mOtof del C ₂ B PCR2, for	ATTACCAGGTGGTGGGCAAGGGAGACAAC
pEGFPN1mOtof del C ₂ B PCR2, rev	GCTGCTCTTCTGCACTGATG
pEGFPN1mOtof del C ₂ C PCR1, for	AAGGACAGCCAGGAGACAGA
pEGFPN1mOtof del C ₂ C PCR1, rev	AGTTGCGCGTCCGTGCCCACTGCCGTTCC
pEGFPN1mOtof del C ₂ C PCR2, for	GTGGGCACGGACGCGCAACTACACTGCTG
pEGFPN1mOtof del C ₂ C PCR2, rev	ACAGAGGCGTGTGTCAGGATCT
pEGFPN1mOtof del C ₂ F PCR1, for	ATGTTGACAGTGGCCGTGTA
pEGFPN1mOtof del C ₂ F PCR1, rev	CATTCTATTCTCGTACTTCTTGGGTTTCC
pEGFPN1mOtof del C ₂ F PCR2, for	GAAGTACGAGAATGAGAATGATGAGTTTGAGC
pEGFPN1mOtof del C ₂ F PCR2, rev	GCTGAACTTGTGGCCGTTTACG
pEGFPN1mOtof RXR PCR1, for	CAATGATTGACCGGAAAATGGGG
pEGFPN1mOtof RXR PCR1, rev	CACAGCACACGGCAGCGCCGGAGAAGCCTGACCGTGG TGTTCCAGCTGGGGGCTGAGCGGTCTGG
pEGFPN1mOtof RXR PCR2, for	CGGCGTGCCGTGTGCTGTGCAATGGGGGCTCCTCCTC TCACTCCACAGGGGAGGTTGTAGTAAGC
pEGFPN1mOtof RXR PCR2, rev	CTCTTTACAGAGGCGTGTGTCAGG

Table A2: Used primers for obtaining point mutation deletion constructs. For better clarity recurrent primers are highlighted.

Name of primer	Sequence of primer 5' -> 3'
pEGFPN1mOtof I515T 1, for	CGTTCATCGGTGAGAACAAG
pEGFPN1mOtof I515T 1, rev	GCGCAGGTCGGTGAAGTGGGTGCCGATGG
pEGFPN1mOtof I515T 2, for	ACCCAATTACCGACCTGCGCAAGATTTCC
pEGFPN1mOtof I515T 2, rev	ACAGAGGCGTGTTCAGGATC
pEGFPN1mOtof G541S 1, for	CGTTCATCGGTGAGAACAAG
pEGFPN1mOtof G541S 1, rev	GCGTGGAGCTGTACATGTTACCCAGGCTG
pEGFPN1mOtof G541S 2, for	GAACATGTACAGCTCCACGCGCAACTACAC
pEGFPN1mOtof G541S 2, rev	ACAGAGGCGTGTTCAGGATC
pEGFPN1mOtof R1607W, for	CGTTCATCGGTGAGAACAAG
pEGFPN1mOtof R1607W, rev	TCATGGGGTCCCACCAGATATTGTAGCCATGTATG

Table A3: Used primers for identification of differences between mouse and human otoferlin. For better clarity recurrent primers are highlighted.

Name of primer	Sequence of primer 5' -> 3'
PCR RXR motif, for	TCATCTACCGACCTCCAGACC
PCR RXR motif, rev	CACATCCACCTTGACCACAGC
PCR amino acid stretch, for	AAGGACAGCCAGGAGACAGA
PCR amino acid stretch, rev	ATCTTGTCTTTGGGGCTCCT

Table A4: Used primary antibody for immunofluorescence stainings as well as proximity ligation assays

Target	Source	Dilution	Name	Provider
Calbindin	goat	1:150	Calbindin D28K (C20)	Santa Cruz
CtBP2	mouse	1:200	Purified Mouse Anti-CtBP2 Clone 16/CtBP2 (RUO)	BD Bioscience
CtBP2	rabbit	1:200	rabbit polyclonal, affinity purified	Synaptic Systems

Dynamin 1/2/3	rabbit	1:500	rabbit polyclonal, antiserum	Synaptic Systems
GFP	rabbit	1:500	GFP Tag Antibody, Alexa Fluor® 488 conjugate, Molecular Probes™	Thermo Fisher Scientific
Hemagglutinin	rabbit	1:300	Anti-HA tag antibody CHIP Grade	Abcam
Myosin 6	rabbit	1:200	Myosin-VI Rabbit Polyclonal Antibody	Proteus Biosciences
OPA1	rabbit	1:400	Anti-OPA1 antibody [EPR11057(B)]	Abcam
Otoferlin	mouse	1:300	Monoclonal Otoferlin antibody [13A9]	Abcam
Otoferlin	rabbit	1:500	Polyclonal rabbit antibody against Otoferlin	Synaptic Systems
Ribeye	rabbit	1:1000	U2656 (see Schmitz et al., 2000)	
VGlut3	rabbit	1:300	rabbit polyclonal, affinity purified, KO verified	Synaptic Systems

Table A5: Used secondary antibody for immunofluorescence stainings

Target	Source	Dilution	Name	Provider
mouse	goat	1:200	goat anti mouse 405 IgG (H+L)	Invitrogen
mouse	goat	1:200	goat-anti-mouse 568 IgG H+L	Life Technologies
mouse	goat	1:200	goat anti-mouse 594 IgG (H+L)	Invitrogen
rabbit	goat	1:200	goat anti-rabbit 488	Invitrogen
rabbit	goat	1:200	goat-anti-rabbit 568 IgG (H+L)	Life Technologies
goat	donkey	1:200	donkey anti-goat 568	Invitrogen
mouse	donkey	1:200	donkey anti mouse 488	Thermo Fisher Scientific
rabbit	donkey	1:200	donkey anti rabbit 488 IgG (H+L)	Invitrogen
		1:200	Phalloidin Atto 488	Sigma

Curriculum Vitae

Dipl. Biol. Alexandra Müller

Personal Data

Name: Alexandra Müller
Address: Teichstraße 67
37085 Göttingen
E-mail Address: Alexandra_mueller@t-online.de
Date/Place of birth: 31.07.1984/Siegen, Germany
Nationality: Germany

Education

2012- present PhD in Göttingen Graduate School for Neurosciences, Biophysics, and Molecular Biosciences, focused on Sensory and Motorneuroscience/ University of Göttingen/ Göttingen/ Germany
PhD-Thesis in the Institute for Auditory Neuroscience: "Molecular studies of the synaptic protein otoferlin"

2011 – 2012 Clinical diagnostics of chromosomes, MVZ Institut für Labormedizin und Klinische Genetik Rhein/Ruhr GmbH, Essen

2004 – 2010 Diploma in Biology at the Technical University of Kaiserslautern/Kaiserslautern/Germany
Diploma Thesis in the Department of Biology of the Technical University of Kaiserslautern, Division of Ecology
"PLC-vermittelte Sekretion GPI-verankerter Proteine ins Medium und der Einfluss der Dicer Homologe auf die Serotypexpression bei *Paramecium tetraurelia*"

Conferences / Symposia

Poster presentation:

11th Goettingen Meeting of the German Neuroscience Society: A. Müller, H. Al-Moyed, C. Lenz, S. Meese, K-T. Pan, H. Urlaub, E. Reisinger: "Analysis of Stability and Degradation of Otoferlin at normal and elevated Temperature"

Publications

Hair cell synaptic dysfunction, auditory fatigue and thermal sensitivity in otoferlin Ile515Thr mutants.
Strenzke N, Chakrabarti R, Al-Moyed H, Müller A, Hoch G, Pangrsic T, Yamanbaeva G, Lenz C, Pan K-T, Auge E, Geiss-Friedländer R, Urlaub H, Brose N, Moser T, Wichmann C, Reisinger E (2016) EMBO J 35 (23):2519–2535

Selective and programmed cleavage of GPI-anchored proteins from the surface membrane by phospholipase C.
Müller A, Klöppel C, Smith-Valentine M, Van Houten J, Simon M
Biochim Biophys Acta. 2012 Jan;1818(1):117-24. doi: 10.1016/j.bbamem.2011.10.009. Epub 2011 Oct 14.

Two isoforms of eukaryotic phospholipase C in *Paramecium* affecting transport and release of GPI-anchored proteins in vivo.
Klöppel, C, Müller, A, Marker S, Simon S
Eur J Cell Biol. 2009 Oct;88(10):577-92. doi: 10.1016/j.ejcb.2009.05.002. Epub 2009 Jun 21.